Faculty of Engineering

Development and Characterization of Polyvinylidene Fluoride Incorporated with Bamboo Nanocellulose/Graphene/Titanium Dioxide Nanocomposite Membrane for Dye Wastewater Treatment

Ain Zaienah Sueraya

Master of Engineering
2026

Development and Characterization of Polyvinylidene Fluoride Incorporated with Bamboo Nanocellulose/Graphene/Titanium Dioxide Nanocomposite Membrane for Dye Wastewater Treatment

Ain Zaienah Sueraya

A thesis submitted

In fulfillment of the requirements for the degree of Master of Engineering

(Chemical Engineering)

Faculty of Engineering
UNIVERSITI MALAYSIA SARAWAK
2026

DECLARATION

I declare that the work in this thesis was carried out in accordance with the regulations of Universiti Malaysia Sarawak. Except where due acknowledgements have been made, the work is that of the author alone. The thesis has not been accepted for any degree and is not concurrently submitted in candidature of any other degree.

……

Signature

Name: Ain Zaienah Sueraya

Matric No.: 22020207

Faculty of Engineering

Universiti Malaysia Sarawak

Date: 20th January 2026

ACKNOWLEDGEMENT

Firstly, I would like to thank my supervisor, AP Dr. Md Rezaur Rahman, for his persistent support, help, and professional feedback throughout my research studies. His expertise and encouragement have been crucial in completing this thesis and my growth as a researcher.

Thank you to my co-supervisors, AP Dr. Devagi Kanakaraju and Dr. Khairul Anwar Mohamad Said, for their encouragement, prudent suggestions, and motivating words. Their insights contributed greatly to this research, and I truly appreciate the learning opportunities posed by their differing views.

Next, I would also like to express my deepest gratitude to my family for supporting and motivating me through every step of the journey with your immeasurable love. I cannot thank you all enough for providing me a strong foundation to lean on in times of distress. To my parents, I am grateful for every sacrifice you made and believing in me when I struggled to find faith in myself. Your undeterred love has empowered me constantly. To my siblings, your support means everything to me. Reaching this stage would have become an unmanageable task without your unwavering love and strength.

I would also like to thank my senior, Anthonette James, for her wise mentorship, kindness, and warm-hearted motivational words. Her guidance means so much to me as it helped me a lot throughout the journey in completing my research.

To my best friends, thank you for always being my side and ready to help me whenever I needed it. I sincerely appreciate your support whether it was a small favour or

simply motivations on a rough day, your presence means more than I could ever express. I am very grateful for our friendship as your constant support, patience and willingness to lend a hand helped me lighten any burden I had during this journey.

To Team FR, words will never be enough to convey the impact of your presence in my life. We've shared countless struggles, frustrations, and breakthroughs together. There were moments during this journey where it felt very overwhelming, and you all became my source of strength and resilience. The bond that we share based on mutual understanding and support has been a vital part of this journey and I will forever be grateful to all of you who walked by my side throughout this journey.

To Heemangdan, thank you for your endless love and warm-hearted support. You provided me with peace and joy where it has truly helped me in the moment when I needed it the most. Your presence in my life has been incredibly healing and heartwarming. Thank you for being my emotional support, even from afar, and reminded me that I am not alone in this. I truly treasure every encouragement you gave as your positivity and belief in me gave me hope especially during moments I felt like giving up.

Whether big or small, every contribution made for this journey is deeply appreciated. Thank you once again to everyone involved in this journey together with me.

ABSTRACT

The increasing global demand for clean water has intensified research into advanced membrane technologies for water purification and wastewater treatment. While polyvinylidene fluoride (PVDF) membranes are widely recognized for their mechanical strength and chemical stability, their practical application is often limited by low permeability, insufficient dye rejection efficiency, and high fouling tendencies. To address these challenges, this study investigates the incorporation of functional nanomaterials including graphene (GR), titanium dioxide (TiO_2), and bamboo-derived nanocellulose (NC) into PVDF membranes to enhance their structural, chemical, and filtration properties. Three nanocomposite membranes were fabricated via the phase inversion method using N-methyl-2-pyrrolidone (NMP) as the solvent with PVDF as the polymer which are GR/NC, GR/TiO_2, and GR/NC/TiO_2 nanocomposite membranes. Each formulation was subjected to comprehensive characterization using Field Emission Scanning Electron Microscopy with Energy Dispersive X-ray analysis (FESEM-EDX), X-ray Diffraction (XRD), Fourier-Transform Infrared Spectroscopy (FTIR), and Ultraviolet-Visible (UV-Vis) spectroscopy. In the first part of the study, the study evaluates the GR/NC nanocomposite membranes. The membrane with the formulation of 20 wt% GR and 80 wt% NC achieved a remarkable water flux of 435.15 ± 1.73 L/m².h.bar approximately four times greater than that of pristine PVDF (110.87 ± 2.50 L/m².h.bar) along with the highest methylene blue (MB) dye removal efficiency of 94.47% (± 0.18). The superior dispersion of NC contributed to enhanced structural integrity and fouling resistance, leading to improved membrane reusability. The second part of the study focused on GR/TiO_2 nanocomposite membranes. The membrane with the formulation of 80 wt% GR and 20 wt% NC demonstrated optimal performance, with a sponge-like morphology and uniform nanoparticle distribution. XRD and FTIR

analyses confirmed that PVDF crystallinity was preserved while TiO_2 crystallinity was suppressed, enhancing membrane hydrophilicity. This ratio resulted in the highest water permeability and MB dye rejection alongside excellent antifouling behaviour compared to other ratios. The final phase of the study evaluated a nanocomposite membrane composed of bamboo nanocellulose, graphene, and TiO_2 (NC/GR/TiO_2). Scanning Electron Microscopy (SEM) images revealed a highly porous and interconnected network structure with homogeneously distributed nanomaterials. XRD patterns indicated modified PVDF crystallinity with reduced peak intensity, suggesting structural modification. This membrane achieved the highest overall water flux of 512.76 L/m².h.bar and a strong dye rejection rate of 92.13%, significantly surpassing the pristine PVDF membrane (109.48 L/m²·h·bar and 54.28% rejection, respectively). While its dye removal was slightly lower than the GR/NC membrane, its antifouling test showed superior results with a flux recovery ratio (FRR) of 95.95% and sustained dye removal of 86.18% after one reuse cycle. Therefore, the synergistic integration of bamboo-derived nanocellulose, graphene, and titanium dioxide significantly improves the permeability, dye removal efficiency, antifouling properties, and reusability of PVDF membranes. Among the three formulations, the GR/NC membrane achieved the highest dye removal, while the NC/GR/TiO_2 membrane demonstrated the best overall performance balance, particularly in terms of permeability and fouling resistance. These findings highlight the promising potential of renewable nanomaterials like bamboo nanocellulose in the development of highly efficient and sustainable membranes for the treatment of dye-contaminated wastewater.

Keywords: Nanocomposite membrane, nanocellulose, graphene, titanium dioxide, polyvinylidene fluoride, water purification

Kajian mengenai Nanoselulosa Buluh yang Digabungkan dengan Membran Nanokomposit Polivinilidena Fluorida Grafen/Titanium Dioksida

ABSTRAK

Peningkatan permintaan global terhadap sumber air bersih mendorong penyelidikan intensif dalam teknologi membran canggih untuk rawatan air sisa. Membran polivinilidena fluorida (PVDF) terkenal dengan kekuatan mekanikal dan kestabilan kimianya, namun penggunaannya dalam aplikasi praktikal terhad oleh kebolehtelapan rendah, kecekapan penyingkiran pewarna tidak mencukupi, dan kecenderungan kekotoran tinggi. Oleh itu, kajian ini menyiasat penggabungan bahan nano berfungsi termasuk grafen (GR), titanium dioksida (TiO_2), dan nanoselulosa (NC) daripada buluh ke dalam membran PVDF bagi meningkatkan sifat struktur, kimia dan penapisan membran tersebut. Tiga membran nanokomposit telah difabrikasi melalui kaedah fasa penyongsangan menggunakan N-methyl-2-pyrrolidone (NMP) sebagai pelarut dan PVDF sebagai polimer, iaitu membran GR/NC, GR/TiO_2, dan GR/NC/TiO_2. Setiap formulasi dinilai menggunakan Mikroskop Elektron Imbasan Pancaran Medan dengan Analisis Sinar-X Serakan Tenaga (FESEM-EDX), Plot Sinar-X Difraksi (XRD), Spektrometer Inframerah Transformasi Fourier (FTIR), dan Spektrometer Ultralembayung (UV-Vis). Pertama sekali, kajian dijalankan bagi membran nanokomposit graphene dan nanoselulosa (GR/NC). Formulasi 20 wt% GR dan 80 wt% NC mencatatkan fluks air sebanyak 435.15 ± 1.73 L/m².j.bar, hampir empat kali ganda lebih tinggi berbanding membran PVDF asli (110.87 ± 2.50 L/m².j.bar) serta kecekapan penyingkiran pewarna metilena biru (MB) tertinggi sebanyak 94.47% (± 0.18). Penyebaran NC yang seragam meningkatkan integriti struktur membran, sifat antikotoran, dan kebolehkitaran semula membran. Bahagian kedua kajian iaitu nanokomposit GR/TiO_2 menunjukkan formulasi 80 wt% GR dan 20 wt% NC mempunyai morfologi seperti span dan

pengagihan nanopartikel yang homogen. Analisis XRD dan FTIR mengesahkan bahawa kekristalan PVDF dikekalkan manakala kekristalan TiO_2 dikurangkan, yang menyumbang kepada peningkatan hidrofilisiti. Formulasi ini menghasilkan kebolehtelapan air dan penyingkiran MB tertinggi, serta menunjukkan prestasi antikotoran cemerlang berbanding formulasi yang lain. Bahagian terakhir kajian menilai membran nanokomposit ternari iaitu GR/NC/TiO_2. Analisis SEM menunjukkan struktur membran yang berliang dan saling berhubung dengan pengagihan nanobahan yang sekata. Corak XRD menunjukkan penurunan intensiti puncak, menandakan pengubahsuaian struktur dan peningkatan hidrofilisiti. Membran ini mencapai fluks air keseluruhan tertinggi iaitu 512.76 L/m²·j·bar dan kadar penyingkiran pewarna sebanyak 92.13%, jauh mengatasi membran PVDF asli (109.48 L/m²·j·bar dan penyingkiran 54.28%). Walaupun kecekapan penyingkiran pewarna lebih rendah berbanding membran GR/NC, membran ini menunjukkan prestasi antikotoran unggul dengan nisbah pemulihan fluks (FRR) sebanyak 95.95% dan kecekapan penyingkiran pewarna sebanyak 86.18% selepas satu kitaran penggunaan semula. Integrasi sinergistik antara nanoselulosa buluh, grafen dan titanium dioksida telah meningkatkan kebolehtelapan, kecekapan penyingkiran pewarna, sifat antikotoran dan kebolehkitaran semula membran PVDF dengan ketara. Antara ketiga-tiga formulasi, membran GR/NC mencatatkan penyingkiran pewarna tertinggi, manakala membran GR/NC/TiO_2 menunjukkan prestasi keseluruhan terbaik, khususnya dari segi kebolehtelapan dan rintangan kotoran. Penemuan ini menunjukkan potensi besar nanobahan boleh diperbaharui seperti nanoselulosa buluh dalam pembangunan membran yang cekap dan mampan untuk rawatan air sisa yang tercemar pewarna.

Kata kunci: *Membran nanokomposit, nanoselulosa, grafen, titanium dioksida, polivinilidena fluorida, penulenan air*

TABLE OF CONTENTS

LIST OF TABLES

LIST OF FIGURES

Page

LIST OF EQUATIONS

LIST OF ABBREVIATIONS

AFM	Atomic Force Microscope
DLBF	Delignified Bamboo Fibre
DWBF	Dewaxed Bamboo Fibre
DMF	Dimethylformamide
DMSO	Dimethylsulfoxide
FESEM-EDX	Field Emission Scanning Electron Microscopy with Energy Dispersive X-Ray
FRR	Flux Recovery Ratio
FTIR-ATR	Fourier Transform Infrared Spectrophotometer Equipped with Attenuated Total Reflectance
FTIR	Fourier-Transform Infrared Spectroscopy
GR	Graphene
GO	Graphene Oxide
R_{ir}	Irreversible Fouling
CH_2	Methylene
MB	Methylene Blue
MMM	Mixed Matrix Membrane
DMAC	N,N-Dimethylacetamide
NC	Nanocellulose
NFC	Nanofiber Cellulose
NMP	N-Methyl-2-Pyrrolidone
PAN	Polyacrylonitrile

PES	Polyethersulfone
PVDF	Polyvinylidene Fluoride
R_r	Reversible Fouling
SEM	Scanning Electron Microscopy
SCNF	Sulphated Cellulose Nanofibril
TFC	Thin Film Composite
TiO_2	Titanium Dioxide
R_t	Total Fouling
TEM	Transmission Electron Microscopy
UF	Ultrafiltration
UV-Vis	Ultraviolet-Visible Spectroscopy
XRD	X-Ray Diffraction

CHAPTER 1

INTRODUCTION

1.1 Research Background

The continuous requirement for safe water, the increase in energy utilization, cost-effectiveness, and the decline in natural resources, are among the main reasons for developing various technologies to produce clean water for the human population (Saleem & Zaidi, 2020). According to Saud et al. (2022), the prediction for the overall world population in the upcoming thirty years is an increase of more than 40%, increasing industrial, domestic, and agricultural water sources. On top of that, the demand for water sources will escalate drastically in developing countries as the demand for clean water sources is comparatively higher concerning the population of the countries (Saud et al., 2022). Based on the study by Baghel and Baranwal (2022), the amount of ocean water that is determined in the overall water amount on Earth is around 97.5%, and the remaining percentage, which is 2.5%, is the amount of fresh water accessible for human usage. Since ocean water is salty, it is unsafe for human consumption, showing water treatment's importance. Besides, despite significant progress in increasing access to clean water sources, billions still lack these essential services, especially in urban and rural areas (Nannan et al., 2022). Hence, the purification and treatment of water sources are crucial for the survival of the human population and the planet (Salama et al., 2021). Nannan et al. (2022) also mentioned that access to sustainable and safe water sources should be highly prioritized, especially in urban and rural communities. The report by World Water Council mentioned that it is very likely that almost 3,900 million people will face shortages in water supply by 2030 (Saud et al., 2022).

As the crucial role of clean water sources in maintaining healthy ecosystems has become widely recognized, there has been a rapid development and implementation of new water treatment technologies (Oladoyinbo et al., 2024; Shi et al., 2023). Water treatment technologies include microfiltration, ultrafiltration, reverse osmosis, membrane distillation and others for different purposes of water treatments (Ezugbe & Rathilal, 2020; J. Wang, Chen, et al., 2023). Besides the increasing water demand, it is also crucial to improve the water treatment methods as there are various reasons for the pollution of the current water sources due to industrial activities. This fact is also mentioned by Qiao et al. (2021) where a study states that the water pollution issue is very severe due to the development of industrialization. Water pollution refers to the presence of pollutant compounds in the water that are hazardous to people, plants, or property, where the pollutants are substances that can change the natural properties of water (Abdi-Soojeede & Nour, 2022). According to Abouzeid et al. (2019), two types of water pollutants can be found in wastewater: chemical and biological. The chemical contaminants of wastewater include organic and inorganic particles, pharmaceuticals, heavy metals, toxins, hormones, and other harmful substances. Water contaminants such as dyes, organic compounds, heavy metals, saturated salts, oil emulsion, and pharmaceutical effluents are reported posing significant challenges, endangering the safety of both aquatic life, humans and ecosystem (Chandio et al., 2020; Muhammad & Usman, 2022; Norfarhana et al., 2022; Pachaiappan et al., 2022; Qamar et al., 2022; Zeng et al., 2022). Effective treatment of these emerging contaminants is however substantially constrained with water treatment technologies.

There are various technologies for wastewater treatment mentioned by Saleh et al. (2022) including photocatalysis, chemical precipitation, adsorption, flotation, coagulation/flocculation, ion exchange, reverse osmosis, electrochemical treatment,

ultrafiltration, and nanofiltration. Ranjit et al. (2021) state that the conventional wastewater treatment method uses a combination of physical, chemical, and biological procedures to eliminate the biological decomposition of organic matter, nutrients, dissolved solids, and suspended solids. Even though many technologies can be used for wastewater treatment, various issues are involved with conventional wastewater treatment technologies that need to be considered. For example, Qiao et al. (2021) state that the electrochemical treatment or chemical precipitation methods are ineffective in removing metal ions when the ion concentration is less than 100 mg/L or when the ion product is less than the K_{sp}. In addition, Qiao et al. (2021) also mentioned that other conventional technologies, like reverse osmosis and ion exchange, require high energy and costs in the long run. Thus, it is crucial to identify the best wastewater treatment method as pollutant management is a crucial issue due to high amounts of hazardous pollutants in wastewater cannot be removed effectively by the majority of the current wastewater purification and separation technologies (Crini & Lichtfouse, 2018; Ge et al., 2019; Y. Zhang & Park, 2019).

Membrane technology is one of the novel and viable methods to address the issues that are faced by the conventional methods as it has outstanding qualities like better selectivity, increased life span, high separation efficiency, cost-effective, and minimal maintenance, along with good mechanical, chemical and thermal stability (Mansoori et al., 2020). In contrast to conventional technologies, membrane technologies have various major advantages, including ease of operation, production of reusable water, high automation potential, scalability, and small environmental imprint (Im et al., 2019; Noguchi et al., 2019). However, according to Kumari et al. (2020), membrane technology has several limitations, including costs when working at high hydraulic pressure, membrane fouling, recyclability, water flux, and selectivity. Therefore, several novel elements are researched and used to

enhance the membrane technologies to solve previously mentioned issues. Membranes can be polymeric, carbonaceous, hybrid/nano-hybrid, porous/non-porous, or organic/inorganic based on the material (Kamran et al., 2022). It is also mentioned that different membrane components have distinctive qualities that are used to eliminate particular contaminants (Kamran et al., 2022).

Ultrafiltration (UF) membrane is a unique membrane filtration technology that can remove particle materials in solution where it is normally used to purify macromolecular solutions (Youcai, 2018). UF membranes are also able to produce highly pure water treatment that contains no pathogenic waste (C. M. Hussain et al., 2022). UF membranes are one of the most efficient membrane filtration processes due to its ease and efficiency in operation, low energy consumption, and its ability to remove a variety of contaminants such as dyes, organic compounds, and suspended solids (Kammakakam & Lai, 2023). The structure of the UF membranes normally have an asymmetric structure that consists of a dense top surface and finger-like pores in the sublayer (B. Khan et al., 2020). Since PVDF has high chemical resistance, mechanical strength, and thermal stability, it remains one of the most preferred polymers in fabrication of UF membranes (Saxena & Shukla, 2021). However, one of the major challenges in UF membrane application is membrane fouling, which reduces water flow through the membrane, shortens its lifespan, and increases operational costs (N. M. A. Omar et al., 2024). These problems can be mitigated by incorporating hydrophilic nanoparticles which are known to enhance membrane performance.

Polyvinylidene fluoride (PVDF) has been used extensively as UF membranes due to its attractive properties such as chemical and physical stability, mechanical strength and has a high solubility in common organic solvents like N-methyl-2-pyrrolidone (NMP), N,N-

dimethylacetamide (DMAc), dimethylsulfoxide (DMSO), and dimethylformamide (DMF) (Wei et al., 2019). Despite that, PVDF is a hydrophobic material and has low surface energy which results in high surface fouling leading to decreased permeability (Z. Wang, Feng, et al., 2023; Wei et al., 2019). Hence, the incorporation of nanoparticles such as graphene (GR) and nanocellulose (NC) that possess excellent physicochemical properties to modify membrane surface characteristics is highly essential in enhancing the efficiency of PVDF membranes

Various studies have reported the successful utilization of TiO_2 as a catalyst for photocatalytic activities, graphene oxide (GO) as a material to remove pollutants from wastewater, and the combination of GO and TiO_2 in PVDF membranes for the removal of dye in wastewater (Alyarnezhad et al., 2020; Dzinun et al., 2020; J. Li et al., 2020; M. Park et al., 2022; Vatanpour et al., 2021; C. Zhu et al., 2017). However, the synergistic effects of combining GR and TiO_2 have not been explored. GR is a two-dimensional material consisting of a single layer of carbon atoms with a honeycomb lattice structure, has excellent physicochemical properties such as exceptionally high mechanical strength, thermal conductivity, and high surface area (Chakraborty & Hashmi, 2018; Namakka et al., 2023; Srivastava & Adesina, 2022). Previous studies reported significant performance of GR-based nanocomposite membranes with high molecular separation properties (Kumari et al., 2021).

NC on the other hand is a promising material with unique characteristics and great potential in water purification systems (Jaffar et al., 2022; Sharma et al., 2020; Tan et al., 2020). NC is environmentally abundant with excellent properties such as hydrophilicity, high adsorption capacity, mechanical stability, biodegradability, and potentials for renewability (Faiz Norrrahim et al., 2021; Reshmy et al., 2022; Z. Wang, Chen, et al., 2023). Although NC conventionally serves as pore former by interacting with polymer matrix

resulting to the formation of a porous structure with an improved membrane permeation properties (Zubair et al., 2024), NC modified membranes are efficient in the removal of various contaminants like dyes (James, Rezaur Rahman, et al., 2024), heavy metals, and oils (Faiz Norrrahim et al., 2021). Moreover, the incorporation of nanocellulose was found to promote hydrophilicity, reducing membrane fouling and maintaining operational efficiency over extended application.

TiO_2 is a white powder distinguished by its large specific surface area. Notably, the integration of TiO_2 into membrane materials has been reported to enhance the hydrophilicity of the membrane surfaces (Jafari & Sillanpää, 2020; Sakarkar et al., 2021). In addition, TiO_2 acts as a biofouling mitigator which is able to degrade organic pollutants, rendering it as a novel material to be incorporated in membrane fabrication (X. Yang et al., 2021). The study shows that the incorporation of TiO_2 in membranes are able to improve flux, dye removal, and has better antifouling performance under various operating conditions (Mohamat et al., 2023). Therefore, by combining the unique properties of these three materials, the NC/GR/TiO_2 nanocomposite membrane is able to improve the water permeation along with the antifouling capabilities and reusability of the membrane.

Combining the synergistic effects of NC, GR and TiO_2 in the PVDF membrane material is expected to enhance the hydrophilic and surface properties of the PVDF membrane and ensure effective wastewater treatment operations. This research presents a novel approach to dye contaminated wastewater remediation with enhanced antifouling performance of PVDF membrane through the development of a NC/GR/TiO_2 PVDF nanocomposite membrane. In order to achieve the optimum composition for NC/GR/TiO_2 PVDF membrane, two experiments were conducted beforehand to determine the optimum composition for NC/GR and GR/TiO_2. Firstly, NC and GR were subsequently incorporated

into PVDF via chemical blending approach to produce the NC/GR PVDF nanocomposite membranes via phase inversion. Similar methodology was done for GR/TiO_2 PVDF nanocomposite membranes along with NC/GR/TiO_2 PVDF nanocomposite membranes. The unique combination of NC, GR, and TiO_2 within the PVDF matrix not only improved the membrane's structural integrity and permeability but also significantly increased its adsorption capacity for methylene blue dye.

1.2 Problem Statements

The rapid expansion of urban areas, industries along with the increasing population results in a surge in demand for clean water which poses serious challenges in effective wastewater treatment and sustainable water supply (Obaideen et al., 2022; Siddique, 2022; Silva, 2023). Membrane-based filtration has emerged as a promising solution for water purification, especially in dye removal from industrial effluents (Kolya & Kang, 2023). However, conventional PVDF membranes have low permeability, poor hydrophilicity, low dye-rejection, and high fouling tendency (Kang & Cao, 2021; Nawaz et al., 2021). These disadvantages limit the usage of membranes in practical water treatment systems and pose a challenge to their applications in practical water treatment systems.

To mitigate the challenges posed by PVDF membranes, the incorporation of functional nanomaterials has emerged as a promising direction of research. NC, GR, and TiO_2 exhibit functional characteristics which are beneficial for the enhancement of the membrane performance (Ben Dassi & Chamam, 2025; Garg et al., 2024). GR possesses remarkable mechanical strength alongside high surface area and structural reinforcement (Lü et al., 2021; F. Zhang et al., 2022). TiO_2 improves surface hydrophilicity while contributing surface roughness, which are both necessary for enhanced water transport and reduced membrane fouling (Bilal et al., 2024; Davari et al., 2021; Matindi et al., 2022). NC is

renewable and biodegradable and naturally hydrophilic, which enhances pore formation and water affinity while increasing membrane flexibility (Khorsandi et al., 2024; Y. Li et al., 2025). Although the discussed nanomaterials have differing favourable characteristics, few studies have systematically evaluated the incorporation of these materials and their synergistic or individual impact on PVDF membrane properties and filtration performance.

This research develops and evaluates three types of nanocomposite membranes, GR/NC, GR/TiO_2, and GR/NC/TiO_2, to mitigate the inherent drawbacks of pristine PVDF. membranes. These membranes are fabricated through phase inversion and characterized in detail for their morphology, crystallinity, dye rejection, water flux, antifouling, and reusability performance metrics. The research conducts an analysis to determine the most optimal combination of nanomaterials which achieves the targeted balance of high permeability, selective filtration, and stable operation over time. It is anticipated that the research will aid in the development of membranes designed to withstand harsh operational conditions while maintaining high efficiency in treating dye-contaminated wastewater.

1.3 Research Gaps

Even with the increase in research targeted toward improving the performance of membranes, major gaps persist in areas like antifouling performance, dye rejection, and membrane permeability. As the performance limitations are highly common in nanocomposite membranes, modified membranes are also subjected to newly produced limitations (Al Harby et al., 2022). Although polymeric nanocomposite membranes have demonstrated higher permeability and antifouling potential than pure polymers, there are still significant challenges in achieving a balance between permeability, selectivity, and fouling resistance (Mubarak et al., 2023). Various laboratory-scale studies have integrated different nanomaterials with polymeric membranes to improve these parameters. Numerous

studies focused on the improvement of a specific factor, but integrating all the factors simultaneously has not been demonstrated.

In addition, there is an insufficient amount of comparative and comprehensive studies that evaluates on different combinations of NC, GR, and TiO_2 with the synergistic effects on the overall structure and functional performance of PVDF membranes. For example, a study by J. Wang et al. (2017) produced a PVDF membrane incorporated with graphene oxide (GO) with TiO_2 and discovered that GO membrane produces a pore channel with a narrow route which limits the dye rejection of the membrane. Other than that, another study also observed that GO incorporated PVDF membranes improved hydrophilicity and antifouling properties, but it focused on the individual modification strategies instead of the combined effect of multiple nanomaterials (Ndeh et al., 2024). Therefore, the comprehensive effects of these nanomaterials on membranes' morphology, dye rejection, antifouling properties, and long-term reusability have not been studied thoroughly.

Therefore, this research aims to address these gaps with consistent fabrication, testing, and characterization of three types of nanocomposite membranes which are GR/NC, GR/TiO_2, and GR/NC/TiO_2. This research also focuses on comprehensive study on the role of each nanomaterial and their synergistic interactions towards fabricating high-performance, reusable, and sustainable membranes designed for the treatment of dye-contaminated wastewater.

1.4 Research Hypothesis

Raw bamboo fibres are dried and grinded to produce NC by using chemical and mechanical methods. The produced NC is expected to exhibit nanoscale morphology, and the structure of NC is determined by using Transmission Electron Microscopy (TEM) analysis. Other than that, nanocomposite membranes are fabricated by using the phase

inversion technique, incorporating NC, GR, and TiO_2 into a PVDF matrix which will exhibit improved morphological, structural, and surface properties.

The incorporation of functional nanomaterials such as NC, GR, and TiO_2 into PVDF membranes is expected to overcome the limitations pertaining to pristine PVDF which are low water permeability, inefficient dye removal, high fouling rates, and limited reusability, thus significantly improving the overall membrane performance.

Each nanomaterial is expected to contribute specific advantages where NC will improve the water uptake while enhancing pore structure and flexibility owing to its hydrophilic and renewable nature, GR will enhance porosity and permeable resistance, and TiO_2 will improve hydrophilicity and surface modification resistant to fouling.

In addition, it is hypothesized that the combination of NC, GR, and TiO_2 in a single nanocomposite membrane (GR/NC/TiO_2) is able to give synergistic effects which will result in an enhanced overall performance compared to membranes that consists of only one or two nanomaterials. This specific nanocomposite membrane is designed with the expectation of the highest water flux along with efficient dye rejection rate, superior antifouling capabilities, and consistent performance even after reusability tests.

It is also hypothesized that the interaction of the nanomaterials will result in greater porosity, hydrophilicity, structural strength, and overall robustness which will enhance membrane efficacy in treating wastewater contaminated with dyes. These enhancements can be analysed via several characterization methods which are FESEM-EDX, FTIR, and XRD. The membranes are expected to demonstrate improved water flux, dye rejection, antifouling performance, and reusability compared to pristine PVDF membranes.

1.5 Research Objectives

The main aim for this research is to develop PVDF nanocomposite membranes incorporated with NC, GR, and TiO_2 for enhanced methylene blue dye removal. To achieve this aim, there are three objectives of this research which are listed below:

i. To synthesis nanocellulose from raw bamboo fibre and determine the nanocellulose structure.

ii. To evaluate the performance of developed nanocomposite membrane.

iii. To compare the effects of different nanomaterial combinations on membrane performance.

1.6 Research Scope

Despite the extensive research that is conducted on the development of nanocomposite membranes in water treatment technologies, there remains a lack of improvements in fundamental aspects such as membrane permeation, dye rejection and antifouling performance. This research focuses on addressing these limitations by incorporating functional nanomaterials like NC, GR, and TiO_2 into a PVDF membrane matrix. This research is done with three experiments with different nanomaterial combinations which are GR/NC, GR/TiO_2 and NC/GR/TiO_2. The fabrication of three types of nanocomposite membranes GR/NC, GR/TiO_2 and NC/GR/TiO_2 will be done via phase inversion method. Other than that, the characterization of the nanocomposite membranes will also be done using various characterization methods such as FESEM-EDX, FTIR, XRD and UV-Vis to determine the morphology, functional groups, crystallinity, and concentration of dye removal respectively. Lastly, the membrane performance will be evaluated in terms

of the water flux, MB dye rejection rate along with antifouling performance and membrane reusability.

CHAPTER 2

LITERATURE REVIEW

2.1 Overview

In this chapter, critical and comprehensive analysis of the study is done where various journals and articles are reviewed. The literature review is conducted to gain better understanding on the research where the patterns of the previous research are analysed to ensure the objectives of the research are achieved. The literature review also focuses on the impact of the nanomaterials on nanocomposite membranes, along with the type, fabrication methods, and mechanisms of the nanocomposite membranes.

2.2 The Impact of Cellulose on Nanocomposite Membranes

Cellulose is one of the primary parts of a plant cell which is the most versatile biopolymer on Earth (Joseph et al., 2020). According to Norizan et al. (2022), cellulose is biodegradable, abundant, natural, and renewable which can be found in algae, plants, animals, bacteria, or fungi. Among those various sources, plants and wood are the main sources of cellulose as it consists of microfibril cellulose, lignin, pectin, and hemicellulose (Norizan et al., 2022). The astonishing properties of cellulose results in high studies of cellulose incorporation as natural polymers in nanocomposite membranes which is discussed in the table below.

Table 2.1: The impact of cellulose on nanocomposite membranes.

Impacts	Explanation	References
More sustainable	As mentioned before, cellulose is obtained from natural sources especially plants and	(Egan & Salmon, 2021;

Table 2.1 continued

	wood. These sources are sustainable and renewable as it can be obtained as by-products from various industries such as agricultural industries and forest wastes. In addition, cellulose is also sustainable as it can be naturally degraded by microorganism even though the degradation of cellulose is dependent on the microbial population. Furthermore, the production of cellulose is readily scalable and does not involve toxic chemicals. On top of that, the production such as enzymatic hydrolysis, does not produce any toxic wastes. Hence, the usage of cellulose in nanocomposite membranes is more sustainable compared to other polymer sources.	El-Gendi et al., 2022; Janaswamy et al., 2022; Yu et al., 2021)
Excellent selectivity	Cellulose has a porous structure that allows the size-sieving mechanism of the nanocomposite membrane where the cellulose has an excellent selectivity in allowing particular sizes of materials to pass through the nanocomposite membrane. This selectivity is due to the effective pore distribution that is formed by the cellulose network which controls the transport of smaller molecules while restricting larger molecules. This mechanism ensures that the cellulose enables the smaller size materials that is desired and remove the larger materials that are not needed. In addition, high degree of polymerization of cellulose facilitates the formation of a networked structure that	(Dong et al., 2022; Lee et al., 2024; Yue et al., 2020; W. Zhou et al., 2024)

Table 2.1 continued

	preserves membrane integrity without substantially increasing pore size. The presence of abundant hydroxyl groups also promotes hydrogen bonding with water molecules which enhances the water affinity and facilitating water transport through the membrane. This is advantageous for nanocomposite membrane that requires filtration application.	
Improved mechanical properties	The mechanical properties of cellulose are attributed by the molecular structure of cellulose where it has high crystallinity because of its superior hydrogen bonds. The cellulose fibres perform as a reinforcement agent in nanocomposite membrane by increasing the strength and stiffness in the structure of the nanocomposite membrane. On top of that, the porous structure of cellulose also has a significant impact on the toughness of the nanocomposite membrane. In addition, cellulose can exhibit synergistic effects by combining with other materials to improve the mechanical properties. Since GR also has superior mechanical properties, the reinforcement of GR and cellulose can produce a synergistic effect that significantly enhance the mechanical properties of nanocomposite membrane.	(Joseph et al., 2020; J. Liu & Lv, 2021; Noor Azammi et al., 2020; Zakuwan & Ahmad, 2018)

In the current study, bamboo-derived nanocellulose is incorporated into PVDF membranes to improve pore structure, targeted transport, and antifouling performance during methylene blue dye filtration as reported in multifunctional PVDF/NC/GR/TiO_2 membranes with improved pore morphology and antifouling performance (James, Rezaur Rahman, et al., 2024). These reported characteristics of nanocellulose, such as its porous structure, high aspect ratio, and abundant hydroxyl groups, directly support its selection.

2.3 The Impact of Graphene on Nanocomposite Membranes

GR is a single layer of graphite which is made up of only carbon atoms that arranged in a honeycomb structure which is a hexagonal pattern extending in a single layer of atoms (Armano & Agnello, 2019). The 2D structure of GR results in various attractive properties of GR (Armano & Agnello, 2019). The properties of GR include high Young's modulus, high thermal conductivity, high molecular barrier abilities, and high electrical conductivity (Rahman et al., 2019; Smith et al., 2019). Thus, the impact of GR on nanocomposite membranes are tabulated in the following table.

Table 2.2: The impact of graphene on nanocomposite membranes.

Impacts	Explanation	References
Improved mechanical properties	GR has an exceptionally great mechanical properties with a high Young's modulus amounting to 1 TPa, break strength of 42 N/m, and tensile strength valued 130.5 GPa. GR also has a low fracture toughness which can be as low as 4.0 ± 0.6 $MPA.m^{1/2}$. The nanocomposite membranes have a significant improve in the mechanical properties specifically in terms of stiffness even with low amounts of graphene.	(Fortunato et al., 2020; Smith et al., 2019)

Table 2.2 continued

Improved barrier properties	GR has a high aspect ratio which can improve the barrier properties of nanocomposite membranes. GR is known to improve the barrier properties of nanocomposite membranes by making the membrane matrix more tortuous, which limits the movement of pollutants, moisture, and unwanted gases. Simultaneously, it can increase selective permeability to water because GR improves pore connectivity and interfacial interactions. In addition, the barrier properties improvement of GR includes gas and moisture barrier properties which can be advantageous for nanocomposite membrane in a variety of applications.	(Ahmed et al., 2023; Ashfaq et al., 2023; Cosquer et al., 2021; Yao et al., 2021)
Anti-corrosive properties	GR also has attractive properties such as anti-corrosion which can be used for commercial uses in various industries. The 2D morphology and chemical inertness of GR contributes to these anti-corrosive properties of GR. Since polymer are permeable to water, chloride, and sulphites, this would be toxic for the nanocomposite membranes. However, GR can be used as fillers to reduce the diffusion of toxic materials to the nanocomposite membrane by generating an anti-corrosive layer on the surface of the membrane.	(Luo et al., 2018; Smith et al., 2019)

According to previous studies on graphene-modified membranes, these graphene characteristics are utilized in this study to enhance membrane permeability and antifouling performance of PVDF-based nanocomposite membranes, especially for improving

methylene blue dye rejection through increased transport tortuosity and improved interfacial interactions (H. Zhang et al., 2025).

2.4 The Impact of Titanium Dioxide on Nanocomposite Membranes

TiO_2 is a non-toxic inorganic compound and is known for its stability along with a multitude of functional properties (Farooq et al., 2024; Nagaraj et al., 2025). It naturally occurs in the three main crystalline forms which are, rutile, brookite and anatase (Eddy et al., 2023). Among these phases, anatase phase is the most prominent in membrane applications due to its higher surface area and reactivity (Dharma et al., 2022). Often used due to its hydrophilic nature, TiO_2 are found in most membranes because of their strong chemical resistance, capability to increase the roughness of the membrane surface, better water permeability, decreased fouling, and overall stronger maintained porosity frameworks (Davari et al., 2021; Tetteh et al., 2021; Y. (Alex) Wang et al., 2022; Y. Zhou et al., 2023). Thus, the impact of TiO_2 on nanocomposite membranes that is illustrated in the table below.

Table 2.3: The impact of titanium dioxide on nanocomposite membranes.

Impacts	Explanation	References
Enhanced antifouling performance	TiO_2 is able to modify surface characteristics of nanocomposite membranes which results in enhancing the antifouling performance of nanocomposite membranes. This is due to the hydrophilic nature and high surface energy of TiO2 which contributes to the production of a hydration layer on the membrane surface. This layer acts as a physical barrier and decreases the adsorption and accumulation of foulants, which includes proteins, dyes, and organic matter.	(Alarif et al., 2023;

Table 2.3 continued

Improved hydrophilicity	The incorporation of TiO_2 into nanocomposite membranes is able to significantly improve the hydrophilicity of the nanocomposite membranes due to the high affinity for the water molecules and polar surface of TiO_2. Nanocomposite membranes with high hydrophilicity exhibits a lower contact angle and improved water permeability, thus, water can diffuse more rapidly and uniformly through the membrane. This is crucial for nanocomposite membranes for water treatment processes as it increases the efficiency of filtration and resistance to fouling.	(Kusworo, Yulfarida, et al., 2023; Nawaz et al., 2021; Xu et al., 2025; T. Zhu et al., 2022)
Improved surface roughness and porosity	The incorporation of TiO_2 into nanocomposite membranes increases the porosity and the surface roughness of the nanocomposite membranes. TiO_2 also affects the kinetics of solvent-nonsolvent exchange during phase inversion process which facilitates the formation of interconnected pore channels and macrovoids. The change in the membrane morphology results in increased availability of surface that are available for filtration and improves overall membrane permeability. In addition, increased surface roughness is able to increase membrane wettability which allows water to spread easier across the membrane surface. Other than that, improved porosity in nanocomposite membranes also	(Cevallos-Mendoza et al., 2022; Gayatri et al., 2023; Goyat et al., 2024; A. U. Khan et al., 2024; M.Hamad et al., 2022; Zhao et al., 2023)

Table 2.3 continued

	enhance separation efficiency as more water molecules can pass through rapidly while maintaining selectivity of pollutants like suspended solids and dyes.	

While GO/TiO_2 systems for antifouling and dye removal applications have been the focus of many previous studies (Kouzi et al., 2025; Mohamat et al., 2023; Oliveira et al., 2022), the current work investigates pristine graphene in combination with TiO_2 and nanocellulose in a PVDF matrix to determine whether synergistic interactions can achieve comparable or improved performance.

2.5 Types of Nanocomposite Membranes

2.5.1 Blend Membrane

Polymer mixing is a general method to acquire new materials and enhance their performance compared to the pure initial components (Mansoori et al., 2020). A blend membrane is fabricated by blending natural or synthetic polymers with nanocellulose or its derivatives (Y. Liu, Ahmed, et al., 2021). It will result in a membrane with enhanced separation performance, improve the permeability and selectivity of the membrane, and increase the flux and swelling capacity of the membrane (Mansoori et al., 2020).

2.5.2 Imprinted Membrane

Molecular imprinting is a synthetic polymer that creates selective molecular recognition properties in a target compound as the recognition sites are structurally and functionally similar to the analyte molecule (G. K. Ali & Omer, 2022). It will result in a membrane with high selectivity as the synthetic receptor sites can memorize and recognize

target species among other species present in the solution (G. K. Ali & Omer, 2022; Mansoori et al., 2020). According to Su et al. (2020), the synthetic process of molecularly imprinted membranes consists of several steps where the formation of the complex is initially done through the covalent or non-covalent bonding of the template molecule and functional monomer. Next, Su et al. (2020) also mentioned that a cross-linking agent is added along with an initiator to polymerize the monomer complexes under photothermal conditions. Lastly, the template molecules are removed from the cross-linked matrix to create binding sites that specifically recognize the template molecule in the presence of other molecules in standard or unknown solutions (Su et al., 2020). In addition, Mansoori et al. (2020) also mentioned that various recent studies fabricated cost-effective and biodegradable membranes with a specific target of pollutants by combining natural polymer materials, including nanocellulose, with the ion/molecular imprinting technology.

2.5.3 Mixed Matrix Membrane

A mixed matrix membrane (MMM) or hybrid membrane is a polymer-based membrane comprising a discrete organic phase, a continuous polymer phase, and organic-inorganic interphase (G. Yang et al., 2020). Yang et al. (2020) also mentioned that the inorganic phase is typically in the form of micro- and nano-sized materials known as fillers or additives. The studies in the development of MMMs are increasing because MMMs combine the advantages of polymers and inorganic fillers in one membrane (Chakrabarty et al., 2022). On top of that, the MMM also has high efficiency and is generally prepared by dispersing porous fillers like metal-organic frameworks (MOFs), carbon nanotubes, silica, and zeolites inside the polymer matrices (Asif et al., 2023). Hence, the selectivity and permeability of MMMs can be improved by choosing a suitable polymer material and a

complementary filler that can improve the interfacial compatibility and dispersion between the polymer and fillers (Asif et al., 2023).

2.5.4 Nanofibrous Membrane

The membranes fabricated using the conventional phase inversion techniques have some drawbacks, including limited permeance, the tendency for fouling, varying pore size and pore size distribution, and poor mechanical strength (Subrahmanya et al., 2021). Hence, nanofibrous membranes are synthesized by using the electrospinning method is an improved method compared to conventional methods as it has higher interconnected porosity, adjustable thickness, and pore size distribution from a few nanometres to several microns, and high surface area for adjusting the surface chemistry (Subrahmanya et al., 2021). Moreover, polysaccharide nanofibers, especially electrospun from cellulose and its derivatives, are thoroughly researched because of their biocompatibility, potential functional ability, natural abundance, non-toxicity, and hydrophilicity (Mansoori et al., 2020).

2.5.5 Thin Film Composite Membrane

Thin film composite (TFC) membranes with improved selectivity and productivity are considered the most effective for water purification out of all the currently available membranes (Mansoori et al., 2020). The primary characteristic of the TFC membrane is the production of an extremely thin active layer that is less than 0.2 μm on a porous substrate (Mansoori et al., 2020). Mansoori et al. (2020) also mentioned that a fully organic TFC membrane could be fabricated using cellulose and its derivatives as the support or active layer in conjunction with another polymer. The production of organic-inorganic hybrid thin-film composite membranes has also been the subject of numerous studies (Mansoori et al., 2020). In producing a hybrid membrane, cellulose can serve as a coating layer on top of a

ceramic substrate, and metallic nanoparticles on a nanoscale can be added to enhance the performance of the thin-film composite membrane.

2.6 Methods of Nanocomposite Membranes Development

Five types of methods can be used to fabricate the nanocellulose-based membrane. Each method has its advantages and disadvantages according to the desired membrane application. Therefore, each method of membrane development is discussed in the following subtopics.

2.6.1 Electrospinning

According to Toriello et al. (2020), electrospinning is a simple method to fabricate ultrafine fibers with narrow and long diameters. Based on Kumar et al. (2019), the components of the electrospinning apparatus include a syringe or capillary tube that acts as a container to hold the polymer solution, a metallic needle known as a spinneret, which is used to get the solution, a high-voltage power source ranging from 10 to 60 kV, and a grounded collector used to collect the nanofibers. According to Shirazi et al. (2020), a polymer must be dissolved in a particular solvent to create a dope solution until it is fully dissolved and degassed, which means it is ready for electrospinning. Subsequently, the dope solution is then injected into the needle to produce nanofibers (Shirazi et al., 2020). Shirazi et al. (2020) also mentioned that a high-voltage source must be used to quicken the jet of the polymer-solvent solution toward the collector. Other than that, Shirazi et al. (2020) also emphasized that the electrical conductivity of the dope solution needs to be high enough to improve the capability of the electrospinning of the dope solution.

Nonetheless, as several polymers emit undesirable conductivity, it is crucial to incorporate appropriate additives (usually salts) into the polymer solution to increase the

conductivity of the polymer (Shirazi et al., 2020). Electrospinning is a process that is well-established where it enables the production of membranes that has open yet continuously interconnected pore structure which exhibits properties like high effective porosity, low basis weight, and large effective surface area (Han et al., 2019). In addition, electrospun nanocellulose shows a significant number of isotropic pores, which are evenly distributed among them because of the random arrangement (Jaffar et al., 2022). Hence, these properties ensure that the nanocellulose-based membranes fabricated by the electrospinning method can be applied to various applications (Zhang et al., 2021).

2.6.2 Freeze Drying

The freeze-drying method uses a freeze dryer, and casting polymeric solution on a flat casting surface creates a film (Jaffar et al., 2022). Subsequently, the casted film is submerged in iced water to fabricate the membrane sheet (Jaffar et al., 2022). In the freeze-drying process, water is sublimated directly from the solid state (ice) to the vapor state, omitting the liquid state and subsequently desorbing from the "dry" layer (Nowak & Jakubczyk, 2020). Flamm (2019) mentions that the freeze-drying system comprises several essential components, including a drying chamber with shelves, a condenser container with a heat exchanger and condenser, an intermediate valve, a refrigeration system, and a vacuum system. The refrigeration system provides the low temperatures required for the shelves and the condenser (Flamm, 2019). Flamm (2019) also explains that the condenser collects the water vapor produced during the sublimation process, where it freezes on the condenser's refrigeration coils. Next, Flamm further explains that the sublimation process occurs due to the vacuum system, which supplies the required negative pressure of the drying chamber for the process. Lastly, the intermediate valve between the condenser and drying chamber is used to be opened during the drying process to enable the release of water vapor and closed

during the freezing process (Flamm, 2019). The freeze-drying method can produce a porous membrane with a honeycomb-like structure, but the downside of this method is it has a relatively low surface area (Nissilä et al., 2021). It is due to the aggregation of the nanocellulose during the formation of the honeycomb structure, and consequently, this will reduce the advantages of the nanocellulose reinforcement in the membrane (Nissilä et al., 2021). The issue can be solved by producing threadlike nanocellulose to decrease the fiber content, resulting in mat-like and partly related material oriented along the freezing direction (Nissilä et al., 2021).

2.6.3 Interfacial Polymerization

Interfacial polymerization is one of the membrane fabrication methods involving two monomers, usually consisting of amine and acyl chloride. The monomers are dissolved in two immiscible solvents (Zhang et al., 2019). The reaction of the two monomers at the interface of a polymer substrate forms an active layer: the membrane with a thickness of around 1-2 μm (Zhang et al., 2019). In addition, the morphological properties of the membrane can be manipulated by changing the type of solvents, monomer, and reaction time (Zhang et al., 2019). Based on Jaffar et al. (2022a), an ultrathin layer film is produced due to the direct contact between the monomers and the rapid polymerization process.

On top of that, the chemical kinetics of the diffusion of monomers through the film can control the polymerization reaction, where the reaction will slow down when the monomers in two solutions separate (Jaffar et al., 2022). The initial interfacial polymerization process starts with soaking polymeric support in an aqueous phase for a few minutes (Mbakop et al., 2021). Subsequently, the process is continued by introducing the organic phase to the membrane to initiate the reaction (Mbakop et al., 2021). This particular

method of membrane fabrication applies to two types of membrane mechanisms which are nanofiltration and reverse osmosis (Jaffar et al., 2022 & Mbakop et al., 2021).

2.6.4 Phase Inversion

According to Gohil and Choudhury (2019), phase inversion is a versatile fabrication method of hollow fiber/flat sheet membrane fabrication, which can be used for ultrafiltration or microfiltration mixed matrix membranes. The mechanism used by this technique is converting a homogenous solution to a solid-state material either through hydration, evaporation, or thermal conversion (Jaffar et al., 2022). There are several methods to achieve phase inversion, but as mentioned by Mbakop et al. (2021), wet phase inversion is the most widely used method in nanocellulose-based membrane production. Firstly, a solvent and polymer are mixed with nanocellulose to produce a casting solution (Jaffar et al., 2022). Subsequently, the casting solution is poured onto the base membrane with the desired thickness of the membranes on the petri dish, followed by immersion in the coagulation bath (Mbakop et al., 2021). Mbakop et al. (2021) further explained that, if possible, the membrane's surface morphology and pore size could be manipulated using solvents with different boiling points and a porous substrate. One of the issues associated with the phase inversion method includes the agglomeration of nanomaterials which is more likely to occur when added to the dope solution for the phase inversion (Gohil & Choudhury, 2019). However, this agglomeration issue can be reduced by chemically modifying the nanomaterials or adding a dispersion agent so that the nanomaterials can obtain a better dispersion (Gohil & Choudhury, 2019). Hence, a suitable solvent and polymer must be selected to solve this issue.

In order to fabricate PVDF-based nanocomposite membranes, the phase inversion technique was utilized for this study because it provides efficient control over pore structure

and nanomaterial dispersion, both of which are essential for achieving high permeance and dye rejection performance (Huo et al., 2023).

2.6.5 Vacuum Filtration

Vacuum filtration is the simplest and most practical technique for producing cellulose composite membranes with layered structures, often known as the "nano paper approach" (Jaffar et al., 2022). This membrane type is usually applied in ultrafiltration applications and fabricates layered structures of NCs-based membranes and nano papers at laboratory and industrial scales (Jaffar et al., 2022; Mbakop et al., 2021). During the final stage of the membrane fabrication, the nanocellulose is densely packed into the membrane/film with a network of pores with varied nano-sized dimensions ranging from 3 to 5 nm (Mbakop et al., 2021). Jaffar et al. added that a thinner film layer is used for separation in the composite membrane, which has significantly reduced mass transfer resistance and increased membrane flux. In addition, different dosages of nanocellulose suspension can be used to customize the morphology and porosity of the membranes according to the desired applications (Mbakop et al., 2021).

Nevertheless, it must be highlighted that the diameter and length of nanocellulose used in membrane production play an important role as it affects the pore size distribution of the membrane (Z. Dai et al., 2019). Furthermore, leaching during filtration or backwashing operations is a persistent issue associated with the vacuum filtration method, as it involves the mechanical infusion of nanomaterials within the polymeric matrix (Mbakop et al., 2021). However, direct vacuum filtration is ideal for various industrial applications due to its advantages, including ultrahigh flux and low film resistance compared to typical commercial ultrafiltration membranes (Jaffar et al., 2022).

2.7 Mechanism of Nanocomposite Membranes

Based on Figure 2.1, six types of membrane mechanisms can be applied in nanocellulose-based membranes: membrane distillation, microfiltration, nanofiltration, pervaporation, reverse osmosis, and ultrafiltration (Sadare et al., 2022; Saud et al., 2022). All membrane mechanisms are pressure-driven, whereas only membrane distillation is thermally driven. Each type of mechanism will be further explained in each subsection.

The performance trends in the GR/NC, GR/TiO_2, and NC/GR/TiO_2 PVDF membranes developed in this study can be evaluated theoretically using these mechanisms, especially regarding permeability, dye rejection, antifouling performance, and reusability.

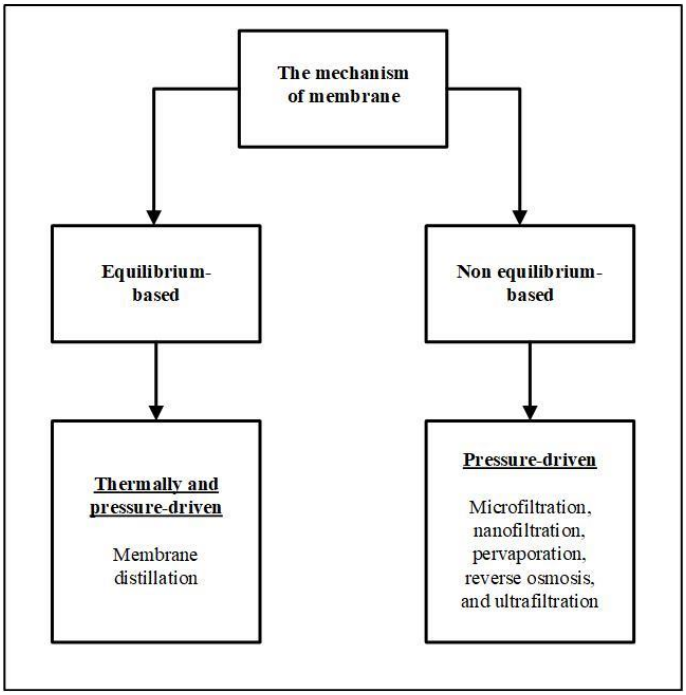

Figure 2.1: The types of membrane mechanisms.

2.7.1 Membrane Distillation

Membrane distillation is one of the processes that has emerged and gained recognition in the current years. It is a non-isothermal membrane-based process that only

allows vapor molecules to pass through the membrane (Kalla, 2021). Kalla (2021) states that the membrane plays a significant role in the membrane distillation process as it has a hydrophobic surface. In addition, the membrane also acts as a barrier for the liquid feed and functions as a porous medium for vapor transport (Kalla, 2021). On top of that, the membrane distillation process is essentially driven by the vapor pressure difference between the permeate and feed (Seraj et al., 2022). For further explanation, the vapor pressure difference is caused by the temperature difference between the permeate and the feed, where the feed is the hot stream, and the permeate is the cold stream (Kalla, 2021; Sadare et al., 2022). Sadare et al. (2022) also mention that only the volatile liquid feed can pass through the membrane pores ranging from 0.1 to 0.5 μm in size and evaporate, not the liquid solution that is distilled. According to Saud et al. (2022), the separation efficiency of the membrane is greatly influenced by the structure of the porous membrane and the volatility of the separating component. The mechanism of the membrane is depicted in Figure 2.2, where the hydrophobic porous membrane allows the movement of vapor from the hot stream to the cold stream.

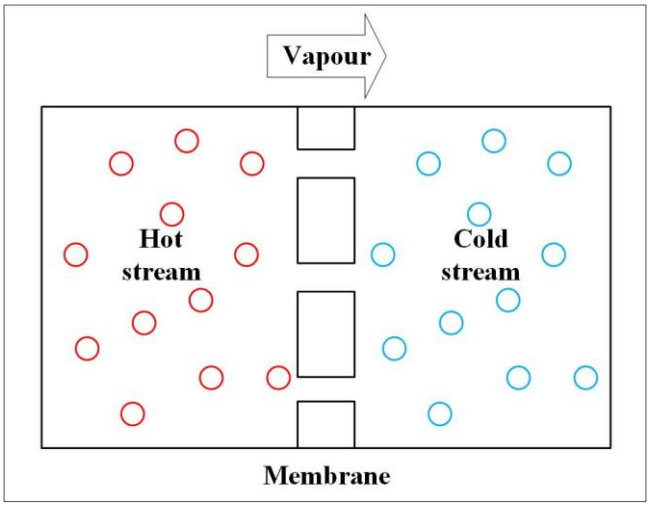

Figure 2.2: The membrane mechanism for membrane distillation.

2.7.2 Pervaporation

As illustrated in Figure 2.3, pervaporation is a type of membrane mechanism where the upper stream of the membrane is in contact with the feed liquid, and a vacuum is utilized in the bottom stream of the membrane (Ismail & Matsuura, 2022). According to Kumar Purkait et al. (2020), pervaporation is an efficient membrane-based separation mechanism that involves the transport of solutes through membranes composed of dense materials. As the fundamental key of mass transport includes the interaction between the membrane and the compound, the major factors that affect the performance of the membrane include the composition and nature of the membrane materials (Purkait et al., 2020). To increase the compound removal efficiency, the permeating components' partial pressure is almost zero (Purkait et al., 2020). On the other hand, it is also mentioned that the liquid mixture is preheated before it is used as a feed stream to achieve higher partial pressure so that the transport rate can be increased.

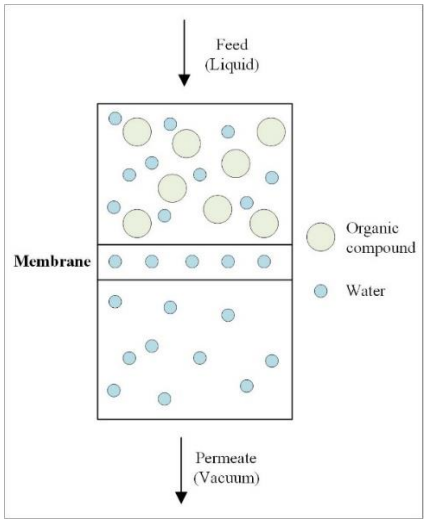

Figure 2.3: The membrane mechanism for pervaporation.

2.7.3 Pressure-driven Membrane Mechanism

According to Ezugbe and Rathilal (2020), pressure-driven membrane mechanisms are one of the most extensively used membranes that depend on hydraulic pressure to achieve separation. The pressure-driven membrane consists of four major mechanisms: microfiltration, ultrafiltration, nanofiltration, and reverse osmosis. The difference between these mechanisms is their pore sizes and pressure requirements. Figure 2.4 illustrates the four types of pressure-driven membrane mechanisms along with the different types of particles.

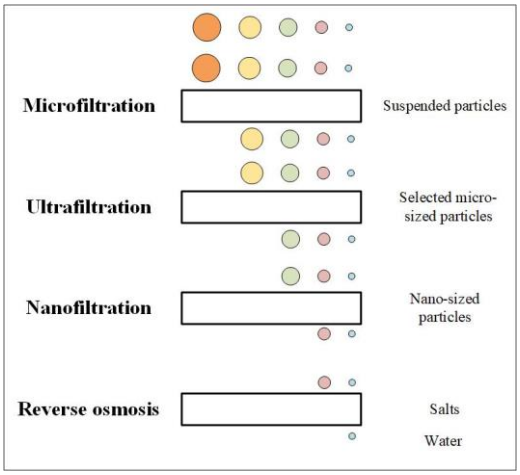

Figure 2.4: Membrane mechanism for pressure-driven membranes.

2.7.3.1 Microfiltration

Microfiltration is one of the oldest membrane mechanisms, which is pressure-driven and used commercially. According to Ray et al. (2020), microfiltration is a mechanism in which the membrane eliminates particles with an average molecular weight of more than 400 kDa. The membranes used for this mechanism have pore sizes ranging from 0.05 μm to 10 μm under the operating pressure of less than 2 bar (Ray et al., 2020). In addition, microfiltration membranes use the principle of physical separation, which can remove micrometer-sized particles, for example, suspended particles, large bacteria, major pathogens, proteins, and yeast cells (Anis et al., 2019). Anis et al. (2019) also mention that microfiltration membranes are flexible since they can remove large-scale pollutants. When the molecular weight of the solute exceeds 500 g/mol, the membrane mechanism will change from solution-diffusion (in reverse osmosis) to molecular filtration, where the membrane pore diameter and particle size determines the separation features (Anis et al., 2019). Based on Sadare et al. (2022), particles with sizes larger than 0.1 μm are typically separated by an open membrane structure. The low hydrodynamic resistance results in the membranes requiring low hydrostatic pressure to ensure a high solvent flux and pollutant rejection

(Sadare et al., 2022). Hence, microfiltration membranes are attractive as they have various pore sizes and low-pressure requirements, resulting in various applications.

2.7.3.2 Ultrafiltration

An ultrafiltration membrane is a specialized membrane separation mechanism that is pressure-driven and can effectively remove pathogens and solid waste from a waste mixture (S. Hussain et al., 2019). It is also mentioned that the final product from ultrafiltration membrane separation is highly pure and contains no pathogenic waste. Ultrafiltration membranes are semi-permeable membranes with pore sizes ranging from 0.005 μm to 0.1 μm, where the membrane acts as a separation barrier between two sides of a pressure difference which are low and high (Giakoumis et al., 2020). This pressure difference is the driving force for separating the solutes, smaller than the membrane's pore size, where the solutes pass through the membrane through a high to low-pressure environment. The ultrafiltration membrane can remove various pollutants or compounds, such as bacteria, colloidal silica, chlorine-resistant pathogens, enzymes, gelatines, iron, manganese, and viruses (Giakoumis et al., 2020). The membrane mechanism for ultrafiltration also separates the molecules with a higher molecular weight and suspended solids, known as molecular weight cut-off by the specialized membrane (Sadare et al., 2022). It also applies to other factors in the ultrafiltration membrane, such as charge, hydrodynamic conditions, and molecular shape.

2.7.3.2 Nanofiltration

The nanofiltration membrane mechanism is a pressure-driven mechanism that falls between the ultrafiltration and reverses osmosis membrane mechanisms. The pore size for nanofiltration membranes ranges from 0.2 nm to 2 nm, whereas the membrane's molecular weight cut-off ranges from 0.2 to 1 kDa. The surface of the nanofiltration membrane is

typically negatively charged to improve the efficiency of dissolved ions removal. Compared to microfiltration and ultrafiltration membranes, nanofiltration membranes perform better when they require lower capital cost, energy consumption, and higher permeability. Nanofiltration has various applications in various industries, such as water desalination, the pharmaceutical industry, and wastewater treatment. Nanofiltration membranes have an average salt rejection that ranges from 10%-90% but cannot achieve a higher salt rejection as reverse osmosis is 99.5%. In addition, when the nanofiltration membranes are in contact with an aqueous solution with varied pH values will result in a surface charge that can repel ionic compounds.

2.7.3.3 Reverse Osmosis

Reverse osmosis membranes are crucial in wastewater treatment as it is used to remove efficiently remove salts and other contaminants (Odabaşi et al., 2021). Reverse osmosis is a pressure-driven membrane mechanism that uses a semi-permeable membrane with pore sizes ranging from 0.5 to 1.5 nm, allowing smaller molecules to pass through (Qasem et al., 2021). The mechanism reverses the normal osmosis process by applying a pressure of 20 to 70 bar, which is higher than the osmotic pressure of the feed solution (Qasem et al., 2021). Qasem et al. (2021) also mention that reverse osmosis membranes can remove particles with a molecular size ranging from 0.25 nm to 3 nm and remove 95 to 99% of charged organic and inorganic salts. Additionally, reverse osmosis membranes can eliminate hazardous chemicals, ions, and micro and macro particles from polluted water (Saud et al., 2022). Since the reverse osmosis membranes are semi-permeable, the salt ions cannot flow back into the feed stream, ensuring the desalination process's efficiency (Saud et al., 2022).

2.8 Comparison of Nanocomposite Membranes with Conventional Membranes

As seen in the table below, there are various advantages and disadvantages of nanocellulose-based and conventional membranes like ceramic/metal-based membranes. Since nanocellulose-based membrane poses more advantages than conventional membranes, it can be deduced that nanocellulose-based membrane is more desirable for achieving wastewater treatment applications of the membrane.

Table 2.4: The advantages and disadvantages of nanocellulose-based membrane and ceramic/metal-based membrane.

Type of membrane	Advantages	Disadvantages	References
Nanocellulose-based membrane	• Cost-effective • Easy end-use disposal • Easy operation • Easy to scale up • Easy to stack • Excellent selectivity • Faster kinetics • Good permeability • High adsorption efficiency • High chemical stability • High efficiency in wastewater treatment • High flexibility • High selectivity based on particle size	• Tendency to membrane fouling • Typically, it has a shorter lifespan • Unable to withstand high temperature • Weak chemical resistance	(Gopakumar et al., 2019; Y. Liu, Liu, et al., 2021; Mansoori et al., 2020; Reshmy et al., 2021; Tan et al., 2020)

Table 2.4 continued

	• Higher capacity for adsorption • Less energy consumption • Lightweight • Low density • Low operating temperature • Non-toxic and environmentally friendly raw materials • Recyclable and reusable • Simple manufacturing process • Strong mechanical properties • Sustainable		
Ceramic/metal-based membrane	• High pressure • High thermal stability • Long life • Strong chemical resistance	• Brittle • High energy consumption • High investment cost • Inconvenient production process • Inflexible • Less selectivity depending on pore size	(Gopakumar et al., 2019; Liu, Liu, et al., 2021; Reshmy et al., 2021)

Table 2.4 continued

		• Low degradability • Unsustainable disposable • Unsustainable manufacturing	

Next, Table 2.5 shows a comparative overview of the nanocomposites membrane compared to conventional membrane systems which are commonly used in wastewater treatment applications. The comparison focuses on the dominant transport mechanisms and the fouling-resistance characteristics, along with the dye separation efficiency where this highlights the conceptual differences between different types of membranes.

Table 2.5: The comparative overview of membrane mechanisms' advantages and disadvantages.

Type of membrane	Dominant Transport/Fouling-Resistance Mechanism	Advantages	Disadvantages	References
PVDF/GR/NC/TiO_2 nanocomposite membrane (this study)	Pore-flow transport, reduced foulant adhesion for antifouling; increased hydrophilicity from NC and TiO_2 and improved pore connectivity from graphene	High dye rejection, improved antifouling and tunable pore structure	Risk of nanomaterial aggregation at high loadings	-

Table 2.5 continued

Commercial PVDF UF membrane	Pore-flow transport, hydrophobic polymer matrix	Established technology, scalable and cost-effective	Lower hydrophilicity and higher fouling tendency	(Kannathasan et al., 2025; Maiti et al., 2025; Ren et al., 2023)
Ceramic UF (Al_2O_3, TiO_2-based)	Pore-flow transport, intrinsically hydrophilic surface	High chemical and thermal stability, and good fouling resistance	High cost and brittle structure	(Brinkmann & Filiz, 2021; Liangdy, 2024; Y. Sun, 2025; Сергієнко et al., 2020)
Commercial NF/RO (polyamide thin film) membrane	Solution-diffusion mechanism	High selectivity	Susceptible to fouling and oxidant sensitivity	(Geng et al., 2024; Lim et al., 2025; Shin et al., 2024; P. Wang et al., 2025)

2.9 Issues in Nanocellulose-Based Membrane Production

2.9.1 Complex Production Process

One of the issues associated with nitrocellulose-based membrane production is the production process which can be quite challenging. As Lasrado et al. (2020) mentioned, it is challenging to develop cost-effective, time-intensive technologies for nanocellulose extractions and fabrication of membranes as most membranes are time-consuming and require high capital costs. This information is also supported by Shen et al. (2022), which state that nanocellulose has higher costs than biofuels, which are not economically friendly.

In addition, Salama et al. (2021) also added that controlling the primary factors of the nanocellulose-based membrane, including specific adsorption, porosity, and permeability, remains a major issue in recent studies. On top of that, nanocellulose-based membranes also require specialized equipment, such as a high-pressure homogenizer, which is expensive and difficult to operate (Y. S. Jiang et al., 2021). As a result, this will limit the scalability of nanocellulose-based membrane production as it requires a complex and costly production process. Lastly, the production process of nanocellulose-based membranes is also greatly influenced by factors such as pH value and temperature to achieve the desired membrane properties, which can also be time-consuming (Pervez et al., 2022).

2.9.2 The High Tendency of Agglomeration

Clustering, most commonly known as agglomeration, is one of the major issues associated with nanocellulose-based membrane productions. Agglomeration is the production of compact films during the dehydration process due to the extensive hydrogen bonding between hydroxyl groups (Jaffar et al., 2022). This agglomeration issue, also known as hornification, reduces the desired characteristics like mechanical strength and the membrane's functionality, resulting in low-flux membranes, particularly for the filtration of small-sized or high-molecular-weight materials (Jaffar et al., 2022). It is because nanocellulose tends to agglomerate, particularly at high loading, which results in non-uniform stress distribution in the membranes (Zaki et al., 2022). Hence, this agglomeration causes the interaction between the nanocellulose loading and the membrane matrix to be reduced, which leads to a decrease in tensile strength after higher loading (Zaki et al., 2022). Jaffar et al. (2022) suggested that surfactant usage, surface modifications, and CO_2 drying can reduce the impact of aggregation. Other than that, the nanocellulose can also be deposited on the surface of the membrane as a thin functional layer (Jaffar et al., 2022).

2.9.3 Homogeneity of Nanocellulose Mixture

Another issue associated with nanocellulose-based membranes includes the difficulty of obtaining a homogeneous mixture of cellulose and inorganic nano adsorbents, which will negatively impact structure, characteristics, and performance (Jaffar et al., 2022). A homogenous mixture of nanocellulose-based membranes consists of two phases. One is a polymer-rich phase, a membrane with an asymmetric structure. The other is a nano cellulose-rich phase with excellent properties (N. Pal & Agarwal, 2021). If a homogenous mixture is not achieved when fabricating a nanocellulose-based membrane, it will negatively impact the membranes' structure, properties and performance (N. Pal & Agarwal, 2021). Hence, it is important to ensure that the mixture of the nanocellulose and the membrane achieves a homogenous mixture to ensure that the nanocellulose-based membrane achieves the desired performance for particular applications.

2.10 Applications of Nanocellulose-Based Membrane in Dye Wastewater Treatment

The textile industry is known to frequently discharge extremely contaminated acidic, alkaline, and coloured effluent, which includes chromium, zinc, chlorine, copper, and alkaline chemicals, which are harmful substances (Parvin et al., 2020). These effluents released to water sources result in severe water pollution, which causes numerous adverse effects on public health and the environment (Parvin et al., 2020). According to Jankowska et al. (2022), prolonged exposure to dye may result in skin irritations and breathing difficulties. In addition, numerous dyes are carcinogenic and mutagenic, increasing the risk of skin cancer. Based on Hussain et al. (2019), the inert nature of dyes and also their complex or large sizes causes the dyes to be more difficult to treat as it is non-biodegradable, thermally stable and resistant towards light and oxidizing agents. These dyes possess a complex aromatic structure which may exhibit anionic, cationic, or non-ionic properties (S.

Hussain et al., 2019). If pollutants in textile effluent are removed without adequate treatment, they might deplete dissolved oxygen in receiving bodies, threatening aquatic life and the ecosystem (Parvin et al., 2020). Therefore, dye removal is crucial in wastewater treatment which is one of the applications of nanocellulose-based membranes. The studies of the membrane efficiency in removing dyes are discussed below.

Nanocellulose-based membranes are known to be very effective in the adsorption of dyes from wastewater. The research by Gopakumar et al. (2019) discusses the potential of nanocellulose-based membranes for dye removal in wastewater treatment. Their research found that nanocellulose-based membranes had a higher permeation flux and rejection of contaminants than conventional membranes. It shows that nanocellulose-based membranes are a viable option for water purification applications. Besides that, the study by Vivod et al. (2018) also mentions that nanocellulose-based adsorbent can effectively remove loose reactive dye during textile laundering. Based on the study, it is also mentioned that when nanocellulose-based adsorbents are applied to a textile industry, they become film-like and efficiently absorb the loose reactive dye from the washing solution, according to the study. The study showed that adsorbent films could retain their properties even after numerous laundering cycles, suggesting that their application in textiles for dye removal could be a cost-effective and eco-friendly solution. In addition, the study discovered that the adsorbent films could remove other pollutants from the washing solution, making them an attractive choice for minimizing the environmental issues caused by wastewater. In addition, the adsorbent films may be modified to the particular requirements of the textile, allowing for further customization. Consequently, the nanocellulose-based adsorbent is cost-effective for removing loose reactive dye from textiles during laundering.

Next, Vilela et al. (2019) investigated the applications of zwitterionic nanocellulose-based membranes for removing Congo red, a commonly used organic dye in the textile industry. Vilela et al. (2019) tested the membranes with various parameters such as pH, ionic strength, and dye concentrations. The study discovered that zwitterionic nanocellulose membranes exhibited significant adsorption capabilities and an efficient dye removal rate. It was attributed to the presence of zwitterionic functional groups, which established a strong electrostatic interaction with the dye molecules resulting in a better adsorption rate. Moreover, the study concluded that the future uses of the membrane for dye removal are promising and recommended further study in this field. Hence, the outcomes of this study show the ability of the zwitterionic nanocellulose-based membranes to remove organic dyes from aqueous solutions.

Lastly, W. Zhang et al. (2020) fabricated a nanocellulose-based aerogel decorated with silver nanoparticles that can retain its structure for organic dyes' rapid, continuous catalytic discoloration. The study shows that nanocellulose-based aerogels can rapidly decolorize organic dyes due to their high specific surface area and large pore volume. Additionally, including silver nanoparticles in the aerogel improves the decolorization of organic dye catalytic activity. It means the modified aerogels are more effective in removing organic dyes than the unmodified aerogels. Furthermore, the shape-retaining property of the aerogels allows them to be reused several times without degrading their performance. It is advantageous for organic dyes' long-term and continuous decolorization, making aerogels a desirable alternative for industrial applications. Therefore, the durable, shape-retaining nanocellulose-based aerogels decorated with silver nanoparticles provide an efficient and sustainable approach for organic dyes' rapid, continuous catalytic discoloration.

CHAPTER 3

RESEARCH METHODOLOGY

3.1 Overview

This chapter discusses the methods that are used to synthesize NC from raw bamboo fibre and the fabrication of three different types of PVDF nanocomposite membranes along with pristine PVDF membrane via the phase inversion technique. The characterization methods and membrane performance evaluation are also discussed in this chapter.

3.2 Materials

Toluene (molecular weight: 92.14 g/mol, purity: 99.8%), ethanol (molecular weight: 46.07 g/mol, purity: ≥ 99.5%), 99.8 wt% acetic acid (molecular weight: 60.05 g/mol, purity: ≥ 99.7%), 35 wt% hydrogen peroxide (molecular weight: 34.01 g/mol, purity: 3%), titanium dioxide (molecular weight: 79.87 g/mol, purity ≥ 99.5%), and sodium hydroxide (molecular weight: 40 g/mol, purity: ≥ 98%). Graphene nanoplatelets (molecular weight: 12.01 g/mol), PVDF (molecular weight: 530,000 g/mol) and NMP (molecular weight: 99.13 g/mol, purity: ≥ 99.0%). Deionized water and distilled water were provided by Universiti Malaysia Sarawak Analytical Lab. Borneo bamboo (*Gigantochloa scortechinii*) culms were collected from Sarawak, Malaysia.

3.3 Synthesis of Nanocellulose

Nanocellulose was synthesized from Borneo Bamboo (*Gigantochloa scorthechinii*) following the procedure described in (James, Rezaur Rahman, et al., 2024) with minor modification. Briefly, the extraction of nanocellulose from bamboo followed three sequential steps viz. dewaxing, delignification, and mercerisation. In the dewaxing process,

400 mL of toluene and 200 mL of ethanol were transferred into a 1000mL round conical flask to treat 10 g of raw bamboo fibre. The resulting solution was placed into a cellulose thimble and dewaxed for 2 hours at 250°C using Soxhlet extractor to eliminate any pigments, waxes, and oil. Then, the dewaxed bamboo fibres (DWBF) were then dried at 70°C overnight. In the delignification step, DWBF was acidified at 130°C for 2 hours by using 106.2 g of acetic acid and 82.3 g of hydrogen peroxide in the presence of TiO_2 catalyst. The delignified bamboo fibre (DLBF) was then neutralize to pH 7 using deionized water before drying at 70°C. In the final mercerization stage, sodium hydroxide was employed to remove pectin and hemicellulose from the DLBF. This procedure was conducted in an autoshaker at 150 rpm and 80°C for a duration of 2 hours. Following this, the sample was stirred continuously for an additional 8 hours to yield cellulose with enhanced purity and minimal residual starch or impurities. The resultant sample was then filtered, neutralized to a pH of 7 using deionized water, and dried overnight at 30°C for subsequent characterization.

3.4 Preparation of Nanocomposite Membranes

85 g of NMP was measured and poured into a beaker. Then, the nanoparticles which are GR/NC, GR/TiO_2, and NC/GR/TiO_2 with the ratio according to Table 3.1, 3.2, and 3.3 respectively was poured into the laboratory glass bottle which contains the NMP solution. This ratio is 1 wt% relative to the weight of PVDF which is optimum for membrane performance without causing agglomeration (Boruah et al., 2023; Safarpour et al., 2022). For Table 3.1, the ratio is selected to study the membrane performance with higher amounts of GR or NC with intervals of 10%. For Table 3.2, the ratio is up until 60% of TiO_2 as excess amounts of TiO_2 can cause agglomeration. Lastly, Table 3.3 is based on the best ratio of Table 3.1 and 3.2. The solution was then stirred at 250 rpm for 1 hour with the temperature of 80°C. Subsequently, the nanocomposite solution was transferred into laboratory glass

bottle and ultrasonicated for 2 hours. Then, 15 g of PVDF was added into the glass bottle and the solution was continuously stirred at 80°C and 250 rpm for 24 hours. Then, the casting solution is continuously stirred at 60 °C during the casting process and the membrane thickness is controlled at 0.05 mm with a tape on the glass plate. The resulting solution was then transferred to a glass plate using casting rod to obtain nanocomposite membrane sheets followed by washing with ultra-pure water to remove residual solvents The nanocomposite membrane sheets were then cut into small circular pieces and soaked in ultra-pure water in a petri dish until required for nanocomposite membrane testing.

Table 3.1: The ratio of GR/NC nanocomposite solution.

Sample	GR:NC ratio	Mass of GR (g)	Mass of NC (g)
80% GR	80:20	0.120	0.030
70% GR	70:30	0.105	0.045
60% GR	60:40	0.090	0.060
50% GR	50:50	0.075	0.075
40% GR	40:60	0.060	0.090
30% GR	30:70	0.045	0.105
20% GR	20:80	0.030	0.120
100% PVDF (Pristine)	0:0	0	0

Table 3.2: The ratio of GR/TiO_2 nanocomposite solution.

Sample	GR:TiO_2 ratio	Mass of GR (g)	Mass of TiO_2 (g)
80% GR	80:20	0.120	0.030
70% GR	70:30	0.105	0.045
60% GR	60:40	0.090	0.060
50% GR	50:50	0.075	0.075

Table 3.2 continued

40% GR	40:60	0.060	0.090
100% PVDF (Pristine)	0:0	0	0

Table 3.3: The ratio of NC/GR/TiO_2 nanocomposite solution.

Sample	Mass of NC (g)	Mass of GR (g)	Mass of TiO_2 (g)
GR/NC/TiO_2	0.12	0.12	0.03
100% PVDF (Pristine)	0	0	0

3.5 Characterization

3.5.1 TEM Analysis

The transmission electron microscopy (TEM) analysis was conducted to determine the size and morphology of the nanocellulose that was synthesised in Section 3.3. 50 mL of ethanol was poured into a beaker and then, 0.025 g of NC was added into the same beaker. Subsequently, this solution was sonicated for 20 minutes, and approximately 1 mL of the solution was dropped onto the copper grid. The copper grid was then dried in the oven at 45°C overnight. The copper grid was then analysed by JEL JEM-1230 TEM with magnifications ×60,000, and ×120,000.

3.5.2 FESEM-EDX and SEM-EDX Analysis

The morphology of the nanocomposite membrane surface and cross sections were measured by using Jeol Field Emission Scanning Electron Microscopy machine for FESEM analysis and Hitachi Scanning Electron Microscopy for SEM analysis with a magnification of ×10,000 and ×20,000 for the surface and two magnifications which are ×1,000 and ×5,000 for the cross sections. The nanocomposite membrane surface was prepared by cutting a small

piece of the membrane sheet. The nanocomposite membrane cross section was prepared by freezing the nanocomposite membrane sheet in liquid nitrogen and immediately cutting the nanocomposite membrane to obtain the cross section. Then, the nanocomposite membrane was coated with gold to enhance samples imaging. In addition to the FESEM and SEM analysis, EDX was also conducted to determine the elemental compositions of the nanocomposite membranes.

3.5.3 FTIR Analysis

The functional groups of the nanocomposite membranes, and pristine membrane were determined using Shimadzu Fourier Transform Infrared Spectrophotometer (FTIR) equipped with attenuated total reflectance (ATR) with the spectral range of 4,000 cm^{-1} to 400 cm^{-1}.

3.5.4 XRD Analysis

The crystalline structure of the nanocomposite membranes and pristine membrane were measured on a Rigaku SmartLab Powder X-ray Diffractometer with Cu Kα (λ = 1.5418 Å) radiation in the 2θ range from 5° to 90° with the step size of 0.01° and scan speed of 2°/min.

3.5.5 Membrane Porosity and Mean Pore Size Measurement

The porosity of the nanocomposite membranes and pristine membrane were calculated using the gravimetric method which was based on the weight of water in the membrane pores. Employing the procedure of (Tavakolmoghadam et al., 2019).

$$\varepsilon = \frac{\left(\frac{W_{w,m} - W_{d,m}}{\rho_{water}}\right)}{\left(\frac{W_{w,m} - W_{d,m}}{\rho_{water}}\right) + \left(\frac{W_{d,m}}{\rho_{PVDF}}\right)} \times 100\% \qquad \text{Equation 3.1}$$

Where,

ε = Membrane porosity

$W_{w,m}$ = Weight of wet membrane

$W_{d,m}$ = Weight of dry membrane

ρ_{water} = Density of water (0.998 g/cm^3)

ρ_{PVDF} = Density of PVDF (1.740 g/cm^3)

The mean pore radius was determined using the Guerout-Elford-Ferry equation in the methodology of (K. Jang et al., 2022), while the mean pore size was determined by multiplying the mean pore radius by 2.

$$\text{Mean pore radius} = \sqrt{\frac{(2.9 - 1.75\varepsilon) \times 8\eta l Q}{\varepsilon \times A \times \Delta P}} \quad \text{Equation 3.2}$$

Where,

Ƞ = Viscosity of water (8.9 × 10^{-4} Pa.s)

l = Thickness of membranes (m)

Q = Volume of permeated water per time (m^3/s)

A = Effective area of membrane (m^2)

ΔP = Operational pressure (Pa)

3.5.6 Membrane Permeation Test

The membrane permeation test of the pristine and nanocomposite membranes consists of water flux test, methylene blue (MB) dye rejection test where the membrane system is depicted in Figure 3.1 and also the membrane reusability test. The feed was

pumped to the membrane system while the nanocomposite membranes were compacted with a backflow that was fed back to the feed, and then, the treated water flowed out as permeate. To determine the water flux, ultra-pure water was pumped to the membrane system with a pressure of 2 bar for 30 minutes for stabilisation of the membrane system. Then, the water flux test was conducted at a pressure of 1 bar for another 30 minutes and results were recorded at 10 minutes intervals. This procedure was repeated 5 times to get an accurate reading and the standard deviation of the results were calculated as well. Similarly, dye rejection test was conducted following same described method but using MB dye as the feed. Three concentrations of MB dye were used in the dye removal test which are 0.5 ppm, 1 ppm, and 1.5 ppm for GR/TiO_2 nanocomposite membranes while one concentration which is 0.5 ppm was used for NC/GR and NC/GR/TiO_2 nanocomposite membranes. As for the reusability test, the same membrane for each type of ratio including the pristine membrane was backwashed with ultra-pure water and then, tested with the dye rejection test for 3 cycles. Then, the concentration of feed and permeate were determined through Shimadzu UV-Vis Spectroscopy with the wavelength of 665 nm. Subsequently, the water flux and dye rejection ratio were obtained as described in Huang et al. (H. Huang et al., 2022) below:

$$J_{flux} = \frac{V}{A \times t \times \Delta P} \qquad \text{Equation 3.3}$$

$$RR = \left(1 - \frac{C_{permeate}}{C_{feed}}\right) \times 100\% \qquad \text{Equation 3.4}$$

Where,

J_{flux} = Water flux (L/m^2.h.bar)

V = Volume of permeate

A = Effective area of membrane (m^2)

t = Recorded time to collect permeate (h)

ΔP = Operational pressure (bar)

RR = Rejection ratio (%)

$C_{permeate}$ = Concentration of permeate (ppm)

C_{feed} = Concentration of feed/initial concentration (ppm)

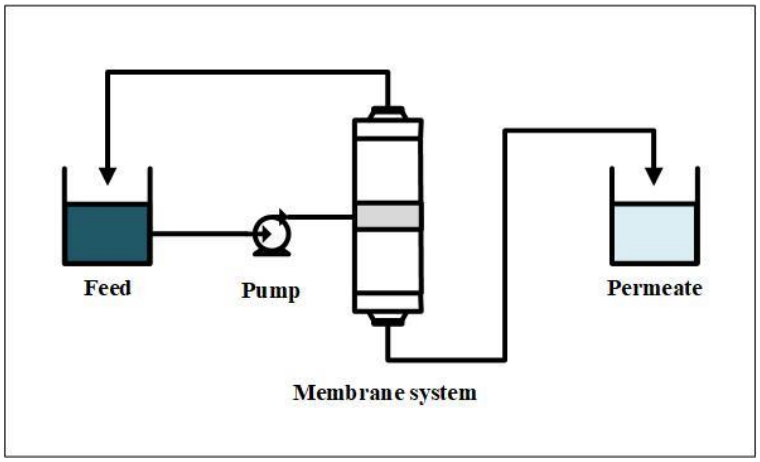

Figure 3.1: Schematic drawing of the membrane system.

3.5.7 Antifouling Performance Test

The antifouling performance of the pristine and nanocomposite membranes were determined by evaluating the flux recovery ratio (FRR), total fouling (R_t), reversible fouling (R_r), and irreversible fouling (R_{ir}) of the membranes. To evaluate the antifouling performance, the pristine and nanocomposite membranes were filtered with ultra-pure water for 60 minutes obtaining the pure water flux, J_{flux}. Subsequently, the feed was replaced with MB dye solution and the membranes filtered the solution for another 60 minutes and the flux of this filtered solution is recorded as $J_{permeate}$. Then, the membranes were soaked in ultra-pure water for 30 minutes for the recovery of the membranes. Lastly, the membrane system was fed with ultra-pure water and the membranes filtered the water for another 60 minutes

to obtain the water flux, $J_{flux,2}$. Based on the values of flux that were obtained, calculations for FRR, R_t, R_r, and R_{ir} of the membranes were calculated by using the equations obtained from Darwish et al. (2023) listed below:

$$FRR = \frac{J_{flux,2}}{J_{flux}} \times 100\% \quad \text{Equation 3.5}$$

$$R_t = R_r + R_{ir} \quad \text{Equation 3.6}$$

$$R_r = \left(\frac{J_{flux,2} - J_{permeate}}{J_{flux}}\right) \times 100\% \quad \text{Equation 3.7}$$

$$R_{ir} = \left(\frac{J_{flux} - J_{flux,2}}{J_{flux}}\right) \times 100\% \quad \text{Equation 3.8}$$

CHAPTER 4

RESULTS AND DISCUSSION

4.1 Overview

This chapter presents the experimental findings from the performance analysis and characterizations of the fabricated nanocomposite membranes. The analysis includes the morphological, structural, and functional assessments of the nanocomposite membranes incorporated with NC, GR, and TiO_2. The discussion focuses on the effects of the nanomaterials on the membrane properties such as water flux, dye rejection, antifouling performance, and reusability. The analysis is done by comparing the nanocomposite membranes with pristine PVDF membrane to analyse the improvements of the membranes.

4.2 EXPERIMENT 1: Graphene/Nanocellulose Polyvinylidene Fluoride (PVDF) Nanocomposite Membrane to Intensify Methylene Blue Dye Removal and Antifouling Performance

4.2.1 Introduction

In the first experiment, a nanocomposite membrane was developed by incorporating GR and NC into a PVDF matrix to enhance MB dye removal and antifouling performance. These nanomaterials are known for their superior properties such as hydrophilicity and structural properties which are expected to improve membrane porosity, dye rejection, and antifouling performance. The nanocomposite membranes were fabricated via phase inversion with different GR/NC compositions to evaluate the changes in membrane structure and performance. The characterization methods were also carried out by using FESEM-EDX, FTIR, XRD and UV-Vis while the membrane performance was assessed by water permeation tests like water flux, MB dye removal, and antifouling performance. This

experiment aims to determine the optimum NC/GR compositions that results in highest dye removal efficiency and overall membrane performance enhancement.

4.2.2 Methodology

Refer to Chapter 3, with Table 3.1 as the nanocomposite membrane composition.

4.2.3 Results and discussion

4.2.3.1 TEM Analysis of Nanocellulose

Figure 4.1 shows the TEM analysis that have been conducted to identify the morphology of nanocellulose. Based on the TEM analysis shown in Figure 4.1 (a) and (b), the nanocellulose particle displayed a spherical morphology after undergoing chemical treatment and repeated ball milling cycles. This observation aligns with previous research, which has similarly reported a transformation of nanocellulose particles from a rod-like fibre morphology to a spherical shape after hydrolysis (El-hadi, 2017; Holilah et al., 2022). In addition, similar structures were also observed by Verma et al., (2024) with 85.6nm approximate diameter. The spherical morphology suggests that the treatment processes were effective, likely reducing the aspect ratio of the particles and leading to the shape change. In addition, this morphology is also highly influenced by the composition ratio and loading in the nanocellulose synthesis. However, the influence of morphology changes on crystallinity and thermal stability is discussed in later sections of this study where XRD results are presented, with reference to previously reported trends in the literature (Dias et al., 2023).

Figure 4.1 (a) shows significant irregular agglomeration of nanocellulose particles, with particles clumped together in certain regions. This agglomeration of particles can be attributed to the strong hydrogen bonds between particle crystallites, which could have resulted to clustered formations. While hydrogen bonding between NC crystallites is a primary driver of agglomeration (El-hadi, 2017), fabrication parameters such as sonication

time, and type of solvent can also influence dispersion (James, Rezaur Rahman, et al., 2024; Sharifalhoseini et al., 2018). Additionally, large agglomerates are reported to impede the convective flux through the membrane material (van den Berg & Ulbricht, 2020). Hence, alternative methods such as electrospinning or surface functionalization of GR could significantly enhance uniform particle distribution within the membrane.

Furthermore, Figure 4.1 (b) indicates that nanocellulose particles contain nanopores, which possibly act as potential active sites for MB dye adsorption applications. The presence of these pores improves the surface area of the material, which is important in applications that require a high MB dye adsorption capacity. This finding aligns with results from studies that suggest increased porosity contributes to enhanced filtration efficiency and permeability.

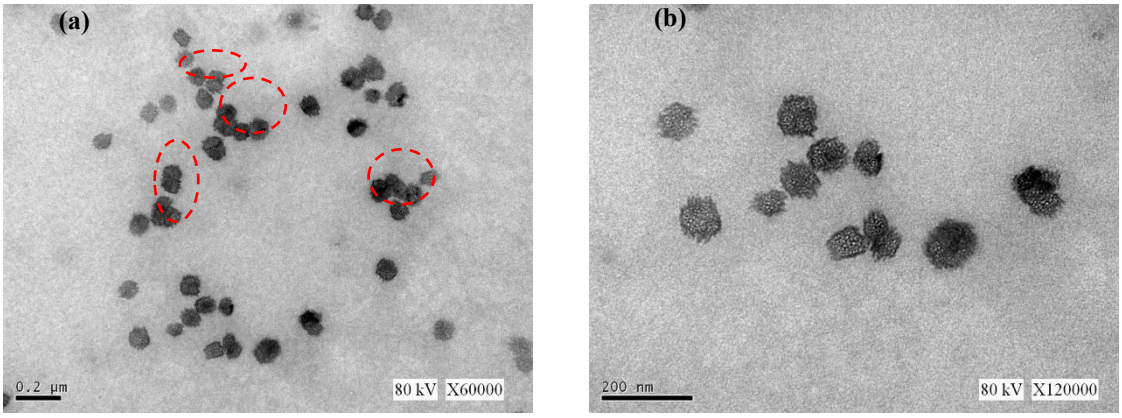

Figure 4.1: The TEM analysis of nanocellulose.

4.2.3.2 FESEM-EDX Analysis of Nanocomposite Membrane

Figure 4.2, 4.3, and 4.4 shows the FESEM analysis for the nanocomposite membranes with varied ratio and pristine membrane for comparison of the surface and cross-section morphologies. Based on the surface morphology of the nanocomposite membrane depicted in Figure 4.2, some of the nanocomposite membranes show cracks on the surface of the membrane. This could be associated with the intrinsic brittle and drying stress of

PVDF material, affecting the membrane surface properties and the permeability of PVDF membranes (Pramono et al., 2017). These inherent limiting properties of PVDF could be alleviated by the addition of plasticizers such as polyethylene glycol (Gontarek-castro et al., 2022). In addition, graphene also affects the surface properties as higher amount of graphene produce cracks on the surface which are open pores distributed throughout the membrane surface. However, it was observed from Figure 4.2 (a) until (g), that the distribution of cracks throughout the membrane surfaces decreases as the amount of graphene decreases with 20% GR exhibiting very minimal cracks due to balanced GR/NC ratio, suggesting minimal need of plasticizers for optimal compositions. A combination of chemical and mechanical stress is able to increase membrane degradation which leads to cracking (Bortot Coelho et al., 2021; Robert et al., 2020). However, it is also possible that the cracking of the membrane surface is due to the drying process of the membrane or the vacuum environment in the FESEM machine (Rudolph et al., 2021).

The cross sections of the membrane were conducted at two magnifications which are ×1,000 and ×5,000 to analyse the membrane pores and the agglomeration in the pores of the nanocomposite membrane respectively. Based on Figure 4.3, all of the nanocomposite membrane shows an asymmetric structure where the membrane has a thin top skin layer that is supported by a finger-like porous sublayer. It can be observed that the increase in the amount of graphene produces a bigger finger-like macro voids compared with low amounts of graphene as seen in 20% GR and 30% GR where the membrane pores appear smaller than other ratios. This is due to the phase separation that occurs, causing the fast exchange of solvent and non-solvent, which leads to precipitation of polymer. This rapid mechanism results in the formation of finger-like macro voids throughout the sublayer (Nursiah et al., 2023). In addition, higher amounts of graphene also cause the phase inversion process to fail

as it acts as a barrier against direct diffusion of solvent and non-solvent molecules which supresses the development of finger-like structure (Karimi et al., 2020). This can be proven by the study done by Mohsenpour et al. (2022) which shows the increase in graphene oxide in PVDF casting solution increases the viscosity and also hinders the exchange of solvent and non-solvent. Therefore, based on Figure 4.3 (g), 20% GR is the suitable amount of graphene that is incorporated in the nanocomposite membrane as it has a thin finger-like structure.

Figure 4.4 shows the cross-section of the nanocomposite membranes at ×5,000 magnification which shows the agglomeration of particles in the membrane pores for some nanocomposite membranes. Based on Figure 4.4 (a) until (c), it can be observed that there is agglomeration of particles in the membrane pores compared to Figure 4.4 (d) until (g) which shows minimal to without agglomeration in the membrane pores. This is due to the hydrophobicity of the graphene material which can cause agglomeration in the membrane pores (Ashok Kumar et al., 2022; Devrim & Bulanık Durmuş, 2022). Hence, the incorporation of hydrophilic groups is able to disperse nanoparticles evenly throughout the membrane pores and reduce agglomeration (Alkhouzaam et al., 2021). Since nanocellulose has hydrophilic properties, this enhances the interaction of the nanocellulose in the polymer matrix which reduces agglomeration and promotes even dispersion (Gan et al., 2020). However, even though nanocellulose disperses evenly throughout the polymer matrix, the incorporation of nanocellulose can also produce agglomeration if the amount of nanocellulose added is too high (H. C. Zhang et al., 2022).

Therefore, 20% GR and 30% GR have a better dispersion of nanoparticles compared to other ratios due to the higher amounts of nanocellulose incorporated in the membrane and these ratios are also a suitable composition as there is no agglomeration due to nanocellulose

observed. The EDX analysis results in Figure 4.5 represents the results for elements composition, carbon and fluoride. The nanocomposite membranes 70% GR to 20% GR have similar carbon content ranging from 60.61% to 63.61%. The membrane pores from FESEM analysis shows that other nanocomposite membranes have agglomerations except 20% GR and 30% GR, but the carbon compositions are in similar range. This means that the nanocomposite membranes are dispersed evenly throughout the membrane pores, as it has similar carbon content. Based on Figure 4.5, it is also observed that the carbon content decreases while the fluoride content increases with increasing amount of GR. This is because the carbon and fluoride contents are dominated by PVDF as the amount of PVDF is higher than the amounts of nanoparticles added into the membrane (Ravi et al., 2021).

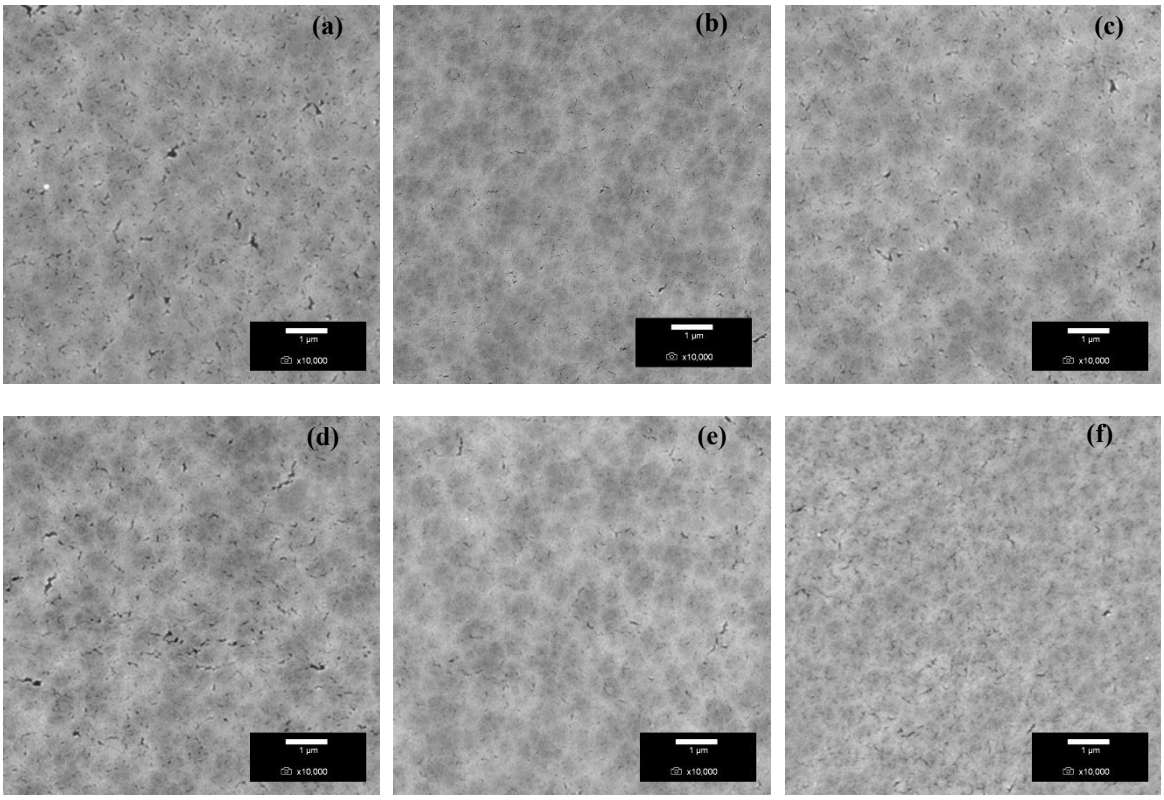

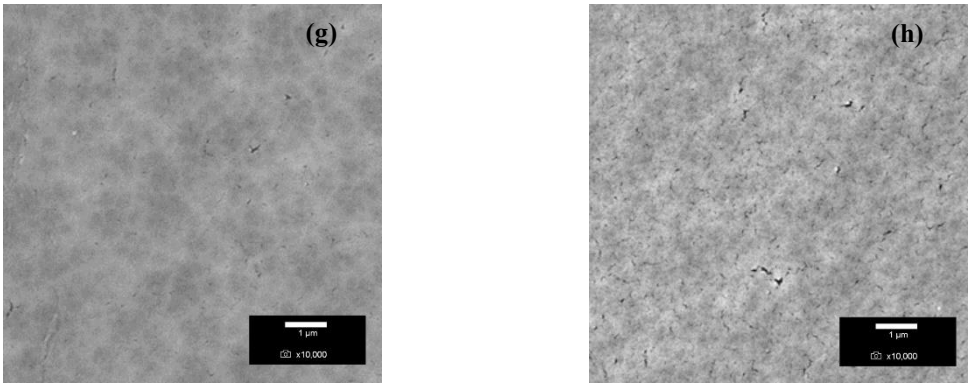

Figure 4.2: The surface morphology results of membranes from FESEM analysis at 10,000× magnification, (a) 80% GR, (b) 70% GR, (c) 60% GR, (d) 50% GR, (e) 40% GR, (f) 30% GR, (g), 20% GR, (h) 100% PVDF.

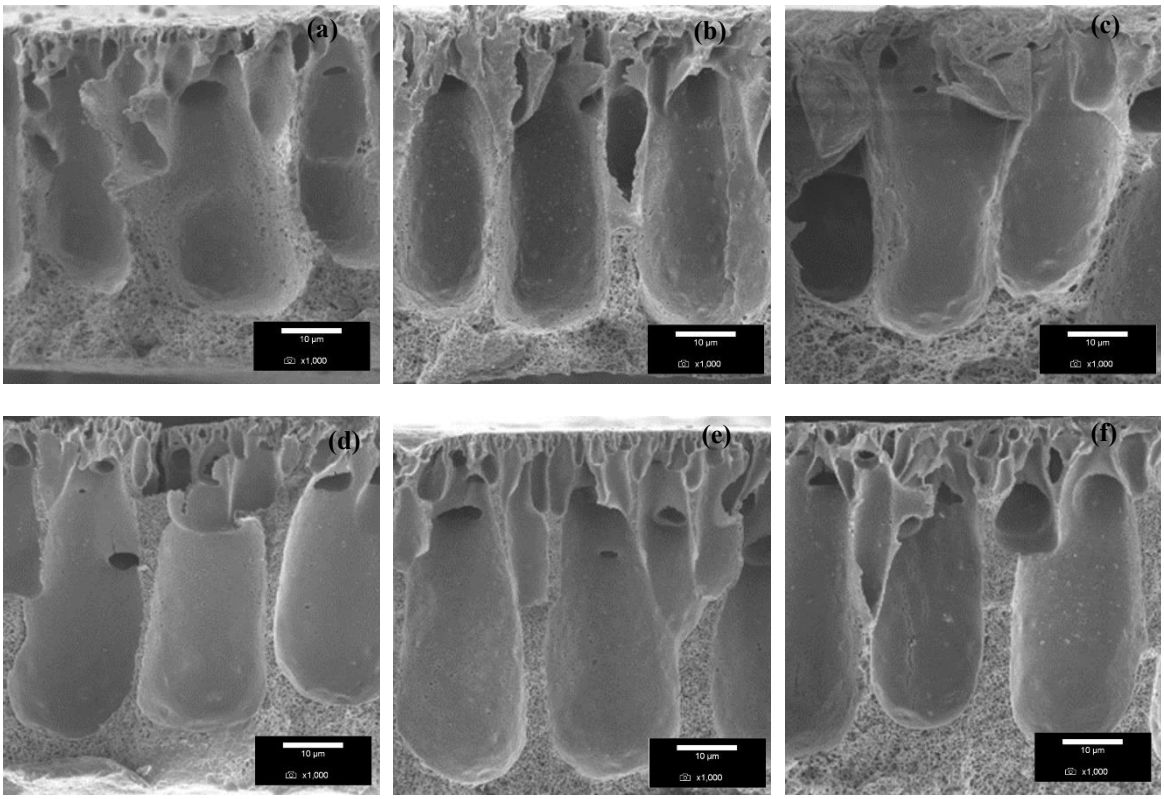

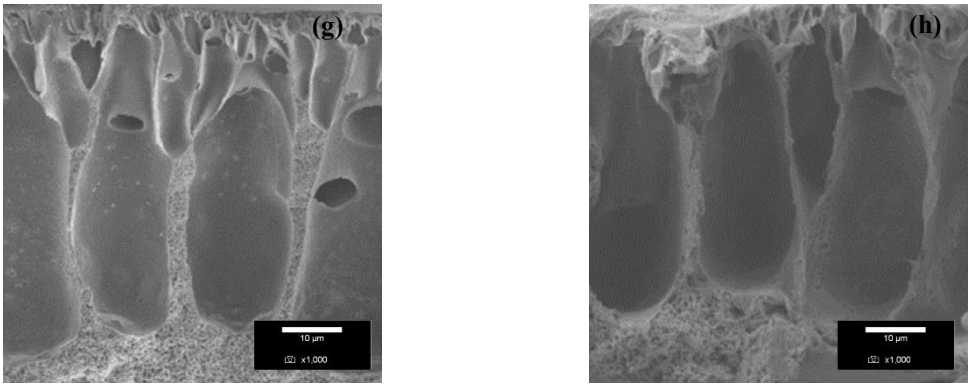

Figure 4.3: The cross-section results of membranes from FESEM analysis at 1,000× magnification, (a) 80% GR, (b) 70% GR, (c) 60% GR, (d) 50% GR, (e) 40% GR, (f) 30% GR, (g), 20% GR, (h) 100% PVDF.

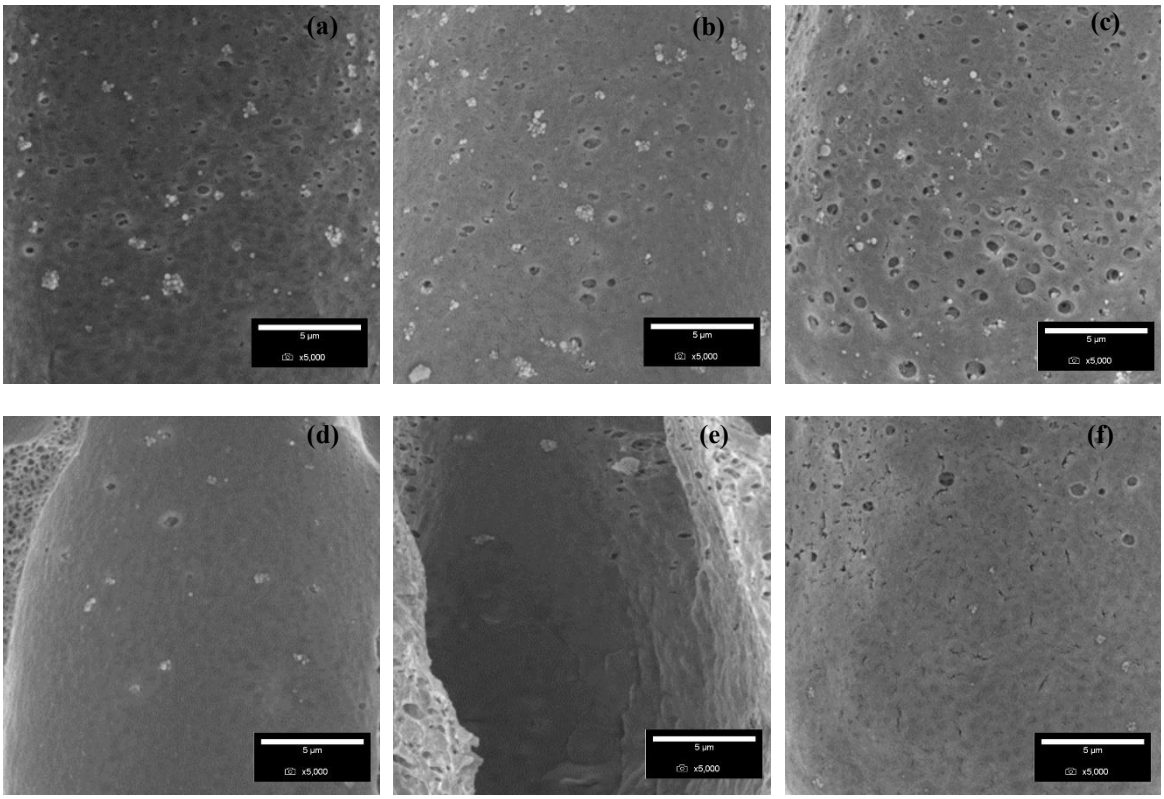

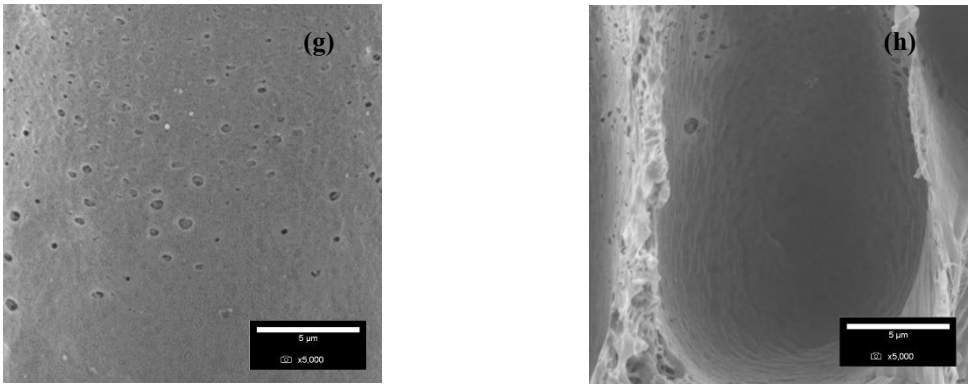

Figure 4.4: The cross-section results of membranes from FESEM analysis at 5,000× magnification, (a) 80% GR, (b) 70% GR, (c) 60% GR, (d) 50% GR, (e) 40% GR, (f) 30% GR, (g), 20% GR, (h) 100% PVDF.

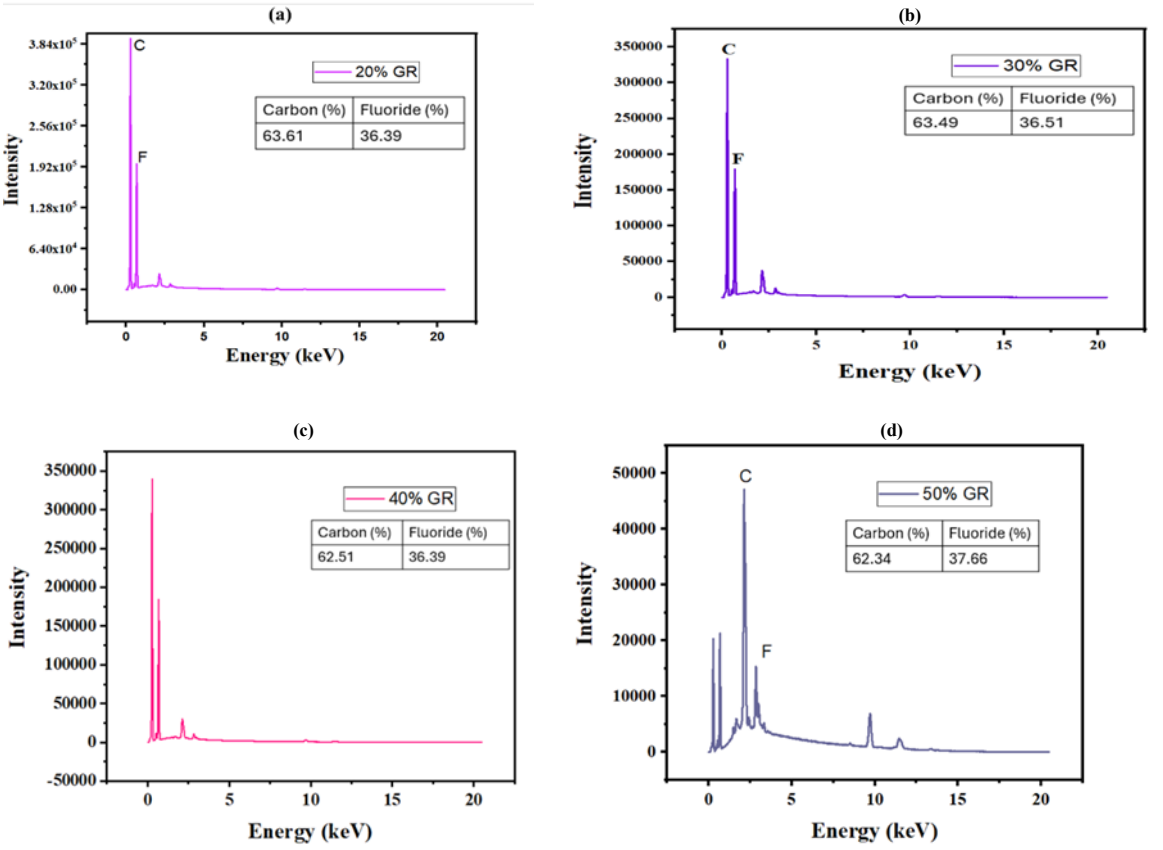

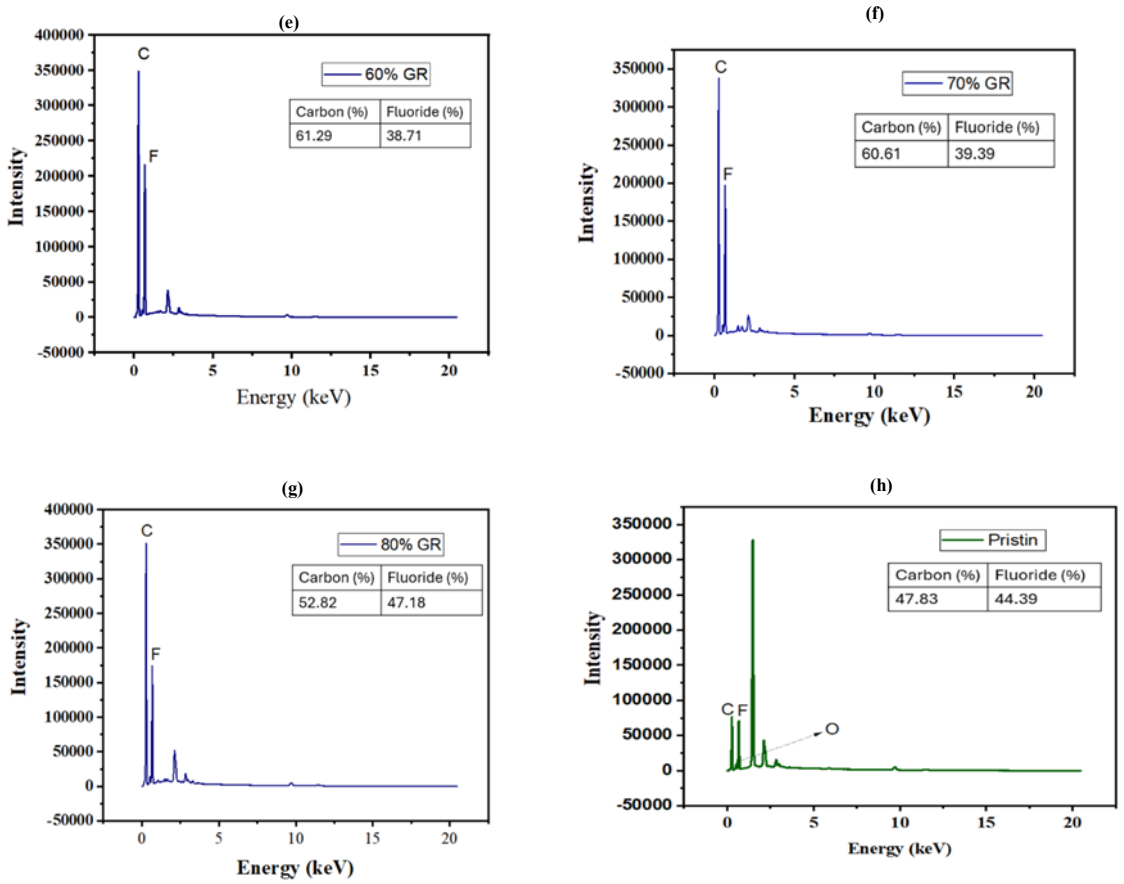

Figure 4.5: The EDX analysis for pristine and nanocomposite membranes (a), 20% GR, (b) 30% GR, (c) 40% GR, (d) 50% GR, (e) 60% GR, (f) 70% GR, (g) 80% GR, (h) 100% PVDF.

4.2.3.3 FTIR Analysis of Nanocomposite Membrane

Figure 4.6 (a) and (b) show the FTIR analysis of pristine and graphene modified nanocomposite membrane which represents the presence of various functional groups in the membranes. Based on Figure 4.6 (a) and (b), it can be observed that the peak characteristics and structure are similar when comparing the FTIR analysis for pristine membrane and nanocomposite membrane. Therefore, this indicates that the addition of nanomaterial does not affect the functional groups present in the membrane. However, it is evident that from Figure 4.6 (b) small concentration of graphene material from 20% to 40% resulted to moderately shallow peaks with relatively undistinctive hydroxyl (-OH) stretching when compared to Figure 4.6 (b). this corroborated the influence of GR materials incorporation on

membrane surface modifications without shift in the peaks position corroborating the findings reported by (Gontarek-Castro et al. 2021). Figure 4.6 (a) and (b) showed the peak at intensity at 1,400 cm^{-1} representing the wagging vibration of CH_2 functional group (Yin et al., 2021), whereas the peak at 1,175 cm^{-1} indicates the presence of CF_2 asymmetrical stretching which is a characteristic peak of PVDF (Nair et al., 2024; W. Zhou et al., 2021). In addition, the peak at 1,065 cm^{-1}, following the findings of (J. Zhang et al., 2022), showed the stretching vibration of -OH groups which indicates the presence of hydrophilic functional groups in the membrane. However, it is imperative to note that -OH vibrations are commonly around 3300 to 3600 cm-1 peak positions (Agale et al., 2025), as shown in Figure 4.6 (a) and (b). These peaks variations could be associated with nature of molecular environment, hydrogen atom or solvent effects which likely shift the position of the -OH stretching frequency. Similarly, the peak at 875 cm^{-1} represents characteristic peak of with the PVDF asymmetrical stretching of C-C functional group (Peng et al., 2023; J. Zhang et al., 2022). However, the peak at 839 cm^{-1} equally represents two types of functional groups which are the CF_2 asymmetric stretching and CH_2 rocking (Gontarek-Castro et al., 2021). On the other hand, the peak at 758 cm^{-1} corresponds to the bending of the C-H functional group (Manfo et al., 2020). It is also mentioned that the peaks at 758 cm^{-1} and 839 cm^{-1} correspond to the α and β phase of PVDF respectively (P. Pal et al., 2020). Hence, this confirms the presence of the PVDF crystalline structure of α and β phase in the nanocomposite membrane which is observed in the XRD analysis. Similarly, the FTIR of NC and GR showed broad peak at 3400cm^{-1} for the individual nanocellulose O-H bond stretching, while the spectral band observed at 1725cm^{-1} corresponds to the GR pi-bond (sp^2), C=C bond (Cui et al., 2021). The spectral characteristics with enhanced broad peak at 3400-3600 cm^{-1} correspond to O-H stretching (James, Rezaur Rahman, et al., 2024; Jangam et al., 2022) of the pure NC material,

specifically in high-NC membranes (20-30% GR). While the peak at 1175 cm^{-1} is associated with presence of hydroxyl groups, and PVDF characteristic peaks (Aziz & Abdel-Karim, 2023; Jeong et al., 2018), corroborating the contribution of NC, GR and chemical stability of PVDF.

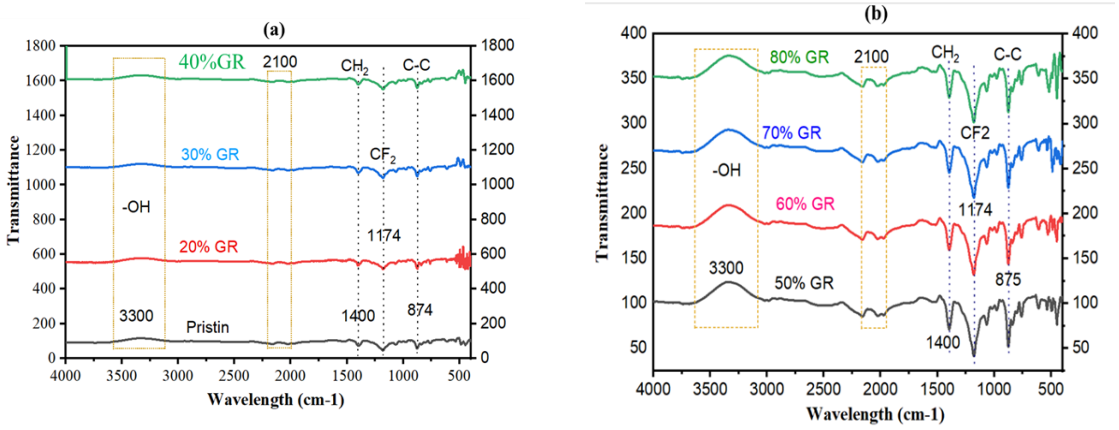

Figure 4.6: Combined FTIR analysis results for (a) Pristine, 20% GR, 30% GR, and 40% GR, (b) 50% GR, 60% GR, 70% GR, and 80% GR.

4.2.3.4 XRD Analysis of Nanocomposite Membrane

The crystallinity of the nanocomposite membranes and pristine membrane were analysed by using the XRD technique and the results are shown in Figure 4.7. Based on the figure, there are three diffraction peaks that can be observed for the XRD analysis of the membranes which corresponds to the crystalline behaviour of PVDF. PVDF is a semi-crystalline polymer that has three main crystalline phase which are α-phase, β-phase, and γ-phase (Saxena & Shukla, 2021). β-phase and γ-phase are polar phase where β-phase is highly polar while α-phase is a non-polar phase which is the most common phase that can be obtained when PVDF is directly melted (Saxena & Shukla, 2021). The results show the diffraction peak at 2θ values of 18.21° and 19.20° is corresponding to refection of α-phase of PVDF at planes (020) and (110) respectively (Anand et al., 2020; H. Zhang et al., 2020). In addition, the diffraction peak at 2θ value of 26.6° represents the β-phase of PVDF at plane

(021) (H. Zhang et al., 2020). Based on Figure 4.7, compared to pristine membrane, it can be observed that the diffraction peaks of the modified membranes decrease with nanocellulose loading. The primary crystalline phase in pristine PVDF conformed with the findings in (Anand et al., 2020; H. Zhang et al., 2020), which are typically the non-polar α-phase shown at approximately 18.21°, 20.0° and 26.6° respectively. Consequently, increasing GR loading into the PVDF matrix induces crystalline phase modifications in GR modified membrane compared to the pristine membrane. These modifications are evident from the gradual attenuation and downshift of the α-phase peaks with increase in GR loading, strengthening the GR-PVDF compatibility. Concurrently, the emergence of new diffraction peak at around 43^{o} which broadens as GR loading increases from 20% to 80% confirmed an increased electroactive β-phase content within the nanocomposite membrane, similar trends were observed in (Rath et al., 2022). The diffraction peaks shown by 40% GR, 50% GR, 60% GR, 70% GR, and 80% GR are due to the nanocellulose properties which inhibits the crystallization of PVDF (Lizundia et al., 2020). Nevertheless, the concentrations of nanocellulose are too high, the diffraction peak can be less pronounced because of the constraining and nucleating behaviour of nanocellulose in forming the crystallization (Lizundia et al., 2020). Therefore, even though nanocellulose is a nucleating agent for PVDF crystallization, excessive amounts of nanocellulose can inhibit the formation of crystalline structure of membrane.

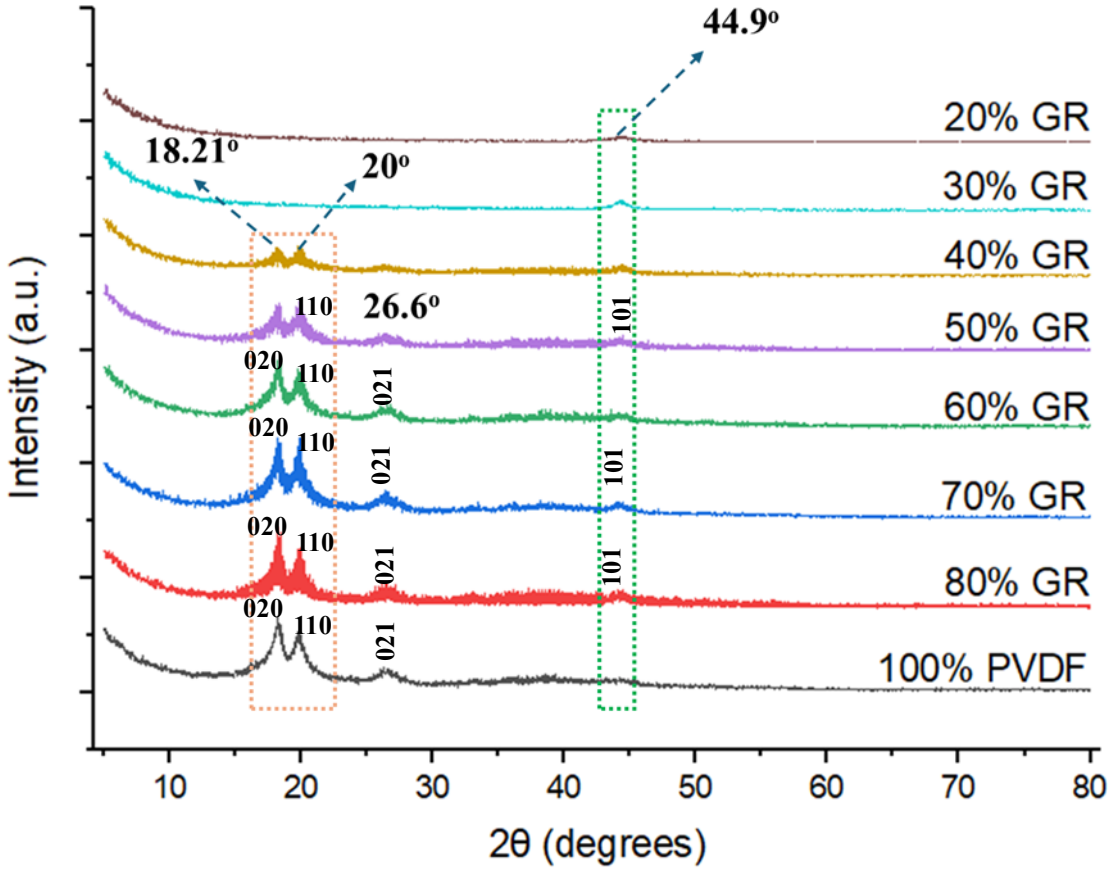

Figure 4.7: Stacked graphs of XRD analysis for pristine and nanocomposite membranes.

4.2.3.5 Measurement of Membrane Porosity and Mean Pore Size for Nanocomposite Membrane

The calculation of the membrane porosity and mean pore size for the nanocomposite membrane is shown in Table 4.1. Based on the table, the porosity of the nanocomposite membrane increases with lesser amount of GR and higher amount of NC. By referring to the FESEM analysis results, all of the nanocomposite membranes have top skin layer that consists of membrane pores with different porosities where this affects the porosity of the membrane (Basko et al., 2023). The thin top skin layer is formed due to the solvent and non-solvent exchange due to loss of solvent, and this change in composition causes phase separation to occur (Ismail et al., 2019). Hence, the solvent used needs to be taken into consideration to improve the porosities of the membrane (Ismail et al., 2019). Based on Table

4.1, all of the nanocomposite membranes have high porosities which are above 80%, which means that the usage of NMP as solvent is able to improve the membrane porosity. This is because NMP is a water-miscible solvent that can form a thinner top-skin layer and suppress the formation of macro voids, which increases the porosity of membranes (L. Lin et al., 2023). In addition, the membrane pore sizes of the nanocomposite membrane are in the range of ultrafiltration membranes which are in between 2 nm to 100 nm (Norrrahim et al., 2021).

Porosity increased with NC content because NC acts as a pore-forming agent during phase inversion, creating interconnected channels (Zubair et al., 2024). While GR is hydrophobic and susceptible to agglomeration. At high loadings (GR greater than 50%), GR platelets are likely to block pore channels and increase casting solution viscosity (M. E. A. Ali et al., 2016; Narayanam et al., 2022), suppressing pore formation which could for the reduced porosity (80.78% at 80% GR). Ultrafiltration membranes have porous skin layer and are highly efficient in dye removal in wastewater (Ismail et al., 2019; Ramutshatsha-Makhwedzha & Nomngongo, 2022; C. Yang et al., 2020). However, the difference in pore sizes affects the permeability and selectivity of the nanocomposite membranes which will be explained further in the next section.

Table 4.1: The porosity and mean pore size of GR/NC nanocomposite membrane.

Sample	Porosity (%)	Mean pore size (nm)
80% GR	80.78 ± 0.36	11.18 ± 0.01
70% GR	82.09 ± 2.18	12.33 ± 0.09
60% GR	82.63 ± 0.55	14.74 ± 0.12
50% GR	83.71 ± 0.24	17.63 ± 0.05
40% GR	84.56 ± 1.36	19.32 ± 0.05

Table 4.1 continued

30% GR	86.52 ± 0.48	20.19 ± 0.12
20% GR	87.50 ± 0.37	20.46 ± 0.06
Pristine	71.24 ± 0.96	11.44 ± 0.20

4.2.3.6 Membrane Permeation Test for Nanocomposite Membrane

Figure 4.8 shows the results for water flux and MB dye rejection ratio for the nanocomposite membranes and pristine membrane. Based on Figure 4.8 (a), it can be observed that the water flux increases as the amount of nanocellulose increases. This can be related to the previous section which is the pore size of the membranes. The increase in pore size can increase the water flux of membranes (Y. Li et al., 2022). As seen in Table 4.1, 20% GR has the largest mean pore size which results in the highest water flux depicted in Figure 4.8 (a). In addition, it can be observed that 70% GR and 80% GR have similar water flux range with the pristine membrane, which means that the water flux is not improved significantly in these two ratios. According to the results in FESEM analysis, the membrane pores of these two ratios consists of agglomeration of nanoparticles. Agglomeration of nanoparticles in the membrane pores can reduce the membrane permeability which makes the membrane to be prone to fouling due to the blockage of the pores as the nanoparticles settle in the pores (Berg & Ulbricht, 2020; H. Jang et al., 2024). Therefore, this means that 70% GR and 80% GR has reduced water flux due to agglomeration of nanoparticles which reduces the membrane permeability.

The incorporation of graphene into PVDF membrane is able to increase the water flux as it increases the membrane porosity, but excessive amounts of graphene cause blocked pores due to agglomeration which reduces the water flux. (Tofighy et al. 2021). It is also

mentioned that excessive incorporation of graphene reduces the hydrophilic properties of the membrane despite having excellent water flux when the amount of graphene is incorporated moderately (Moradi & Zinadini, 2020). On the other hand, the incorporation of nanocellulose also increases the water flux without compromising the membrane selectivity due to the hydrophilicity of nanocellulose (Prihatiningtyas et al., 2021). Nanocellulose has high hydrophilicity because of its abundant hydroxyl groups and hydrophilic functional groups during its preparation process (L. Sun et al., 2020). Thus, 20% GR has the highest water flux value due to its nanocellulose composition and moderate amount of graphene.

Based on Figure 4.8 (b), the MB dye rejection ratio is improved significantly for all types of the nanocomposite membranes compared to the pristine membrane where the MB dye rejection ratio increases as the amount of nanocellulose increases. It can also be observed that 20% GR has the best MB dye rejection ratio which amounts to 94.47% removal of MB dye. Similar to water flux, the dye rejection ratio increases as there is no agglomeration of the membrane pores, allowing efficient dye removal. High hydrophilicity can improve the separation efficiency of membranes and produce high quality water treatment (Kadhim et al., 2020). Based on the research done by Kadhim et al. (2020), the incorporation of graphene oxide has high hydrophilicity on the membrane surface which increases the dye removal efficiency acid black dye and rose Bengal dye. The membrane surface hydrophilicity is crucial as higher hydrophilicity increases permeation and prevents fouling on the membrane surface, which leads to higher dye rejection (Davari et al., 2021). The usage of nanocellulose in membranes are also known to be very effective in dye adsorption as nanocellulose has high hydrophilicity and surface area (Sueraya et al., 2023).

Other than that, another study also mentioned that membranes modified with graphene are able to effectively remove reactive red 195 dye compared to pristine membrane

because of the properties of graphene which causes repulsion between the functional groups of dye (Vatanpour et al., 2021). Even though the efficiency of dye removal due to graphene is recognized, many researchers recommend incorporating a lower concentration of graphene to obtain maximum results for dye rejection as higher amounts of graphene can alter the properties of the membrane (Kadhim et al., 2020). In addition, a study by Y. Huang et al. (2021) also confirmed that nanocellulose can also increase dye rejection rate by the repulsion of the charges of the dye where three types of dye which are methyl blue, methylene blue, and rhodamine B dye are tested to confirm this hypothesis. Hence, 20% GR has the best dye rejection ratio due to the ability of graphene and nanocellulose to effectively remove the dye. Compared to the other ultrafiltration nanocomposite membranes (See Table 4.2), the present study employed GR/NC nanomaterials in the fabrication of the nanocomposite membrane, analysis corroborated marginally higher rejection (approximately 94.5%) which outperforms GO/GBFSG nanocomposite membrane (F. Zhang et al., 2023), TiO2@ZIF-67 PVDF membrane (Prabhakar et al., 2024) and g-C3N4/PAA composite membrane (Z. Qiao et al., 2012), due to NC's pore-forming ability and GR's conductivity.

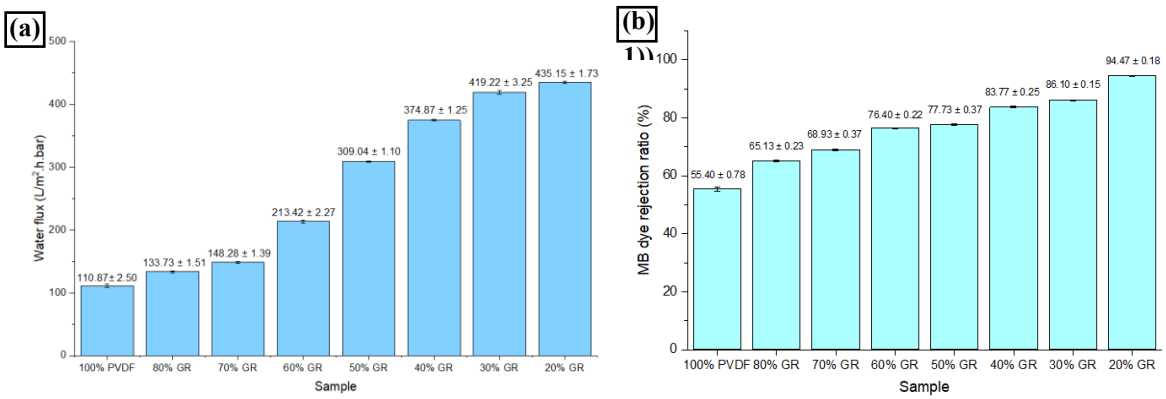

Figure 4.8: The trendline for water flux and MB dye rejection for GR/NC nanocomposite membrane, (a) Water flux, (b) MB dye rejection.

Table 4.2: Comparison of GR/NC nanocomposite membrane performance with other nanocomposite membranes.

Membrane Type	Type of pollutant	Membrane performance (Rejection and separation efficiency)	References
GP-PES membrane	Methyl orange methyl red dyes	55.14 % ± 1.0 67.23 % ± 1.5	(X. Wang et al., 2019)
GO/GBFSG membrane	MB	91 %	(F. Zhang et al., 2023)
TiO_2@ZIF-67 PVDF membrane	Congo dye	92.2 %, (basic medium) 84.3% (neutral medium)	(Prabhakar et al., 2024)
GR/TiO_2 PVDF membrane	MB dye	96.17%	(Sueraya et al., 2024)
GR/NC PVDF membrane	MB dye	94.47% (neutral)	This study

4.2.3.7 Membrane Antifouling and Reusability Test for Nanocomposite Membrane

Membrane fouling is a process where the particles are accumulated or adsorbed onto membrane surfaces or pore by mechanical, physical, or chemical interactions which causes smaller or blocked membrane pores (He et al., 2024; L. Liu et al., 2019). Membrane fouling can reduce the water flux and separation efficiency where this will require vigorous membrane cleaning or replacement of membrane (L. Liu et al., 2019). Hence, it is better to produce membrane with antifouling properties to mitigate this issue and as a result, the membrane is more cost-effective. Figure 4.9 depicts the flux recovery ratio for the pristine and nanocomposite membranes where the flux recovery ratio increases as the amount of nanocellulose increases. The flux recovery ratio is an important parameter in determining the antifouling properties of membrane as higher flux recovery ratio indicates stronger

antifouling performance (Asif Khan et al., 2023). Based on Figure 4.9, 20% GR has the best flux recovery ratio amounting to 85.99% which is significantly higher compared to pristine membrane with only 35.98%. This is because 20% GR has no agglomeration of nanoparticles which was confirmed in the FESEM analysis, and this results in higher flux recovery ratio as the membrane pores are not blocked compared to other nanocomposite membranes (Moradi & Zinadini, 2020).

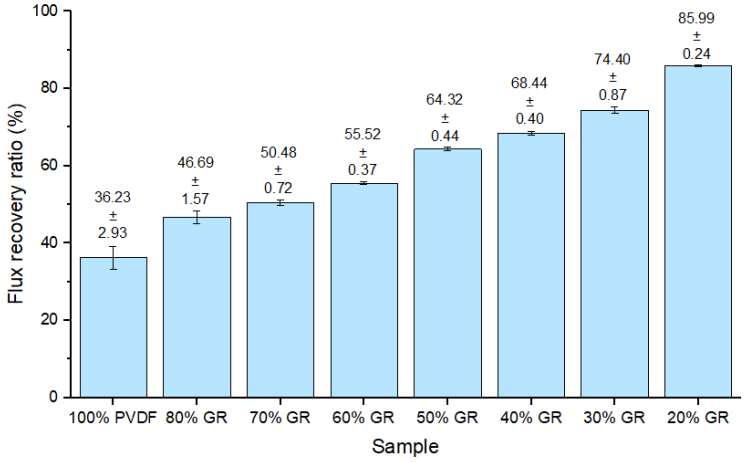

Figure 4.9: Flux recovery ratio of pristine and nanocomposite membrane.

Next, Figure 4.10 shows the antifouling performance of the pristine and nanocomposite membrane which consists of total fouling, irreversible fouling, and reversible fouling ratios. It can be observed in Figure 4.10 that 20% GR has the best antifouling performance where the total fouling is only 15.45% compared to pristine membrane which is 71.88% total fouling of membrane. Other than that, there are two types of fouling which are reversible and irreversible fouling. Reversible fouling refers to pollutants or particles that are attached loosely on the membrane surface and this can be removed effectively by physical cleaning while irreversible fouling refers to pollutants or particles strongly attached to the membrane which can only be removed by chemical cleaning (Leam et al., 2020).

Based on Figure 4.10, it can be seen that the reversible fouling of all the nanocomposite membranes is higher than the irreversible fouling compared to pristine membrane, which means that most of the particles are loosely attached onto the membrane surface of the nanocomposite membranes. This is because the adherence of the dye molecules is weaker on the nanocomposite membranes due to its hydrophilic surface compared to pristine membrane (Moradi & Zinadini, 2020). Therefore, the residual dye particles on the membrane surface can be removed by physical cleaning such as backwashing with water. On top of that, 20% GR has the lowest amount of irreversible and reversible fouling which means that the membrane can be reused effectively.

As depicted in Figure 4.11, all of the nanocomposite membranes are reusable, however, the dye rejection ratio is slightly reduced compared to its previous dye rejection ratio results. This is due to the irreversible fouling on the membrane pores as depicted in Figure 4.10 causing pore blockage which reduces the dye removal efficiency. Based on the study by Hu et al. (2021), six different types of dye are tested to evaluate the dye separation efficiency of a membrane with cellulose and graphene oxide as its composites, and results show that both of the composites are able to improve the antifouling properties of the membrane. On the other hand, the reusability of pristine membrane is only able to remove about half of its original separation efficiency, due to its high irreversible fouling compared to the nanocomposite membranes as seen in Figure 4.10. This is due to the membrane molecules are easily attached to membrane surface and pores of pristine membrane especially when the dye has stronger interactions (Hu et al., 2021).

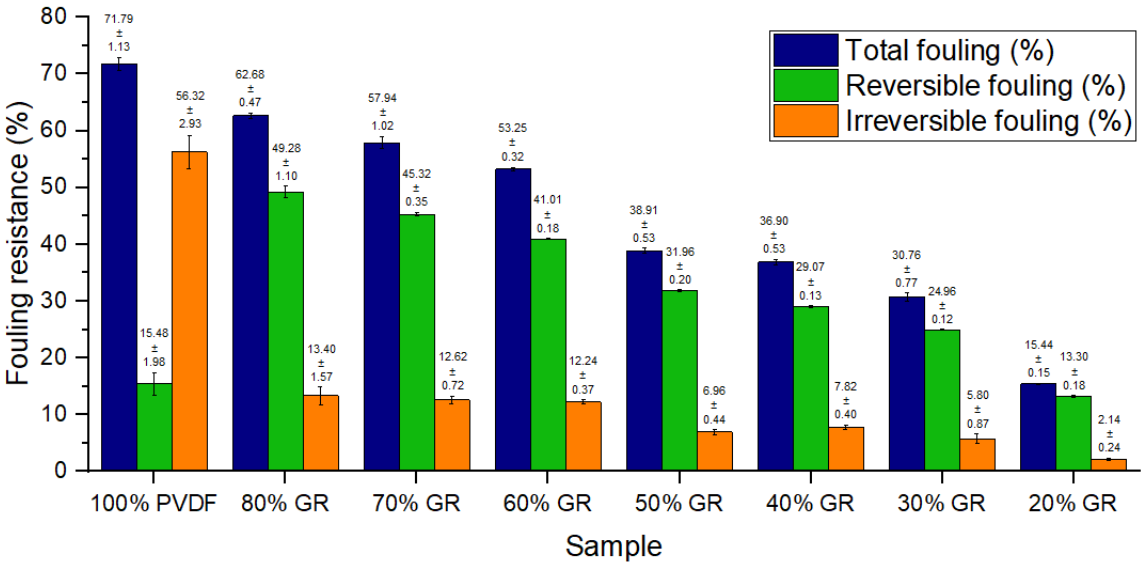

Figure 4.10: Results of total fouling, reversible fouling, and irreversible fouling for pristine and nanocomposite membrane.

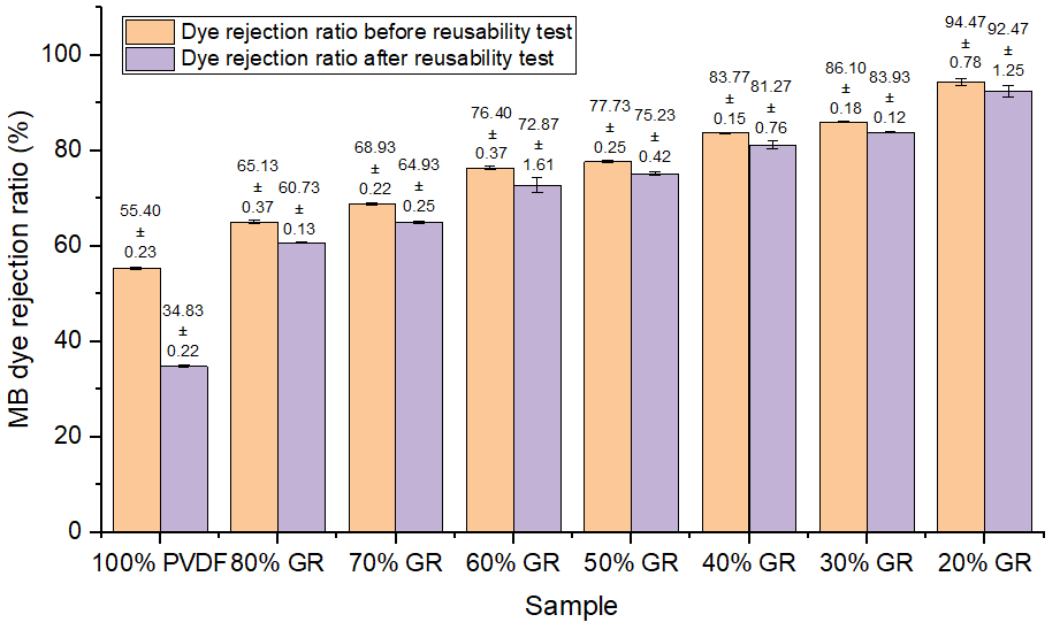

Figure 4.11: Results for membrane reusability test.

4.2.3.8 Evaluation of the GR/NC Nanocomposite Membrane Properties After Degradation Test

This section assessed the stability of the GR/NC nanocomposite membrane at different selected graphene loadings, see Figure 4.11 and 4.12, by analysing the FTIR before

and after exposure to the dye contaminated water. Results revealed changes in bonding characteristics following the exposure of the nanocomposite membrane to methylene blue contaminated water, which were evidenced by shift in peak positions and intensities, corroborating significant chemical interactions between MB dye molecules and nanocomposite membrane functional groups. The observed peaks 800, 872, 875 1176, 1399, 2365, and 3300 cm^{-1} are a critical bond transformation during the chemical interactions between the nanocomposite membrane and dye molecules. From Figure 4.11 (a), prominent band was observed at 3300 cm^{-1} extending to 3447 cm^{-1} corresponding to O-H stretching (Patil et al., 2022) and exhibited a substantial reduction in intensity and moderately shifted post-dye exposure, indicating probable efficient displacement of hydroxyl groups on the surface of the nanocomposite membrane by dye molecules or strong oxidative degradation.

However, it's imperative to note that, while loss of the O-H groups may suggest dye degradation it can also compromised membrane surface hydrophilicity, which may impair water permeability and antifouling performance (James, Rezaur Rahman, et al., 2024; Kuok et al., 2024; Namakka et al., 2024). Poor antifouling performance is highly anticipated as the O-H stretching on the pristine membrane is barely visible compared to all other GR loaded membrane which corroborate the results obtain in Figure 4.10.

Concurrently, the emergence of a peak at 2365 cm^{-1} after dye exposure signifies the possible formation of triple-bonded molecules, such as cyanide C≡N groups. These likely originate from fragmentation of complex MB dye molecules, with byproducts adsorbing onto the membrane surface (Rahman et al., 2024).

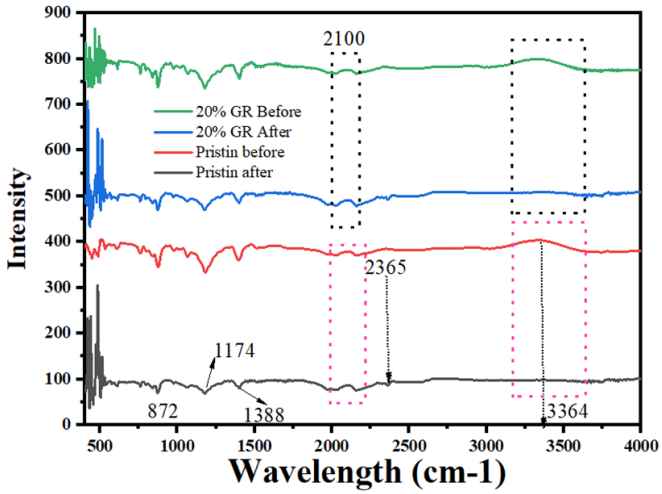

Figure 4.12: Stability analysis, FTIR results of the pristine and 20% GR nanocomposite membranes before and after exposure to dye contaminated water.

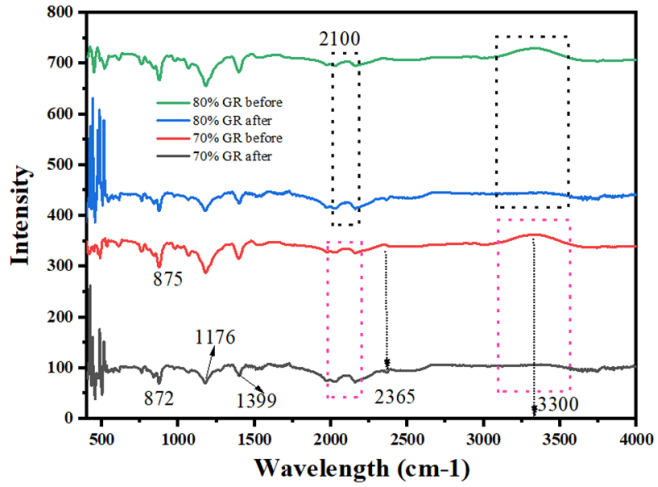

Figure 4.13: Stability analysis, FTIR results of the 70% GR and 80% GR nanocomposite membranes before and after exposure to dye contaminated water.

4.3 EXPERIMENT 2: Impact of Titanium Dioxide/Graphene in Polyvinylidene Fluoride (PVDF) Nanocomposite Membrane to Intensify Methylene Blue Dye Removal, Antifouling Performance, and Reusability

4.3.1 Introduction

The second experiment aims to evaluate the impact of incorporating GR and TiO_2 into PVDF matrix to enhance MB dye removal, and membrane antifouling performance. The functions of GR and TiO_2 are to provide mechanical support, barrier properties,

hydrophilicity and surface roughness, all of which enhances membrane antifouling performance. Membranes with different GR/TiO_2 compositions were fabricated by using phase inversion techniques and evaluated by FESEM-EDX, XRD, and FTIR characterization techniques. In addition, water flux, MB dye removal, and antifouling performance were also assessed. This experiment is focused on the determining of the interactions of GR and TiO_2 and determining which composition provides the most optimum balance of permeable flux and fouling resistance.

4.3.2 Methodology

Refer to Chapter 3, with Table 3.2 as the nanocomposite membrane composition.

4.3.3 Results and discussion

4.3.3.1 FESEM-EDX Analysis of Nanocomposite Membrane

The FESEM analysis of membrane cross section for the nanocomposite membrane were conducted at ×1,000 and ×5,000 magnifications depicted in Figure 4.14 and Figure 4.15 respectively. The cross section at magnification ×1,000 analysed the overall morphology of the nanocomposite membrane, specifically the pores of the nanocomposite membrane. In Figure 4.14, the membrane cross section revealed an asymmetric structure which has a thin top skin layer supported by a finger-like porous sublayer. In addition, it can also be observed that 60% GR demonstrated largest finger-like macro voids which is associated with the significant hydrophilicity of TiO_2 that can cause phase separation (Padmanabhan et al., 2020). The phase separation that occurred was caused by fast exchange of solvent with non-solvent which resulted in the precipitation of polymer, and this fast mechanism causes finger-like macro voids throughout the sublayer (Nursiah et al., 2023). Therefore, the enlarged pore channels observed in Figure 4.14 (c) can be caused by this mechanism. Furthermore, a slow exchange between the solvent and non-solvent results in

delayed de-mixing, which causes the formation of a sponge-like morphology as reported in (Bohr et al., 2023) where this morphology can be observed at the bottom sublayer for the 80% GR and 70% GR. This sponge-like structure enables the nanocomposite membranes to exhibit superior mechanical properties compared to the finger-like structures which is crucial as it is also able to enhance the overall lifespan of the membrane (Cheng et al., 2022).

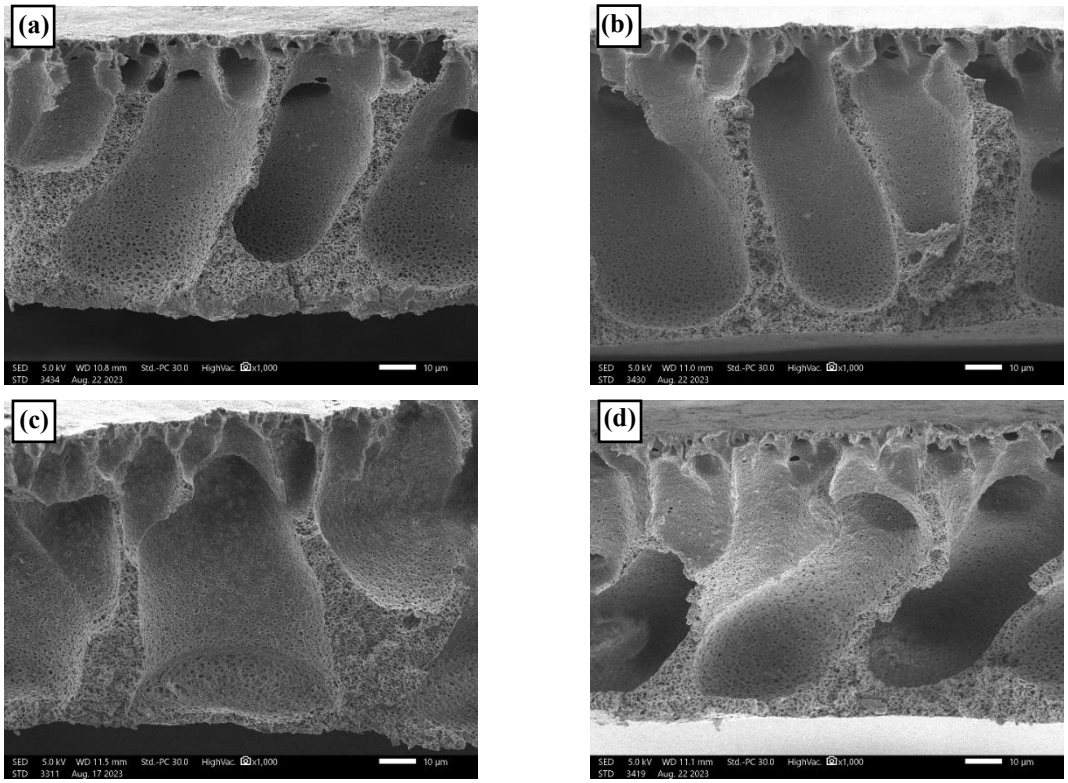

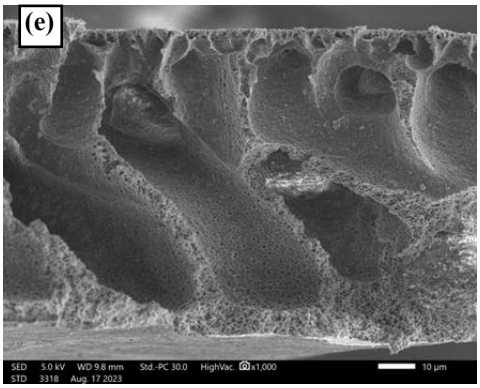

Figure 4.14: FESEM analysis of the cross section of GR/TiO2 nanocomposite membranes at × 1,000 magnification, (a) 80% GR, (b) 70% GR, (c) 60% GR, (d) 50% GR, (e) 40% GR.

Figure 4.15 shows the pore distribution of GR and TiO_2 nanocomposite membrane cross section at ×5,000 magnification which depicts the distribution of GR and TiO_2 inside the membrane pores. Figure 4.15 (e) depicts the cross section of 40% GR which shows the most agglomeration of particles on the nanocomposite membrane pores. Compared to 40% GR, other nanocomposite membrane ratios show minimal agglomeration, while 70% GR and 80% GR shows no agglomeration. However, TiO_2 has high tendency for agglomeration which also decreases its catalytic performance (L. Lin et al., 2023). Thus, this justifies the agglomeration observed in Figure 4.15 (e) since 40% GR has the highest amount of TiO_2. This can also be proven by the EDX analysis in Figure 4.16 where the agglomeration of particles consists of Ti and O components.

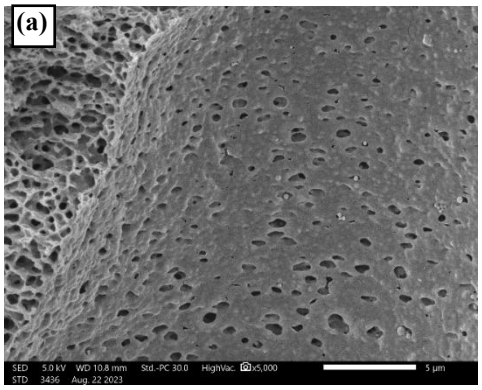

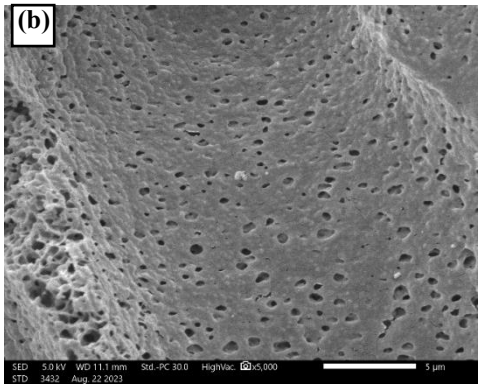

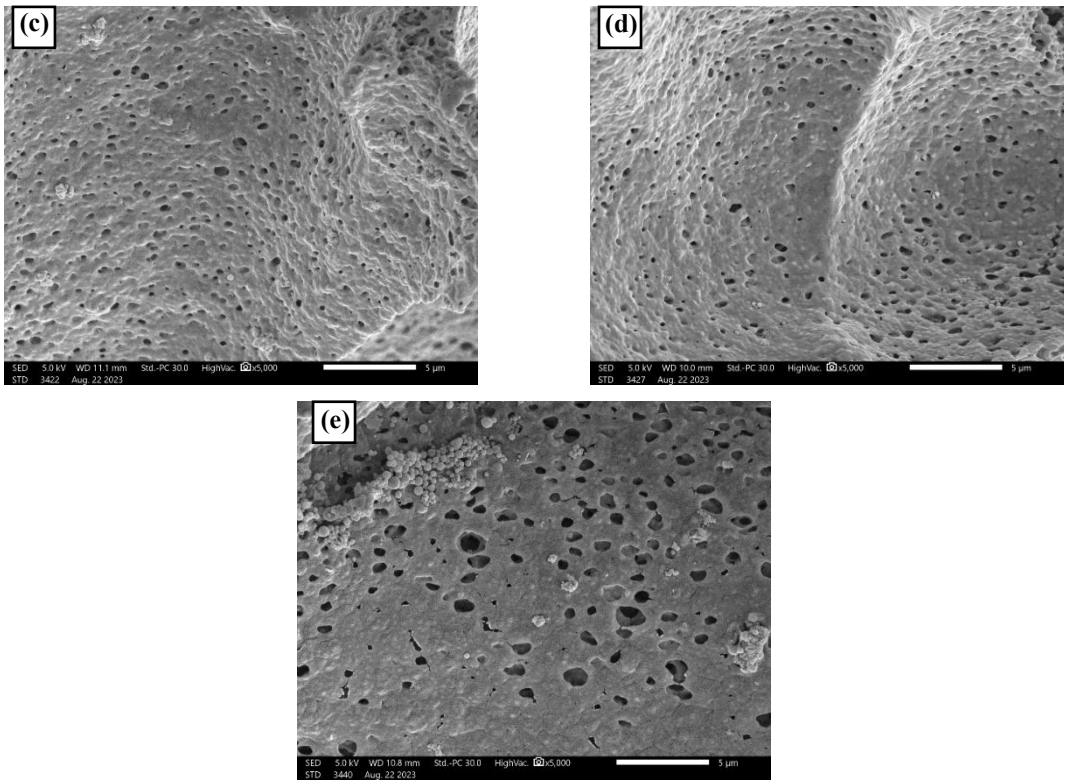

Figure 4.15: FESEM analysis of the cross section of GR/TiO2 nanocomposite membranes at × 5,000 magnification, (a) 80% GR, (b) 70% GR, (c) 60% GR, (d) 50% GR, (e) 40% GR.

EDX analysis was also conducted for the membrane surface at ×20,000 to identify the presence of GR and TiO_2 throughout the membrane. The EDX analysis in Figure 4.16 shows the agglomeration of particles in 40% GR that consists of Ti and O components. Furthermore, similar analysis, shown in Figure 4.17, was conducted for the nanocomposite membrane surface at ×20,000 to analyse the distribution of GR and TiO_2 through the nanocomposite membrane. Based on Figure 4.17, it can be deduced that 80% GR and 60% GR indicated uniform distribution of GR and TiO_2 compared to 40% GR.

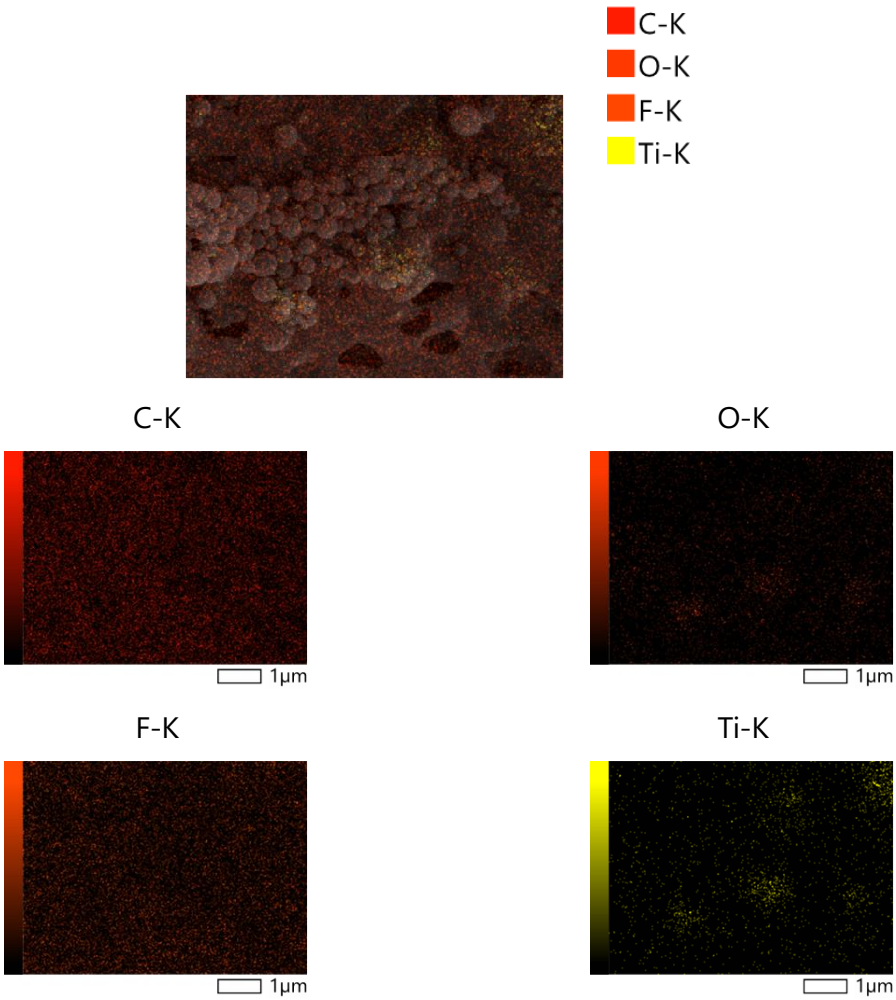

Figure 4.16: EDX analysis of membrane cross section for 40% GR at × 5,000 magnification.

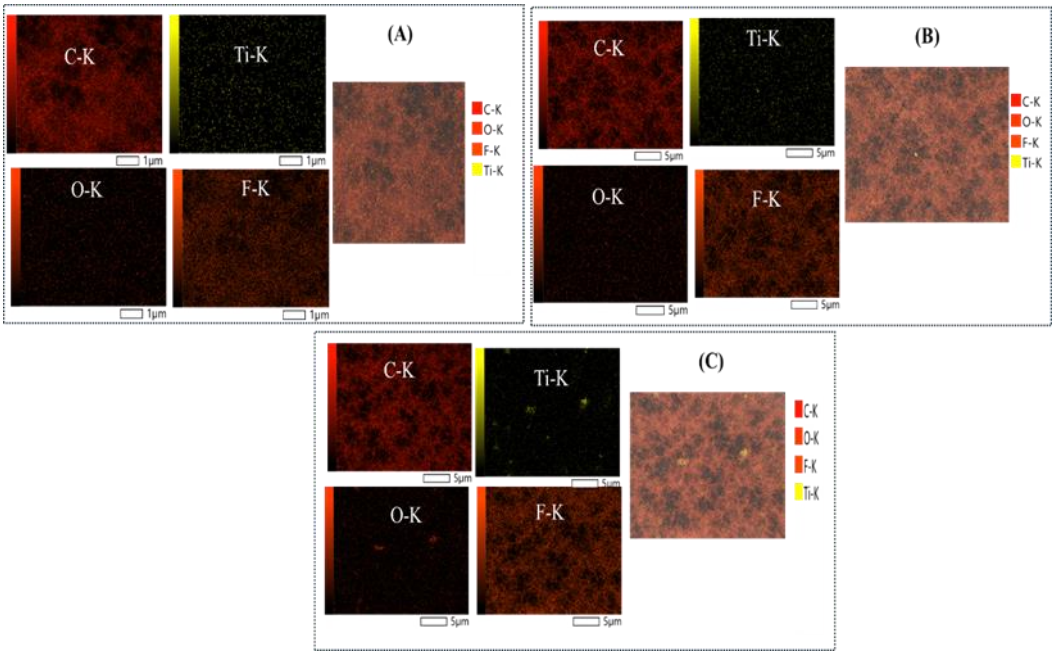

Figure 4.17: EDX analysis of membrane surface at × 20,000 magnification for (a) 40% GR, (b) 60% GR, and (c) 80% GR.

4.3.3.2 FTIR Analysis of Nanocomposite Membrane

The FTIR analysis shows the functional groups present in the nanocomposite membrane with ratios 40% GR, 60% GR, and 80% GR depicted in Figure 4.18. Similar peak structure for all the nanocomposite membranes was observed, indicating that the nanocomposite membranes have similar functional groups despite the difference in ratios of GR and TiO_2. A similar finding is reported by Gontarek-Castro et al. where the incorporation of graphene in the membrane does not change the functional groups present in the membrane. Based on Figure 4.18, first peak that can be observed is at 1,400 cm^{-1} which indicates the wagging vibration of CH_2 functional groups present in the membrane (Yin et al., 2021). The characteristic peak of PVDF can also be observed with the peak at around 1,172 cm^{-1} indicating CF_2 asymmetrical stretching (Nair et al., 2024; W. Zhou et al., 2021). The presence of hydrophilic functional groups in the membrane is also observed with the peak at about 1,070 cm^{-1} representing the stretching vibration of -OH groups (J. Zhang et al.,

2022). The PVDF characteristic peak is observed with the asymmetrical stretching of C-C functional group indicated by the peak at around 877 cm^{-1} (Peng et al., 2023; J. Zhang et al., 2022). In addition, two functional groups such as CH_2 rocking and CF_2 asymmetrical stretching are observed with the peak at around 835 cm^{-1} which also corresponds to the β phase of PVDF (Gontarek-Castro et al., 2021; P. Pal et al., 2020). The peak ranging from 400 cm^{-1} until 700 cm^{-1} represents the stretching of Ti-O-Ti, confirming the presence of TiO_2 compound in all the nanocomposite membrane ratios matrix (Mishra et al., 2021).

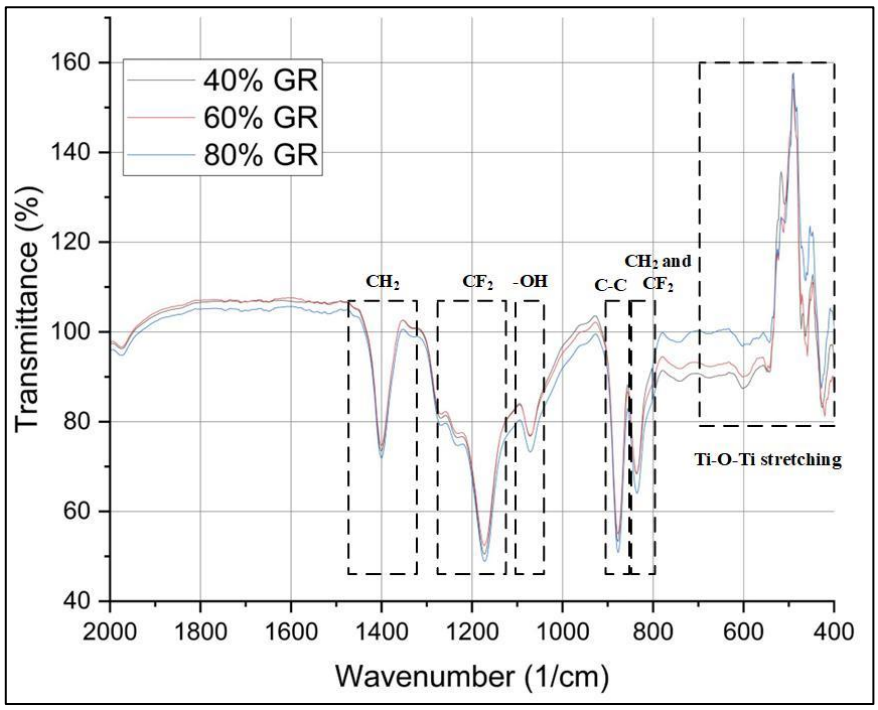

Figure 4.18: The FTIR results for nanocomposite membrane ratios at 40% GR, 60% GR, and 80% GR.

4.3.3.3 X-Ray Diffraction Analysis of Nanocomposite Membrane

X-ray diffraction (XRD) analysis was conducted to investigate the crystallinity of the pristine membrane and nanocomposite membranes. Figure 4.19 presents the key ratios (80% GR, 60% GR, and 40% GR) that exhibited significant differences for the XRD analysis. As observed in Figure 4.19, two prominent peaks at 18.6° (020) and 20.3° (200/110) in the XRD

patterns indicating the crystallinity of PVDF polymer. The peak at 2θ value of 18.6° indicates the primitive structure of PVDF polymer at α-phase while the peak at 20.3° is associated with the β-phase (A. Omar et al., 2023). Additionally, the presence of anatase TiO_2 was confirmed by peaks at 25.4°, 38°, 48.1°, 54.02°, 55.23°, and 62.8°, corresponding to (110), (004), (200), (105), (211), and (204) planes, respectively (Tavakolmoghadam et al., 2019). It can be observed that nanocomposite membrane with ratio of 80% GR only retained anatase peak at 25.4° (110), compared to the membranes with ratios of 60% GR and 40% GR. This means that the incorporation of GR at 80% GR ratio affects the TiO_2 crystallinity at other peaks except for 25.4°. Similar finding is reported where the increase in GR reduces the TiO_2 crystallinity peak which can be caused by micro-strain or inhomogeneities in crystal lattices due to the increase in the concentration of GR (AlShammari et al., 2020). Interestingly, the PVDF crystallinity, as evidenced by the constant peaks at 18.6° and 20.3°, appears to be unaffected by the varied GR concentration. It is also observed that the incorporation of GR and TiO_2 does not affect the crystallinity of PVDF (Khassi et al., 2020).

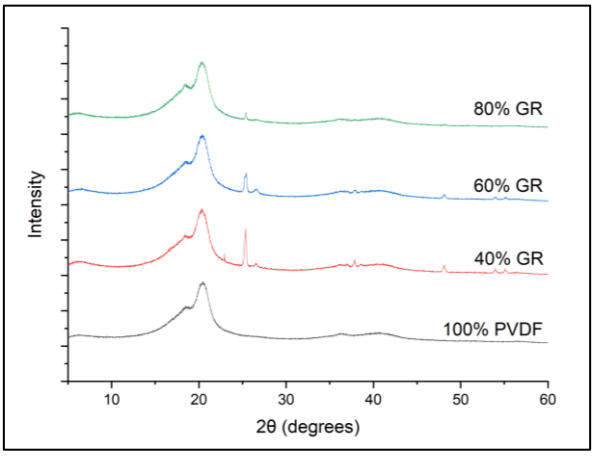

Figure 4.19: Stacked graphs of XRD analysis for 80% GR. 60% GR, 40% GR, and 100% PVDF.

4.3.3.4 Measurement of membrane porosity and mean pore size for nanocomposite membrane

Table 4.3 shows the measurement of membrane porosity and mean pore size for the nanocomposite membrane. The porosity and pore size of the membrane increases as the amount of graphene increases. This is because the phase separation occurs due to the increase in the amount of TiO_2 as it is a hydrophilic component (X. Wang, Ding, et al., 2022). This occurs during fast solvent and non-solvent exchange, where the top skin layer is formed due the concentration of polymer in the skin layer increases and this acts as a barrier to enhance the mass transfer between the solvent and non-solvent (Basko et al., 2023). This skin layer also consists of some pores which has different porosities compared to the sublayer (Basko et al., 2023). Based on the FESEM analysis, all of the nanocomposite membranes formed a thin top skin layer on the membrane which affects the porosity of the nanocomposite membrane. This thin top skin layer is due to the usage of NMP in this experiment. Water-miscible solvents like NMP forms thinner skin layer and can suppress the formation of macro voids and increase the porosity of membranes (L. Lin et al., 2023). Hence, it can be assumed that the usage of NMP as a solvent improves the membrane structure and also the porosity of the membrane. On the other hand, the porosity and thickness of the skin layer in asymmetric membrane also affects the permeability of the membrane (L. Lin et al., 2023). The range of pore size for UF membranes is between 1 until 100 nm where UF membranes are usually fabricated via phase inversion method (Wan & Jiang, 2021). As seen in Table 4.3, all of the mean pore size for the membranes are in the mentioned range for UF membranes. Therefore, it can be deduced that the nanocomposite membranes that are fabricated by the phase inversion method are ultrafiltration membranes. In addition, UF membrane is an excellent candidate for highly efficient dye removal as it has porous skin layers (Awad et al., 2021; Y. C. Lin et al., 2021).

Table 4.3: The porosity and mean pore size of GR/TiO_2 nanocomposite membrane.

Sample	Porosity (%)	Mean pore size (nm)
80% GR	89.08 ± 0.75	87.60 ± 1.40
70% GR	83.17 ± 1.31	87.05 ± 0.66
60% GR	83.31 ± 2.07	78.41 ± 0.77
50% GR	82.45 ± 0.59	74.04 ± 1.33
40% GR	75.81 ± 0.75	68.29 ± 1.25
Pristine	71.24 ± 0.96	63.77 ± 2.18

4.3.3.5 Permeation Test for Nanocomposite Membrane

Figure 4.20 shows the water flux results for the pristine and GR/TiO_2 nanocomposite membranes where a significant trendline can be observed based on the graph. Based on Figure 4.20, the water flux increases as the amount of graphene increases. It can also be observed that 80% GR has a significantly higher water flux which amounts to 320.82 (± 8.32) L/m^2.h.bar compared to pristine membrane which is only 110.87 (± 7.50) L/m^2.h.bar. This is due to the incorporation of GR and TiO_2 which is able to increase the water flux because of the increase in porosity and hydrophilicity of the membrane, however, optimum ratio of GR/TiO_2 is required during membrane fabrication (Junaidi et al., 2021). On the other hand, the water flux results are also dependent on the pore size as larger pore sizes leads to higher water flux (Y. Li et al., 2022). By referring to Table 4.3, 80% GR has the largest mean pore size followed by 70% GR, 60% GR, 50% GR, and 40% GR respectively. Thus, the enhanced water flux in Figure 4.20 can be justified by the increasing pore size that is shown in Table 4.3.

In addition, it can also be observed that 40% GR has low water flux which is in similar range with the pristine membrane even when GR and TiO_2 is added into the membrane. This is due to the agglomeration of TiO_2 that can be observed in the FESEM analysis depicted in Figure 4.15 (e). The agglomeration of TiO_2 causes the decrease in water flux as higher concentrations of TiO_2 leads to the decrease in membrane porosities (Sakarkar et al., 2021). The agglomeration of TiO_2 also reduces the hydrophilicity of the membrane which leads to decreased membrane permeation (Frallicciardi et al., 2022; Sakarkar et al., 2020). Thus, it can be concluded that GR and TiO_2 are well dispersed in 80% GR which also significantly enhance the water flux of the nanocomposite membranes compared to pristine membrane.

Figure 4.21 shows the dye rejection ratio results for three different concentrations which are 0.5 ppm, 1.0 ppm, and 1.5 ppm for pristine and GR/TiO_2 nanocomposite membranes. Based on Figure 4.21, the same trendline for 0.5 ppm, 1.0 ppm, and 1.5 ppm can be observed which is the MB dye rejection ratio increases as the amount of graphene increases. This indicates that the incorporation of graphene enhances the MB dye rejection compared to pristine membrane where 80% GR is able to remove over 40% more MB dye than pristine membrane. This is because the properties of graphene that has unique structure and surface properties which allows selective separation of MB dye (L. Jiang et al., 2021; Wu et al., 2020).

It can also be observed that the dye rejection rate for each membrane ratio is in a similar range despite varied concentrations of MB dye. This could be associated with the rejection mechanism of the membrane, which is size exclusion where the dye molecules are trapped by the nanocomposite membrane. However, possible adsorption and electrostatic interactions between membrane materials (viz., PVDF, TiO_2, and GR) and methylene blue

dye could influence or contribute to the overall dye rejection mechanism. Additionally, GR and TiO_2 have high adsorption capacities, hence their incorporation into membrane surface could provide additional surface area and more adsorption sites. A similar finding is observed in the nanocomposite membrane which incorporates graphene oxide and molybdenum disulfide, which is able to maintain a high dye rejection ratio of MB dye although there are different concentrations of MB dye (Ma et al., 2020). According to the literature, varied concentrations does not affect the dye rejection ratio of the membrane and electrostatic repulsion also occurs between the positively charged MB dye and the negatively charged graphene oxide/PVDF membrane which enhances the dye rejection rate (C. Wang et al., 2022). Thus, it can be deduced that the concentration of MB dye does not affect the dye rejection ratio of the nanocomposite membranes. However, increase in nanocomposite concentration improves the overall dye removal performance.

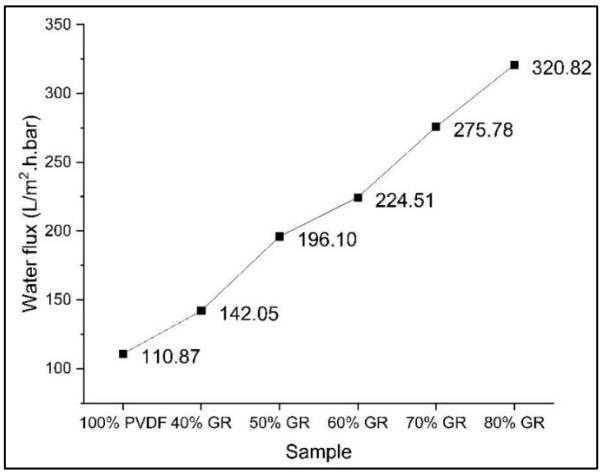

Figure 4.20: The trendline for water flux of pristine and GR/TiO2 nanocomposite membranes.

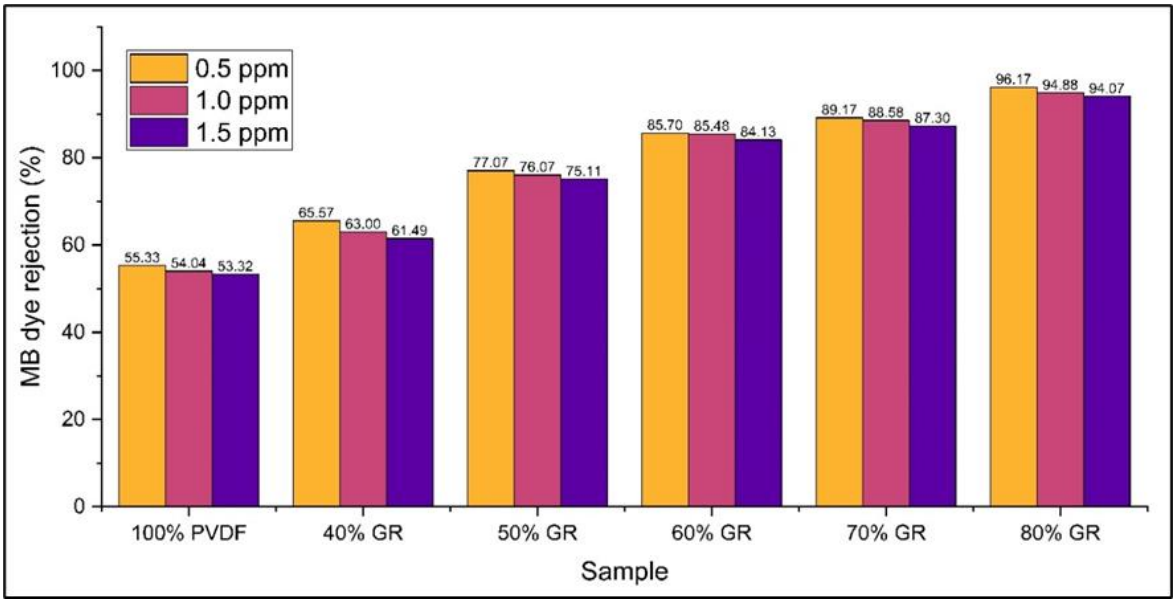

Figure 4.21: The MB dye rejection removal rate for pristine and GR/TiO2 nanocomposite membranes at concentrations 0.5 ppm, 1.0 ppm, and 1.5 ppm.

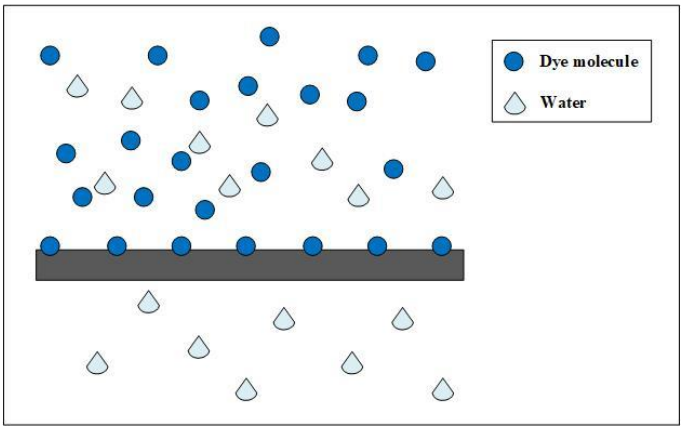

Figure 4.22: Dye rejection mechanism for nanocomposite membrane.

4.3.3.6 Antifouling Performance and Reusability of The Nanocomposite Membrane

Membrane fouling is the process where particles are accumulated onto the membrane surface or within the pore structure by chemical, mechanical or physical interactions which results to blocked or smaller membrane pores (Gul et al., 2021; L. Liu et al., 2019). Membrane fouling causes a decline in membrane flux and separation efficiency, along with extreme costs required to conduct chemical cleaning to reduce the effects of fouling, and membrane replacement (L. Liu et al., 2019; Zulkefli et al., 2021). Therefore, it is crucial to

fabricate membrane with antifouling properties that can overcome this issue, enabling the production to be more cost-effective. Flux recovery ratio (FRR) is evaluated to determine the antifouling performance of membranes, as higher FRR indicates excellent antifouling performance of membranes (Y. Ibrahim & Hilal, 2023; Kusworo, Kumoro, et al., 2023). Figure 4.23 depicts the flux recovery ratio for the pristine and nanocomposite membranes, which shows that the flux recovery ratio increases as the amount of graphene increases. In addition, it can also be observed that all of the GR/TiO_2 nanocomposite membranes had better flux recovery ratio compared to pristine membrane, with 80% GR observed as the best flux recovery ratio.

From Figure 4.24, it can be seen that 70% GR, and 80% GR has better dispersion of MB dye on the membrane surface compared to other ratios including the pristine membrane. It can also be observed that there are concentrated spots in the membranes as circled in Figure 4.24. The concentrated spots are more obvious in the pristine membrane when compared to nanocomposite membranes. This indicates the pore blockage of the membrane due to the dye molecules that are attached to the membrane surface (Jin et al., 2022). As a result, this causes the water flux to decline and decreases the FRR as water is unable to flow through the blocked pores (S. Zhang et al., 2020). A similar finding can be observed where the flux recovery ratio reached 98.16% with the incorporation of GO as the surface properties of the membrane is improved and hence, reducing the fouling (W. Zhang et al., 2022). It is also reported that the addition of GO, TiO_2 and poly (methyl methacrylate) is able to achieve better dispersion and enhance the surface properties of the membrane with the flux recovery ratio of 86.46% (Mohamat et al., 2023).

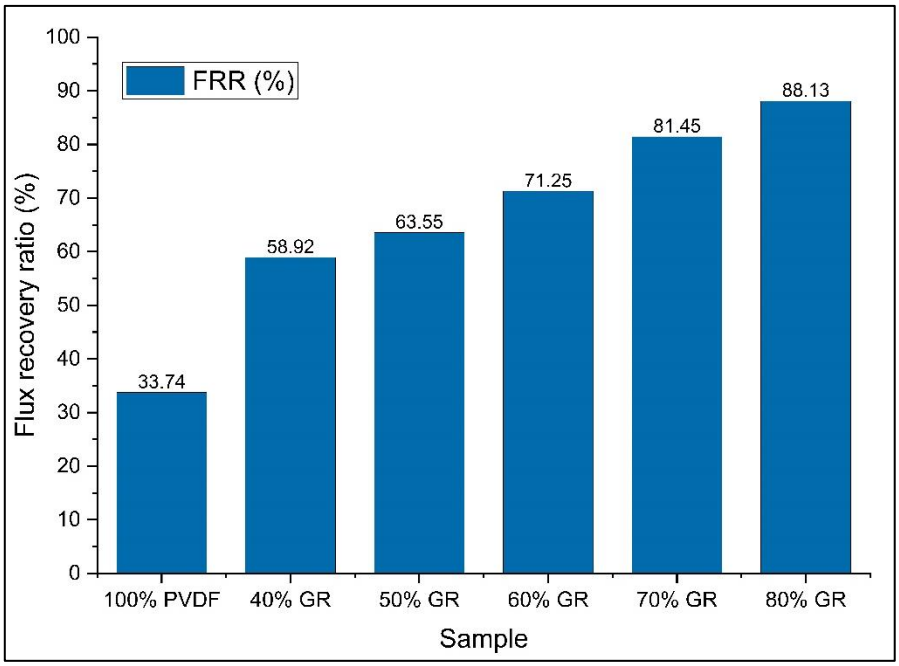

Figure 4.23: The flux recovery ratio of pristine and GR/TiO_2 nanocomposite membranes.

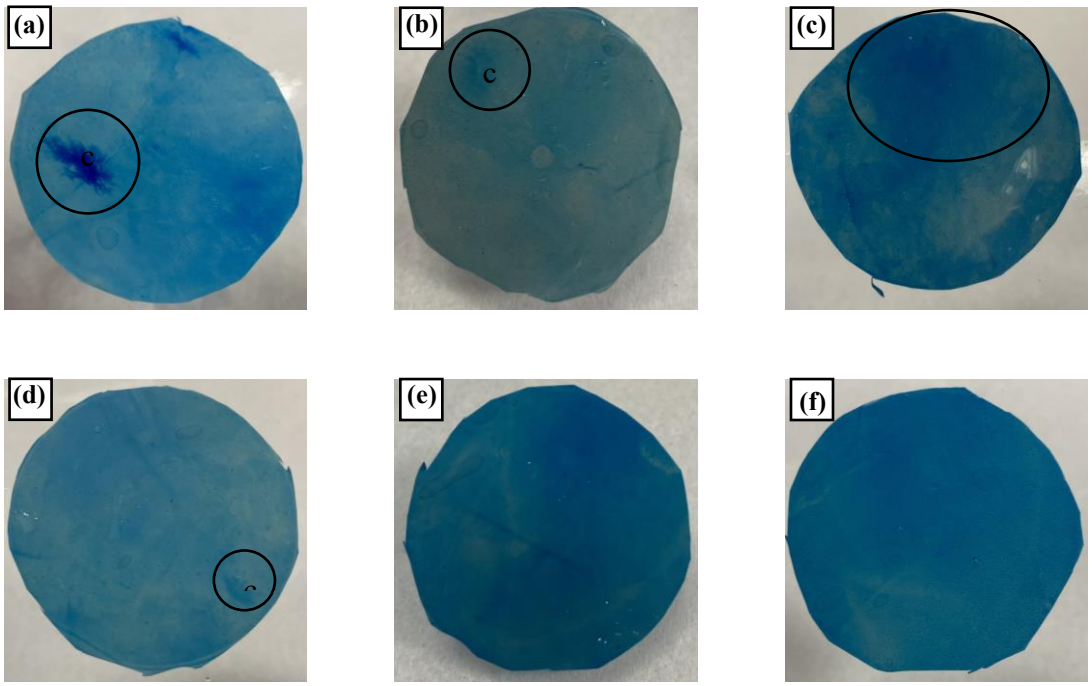

Figure 4.24: Pristine and GR/TiO_2 nanocomposite membranes after MB dye testing, (a) Pristine, (b) 40% GR, (c) 50% GR, (d) 60% GR, (e) 70% GR, (f) 80% GR.

Figure 4.25 depicts the antifouling performance of the pristine and GR/TiO_2 nanocomposite membranes that includes the total fouling, reversible fouling, and irreversible

fouling. Based on Figure 4.25, it can be observed that the incorporation of GR and TiO_2 are able to improve the antifouling properties of the pristine membrane as all of the GR/TiO_2 nanocomposite membrane ratios have less total fouling compared to pristine membrane. Moreover, 80% GR is the best ratio for antifouling performance as the total fouling is only 33.49% compared to pristine membrane which has a total fouling of 72.24%. It is also important to determine the types of fouling whether it is reversible or irreversible fouling. Reversible fouling is loosely attached pollutants on membrane surface that can be removed by simple cleaning methods like backwashing and flushing while irreversible fouling is tightly attached pollutants on membrane surface that requires more vigorous cleaning like chemical cleaning (Hube et al., 2021; Ullah et al., 2021). In addition, repeated chemical cleaning can lead to membrane damage and requires membrane replacement (Ullah et al., 2021). Based on Figure 4.25, it can be observed that 80% GR has the highest reversible fouling compared to irreversible fouling which means that 80% GR only requires simple cleaning process which does not cause damage to the membrane. This is due to the hydrophilic surface of the membrane with the addition of TiO_2 which causes the adherence of dye molecules to be weaker on the nanocomposite membrane surface (Haghighat et al., 2020; Moradi & Zinadini, 2020).

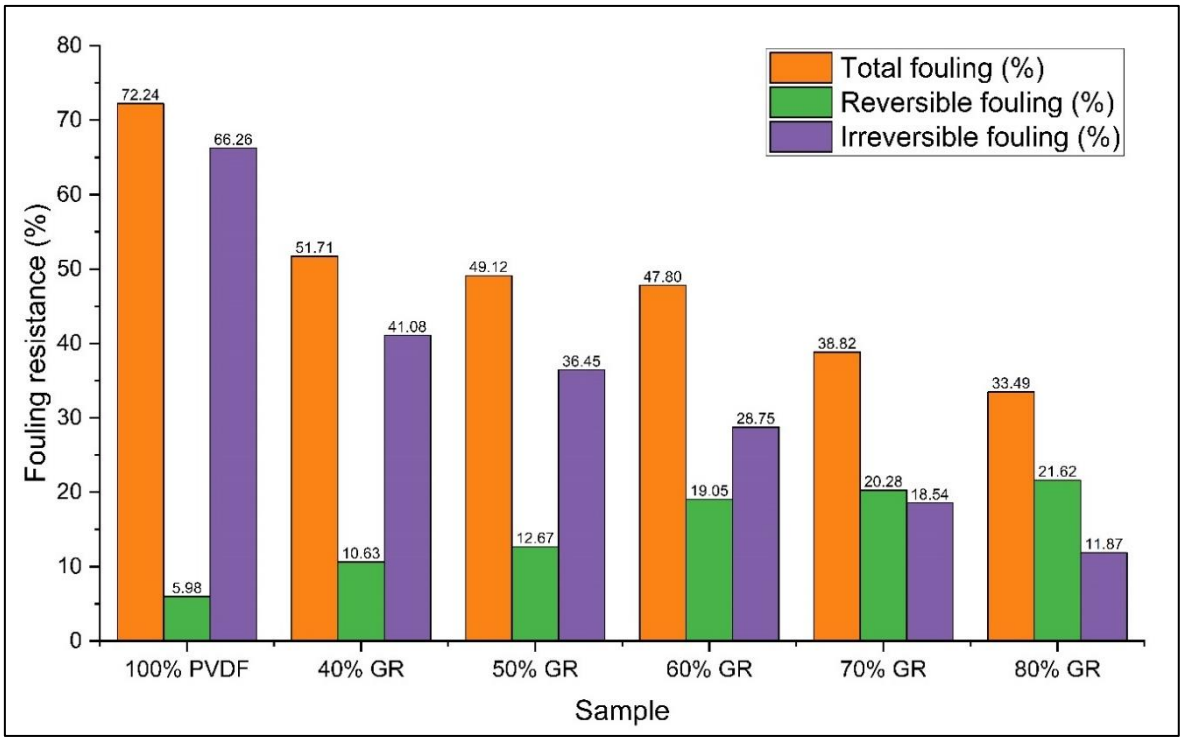

Figure 4.25 The antifouling performance results for pristine and GR/TiO_2 nanocomposite membranes.

Figure 4.26 shows the results of the membrane reusability test for each type of membranes where the reusability test is done by running the membrane with dye rejection test for three cycles. Based on Figure 4.26, it can be observed that 70% GR and 80% GR have the most stability in the reusability test for all three cycles as the membranes are able to retain the MB dye rejection ratio into a similar range with the initial MB dye rejection ratio. This means that the addition of GR and TiO_2 at these two ratios improve the pure PVDF membrane performance which has lower stability during the reusability test. As seen in Figure 4.25, 70% GR and 80% GR still has some fouling, but this can be reduced by backwashing the membrane with water. The high mechanical strength of graphene improves the membrane structure and as a result, the cleaning process does not cause any damage onto the membrane (Memisoglu et al., 2023; Schweizer et al., 2020). Hence, the incorporation of

graphene is able to improve the reusability of the membrane as it able to withstand the cleaning process along with low membrane fouling.

Based on Figure 4.26, it can also be observed that the pristine membrane only removes 36.76% of MB dye in the first cycle compared to its initial removal which is 55.33%. This is due to its high irreversible fouling as seen in Figure 4.25 where this requires vigorous chemical cleaning to improve the fouling of the membrane and improve the reusability. Similarly, 40% GR, 50% GR, 60% GR also has a lower rejection ratio in the first cycle compared to its initial dye rejection ratio. This is due to the agglomeration of nanoparticles causes the membrane structure to become loose which enables the dye molecule to pass through the membrane (Hou et al., 2020). It is reported that Fe (III)/TiO_2 PVDF membrane has an efficiency loss of 8-16% after 3 cycles due to loss of catalytic nanoparticles and reduction of active sites on membrane surface after cyclic uses (C. Yang et al., 2021). It also observed that reduced graphene oxide (rGO)/TiO_2/polyphenylenesulfone (PPSU) membrane is able to maintain the rejection rate at 80% and it declines by 7% after 8 cycles (F. Dai et al., 2021). Similar trend was found in GR/TiO_2 nanocomposite membrane which is supported by the mentioned literature (F. Dai et al., 2021; C. Yang et al., 2021).

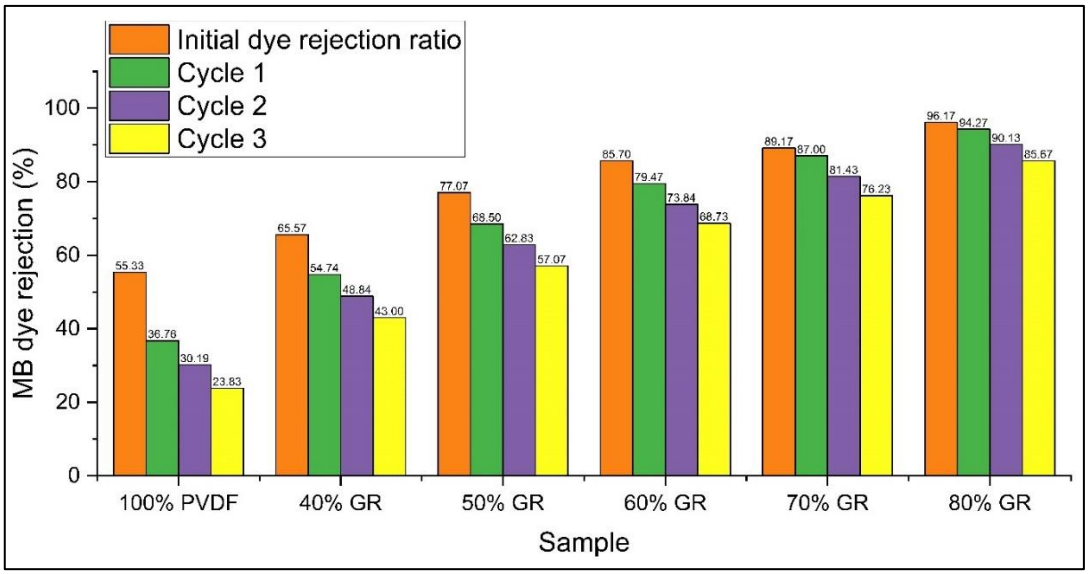

Figure 4.26: The reusability test results for pristine and GR/TiO_2 nanocomposite membranes.

4.4 EXPERIMENT 3: Graphene/Nanocellulose/Titanium Dioxide Polyvinylidene Fluoride (PVDF) Nanocomposite Membrane to Improve Methylene Blue Dye Removal and Antifouling Performance

4.4.1 Introduction

The third experiment is based on the first and second experiment as this experiment combines all three nanomaterials which are NC, GR, and TiO_2 into the PVDF matrix. This specific combination utilizes the key advantages provided by each nanomaterial such as NC contributing hydrophilicity, GR enhancing structure with surface area, as well as TiO_2 for better wettability and antifouling performance, resulting in membranes with more balanced and superior performance. The fabrication of the membrane was done through phase inversion and was characterized by SEM-EDX, XRD, and UV-Vis. The membrane filtration performance was measured as a function of water flux, dye removal, antifouling, and reusability. The focus of this experiment is to investigate the synergistic effects of all three nanomaterials and analyze whether this formulation provides more improvements in performance compared to single or binary nanocomposite membranes.

4.4.2 Methodology

Refer to Chapter 3, with Table 3.3 as the nanocomposite membrane composition.

4.4.3 Results and discussion

4.4.3.1 SEM-EDX Analysis of Nanocomposite Membrane

The scanning electron microscopy (SEM) images of the NC/GR/TiO_2 nanocomposite membrane demonstrate that its morphology is similar to a pure PVDF membrane. Based on Figure 4.27 and 4.28, both membranes are asymmetric and consist of a dense porous upper sublayer and a porous finger-like sublayer which is common in phase inversion membranes (Xia et al., 2024). At higher magnification which is ×5,000, significant differences in the pore structure are observed. The NC/GR/TiO_2 membrane shows a significantly higher density of pores with relatively larger pore sizes compared to the pure PVDF membrane. These differences are due to the presence of hydrophilic nanocellulose and TiO_2 nanoparticles indicating faster solvent and non-solvent exchange during phase inversion, leading to more open macrovoid porous structures (Geleta et al., 2023; J. Zhang et al., 2022).

Interestingly, there were no signs of agglomerations of the nanoparticles in the nanocomposite membrane which shows that NC, GR, and TiO_2 were well dispersed within the polymer matrix. The absence of agglomeration in the nanocomposite membrane is likely due to the hydrophilic nature of nanocellulose and the improved compatibility it provides between the nanoparticles and PVDF matrix. Due to its abundance of hydroxyl groups which is also observed in the FTIR analysis, nanocellulose results in much better dispersion of fillers as well as enhanced interaction with the chains of the polymer making the resultant membrane structure more homogeneous (James, Rahman, et al., 2024; Sueraya et al., 2023). In contrast, it can be observed the pure PVDF membrane shows minimal agglomeration

issue, likely due to slower solvent–non-solvent exchange and lack of nucleating agents during the membrane formation process (FitzPatrick et al., 2025).

Next, the findings of EDX analysis for both membranes are reported in Tables 4.4 and 4.5. The carbon and fluorine values for the pristine PVDF membrane were found to be 90.19% C and 9.81% F respectively, which confirms its chemical structure. The composition of the NC/GR/ TiO_2 membrane deviates from this as carbon was reduced to 84.75% and the membrane contained 3.42% titanium, 2.49% oxygen, and 9.34% fluorine. The addition of Ti and O proves that the incorporation of TiO_2 nanoparticles into the membrane was successful. The incorporation of TiO_2 is able to increase the hydrophilic characteristics of the membrane, along with photocatalytic and antifouling properties (J. Jiang et al., 2022; X. Wang, Li, et al., 2022; Xu et al., 2025). Moreover, the decrease of carbon content in the nanocomposite membrane indicates that the carbonaceous regions of the PVDF structure were substituted with the nanomaterials containing oxygen and titanium.

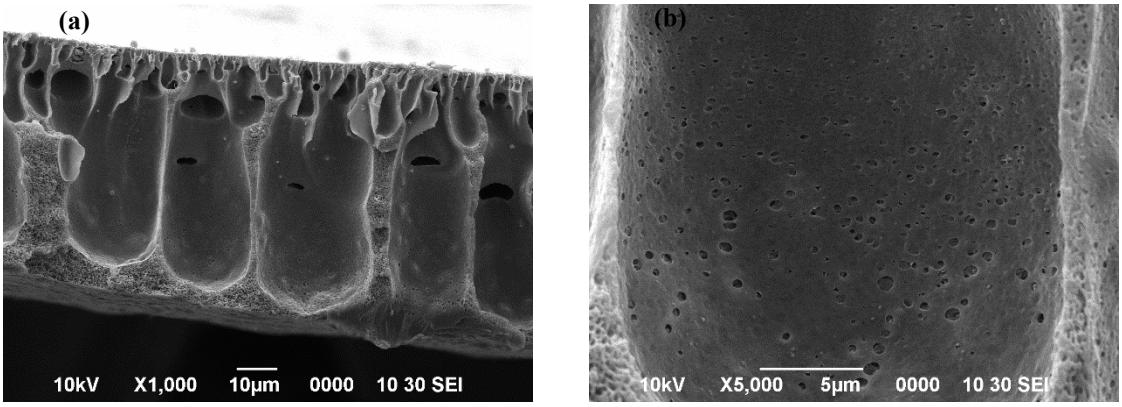

Figure 4.27: SEM analysis of NC/GR/TiO_2 membrane at ×1,000 and ×5,000.

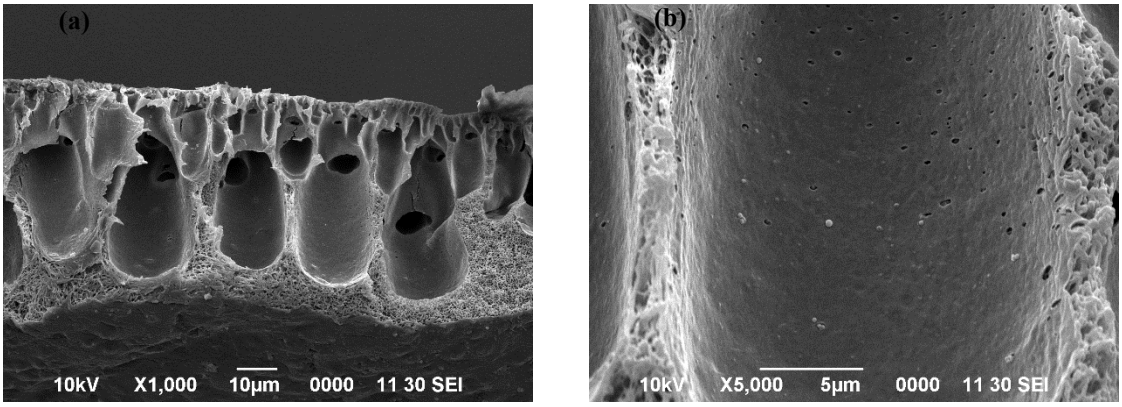

Figure 4.28: SEM analysis of pure PVDF membrane at ×1,000 and ×5,000.

Table 4.4: EDX analysis for pure PVDF membrane.

Elements	Composition (%)
C	90.19
F	9.81

Table 4.5: EDX analysis for NC/GR/TiO_2 membrane.

Elements	Composition (%)
C	84.75
F	9.34
Ti	3.42
O	2.49

4.4.3.2 FTIR Analysis of Nanocomposite Membrane

Figure 4.29 displays the FTIR spectra of both the pure PVDF membrane and the NC/GR/ TiO_2 nanocomposite membrane in the wavenumber interval of 2400 to 400 cm^{-1}. Based on the comparative analysis of the peak characteristics and structure, it can be deduced both membranes display similar peaks which indicates integration of NC, GR, and TiO_2 in the PVDF matrix did not alter the chemical structure of the polymer backbone significantly. This means that the covalent bonding interactions that could potentially form between PVDF and the nanomaterials added do not take place, ensuring intact PVDF membrane structure. Based on Figure 4.29, methylene (CH_2) groups attributed to PVDF polymer have a characteristic peak around 1400 cm^{-1} (M. Ibrahim et al., 2025) while the strong band at approximately 1180 cm^{-1} is assigned to the asymmetric stretching of the CF_2 groups which is a typical vibrational mode of the PVDF crystalline structure (Rihayat et al., 2025). Hence, this peak indicates that the formulation of the nanocomposite membrane does not affect the primary fluorinated carbon backbone of PVDF since this peak is observed in both membranes. In both pristine and nanocomposite membranes, another peak is observed at 1065 cm^{-1} which corresponds to the stretching vibration of hydroxyl (-OH) groups (J. Zhang et al., 2022). This peak confirms the presence of hydrophilic functional groups in the membrane matrix, which were most likely created by the addition of nanocellulose due to its highly -OH group containing structure (Sreedharan et al., 2024). This corresponds with the increase in hydrophilicity and enhancement in antifouling performance associated with NC-based membranes (Taghipour et al., 2024). Another important feature in the spectra is the absorption at 877 cm^{-1} which corresponds to C–C asymmetric stretching as one of the vibrational modes in PVDF (Sueraya et al., 2023). The band around 839 cm^{-1} may also be assigned to CF_2 asymmetric stretch and CH_2 rocking, and it is typical of the β phase

crystalline structure of PVDF (Nie et al., 2024; G. Wang et al., 2024). In summary, the FTIR analysis indicates that the incorporation of NC, GR, and TiO_2 into the PVDF matrix does not change the chemical structure of PVDF functional groups.

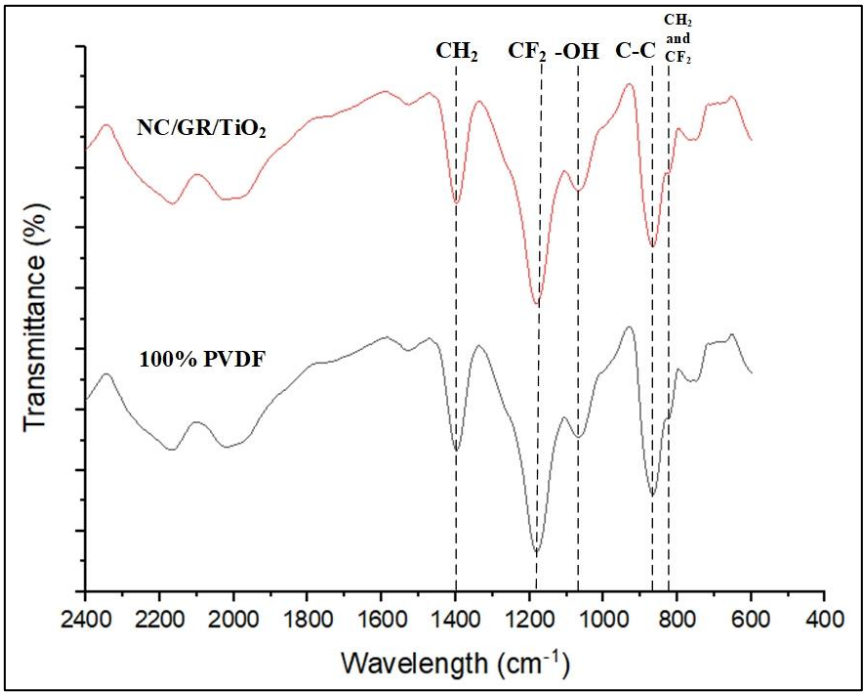

Figure 4.29: FTIR analysis of NC/GR/TiO_2 and pure PVDF membranes.

4.4.3.3 XRD Analysis of Nanocomposite Membrane

Figure 4.30 illustrates the X-ray diffraction (XRD) analysis pertaining to the PVDF membrane and NC/GR/ TiO_2 nanocomposite membrane which were measured over a range of 2θ from 3° to 60°. The diffraction profiles show distinct peaks at 2θ value of 18°, 20°, 38°, and 44° that reflect the crystalline features of the nanocomposite and pristine membranes and the impact of incorporating nanomaterials. The two peaks around 18° and 20° can be noted for distinguishing α-phase of PVDF, (020) and (110) crystallographic planes respectively (Concha et al., 2024). Based on Figure 4.30, the intensity of the two α-phase peaks for both nanocomposite and pristine membranes are similar which indicates that the addition of NC, GR and TiO_2 does not alter the arrangement of crystalline PVDF. This

is because the α-phase is the most thermodynamically stable form out of all crystalline phases of PVDF (Marshall et al., 2021).

Next, the sharp peak on 2θ value of 38° in both membranes are observed which corresponds to the α-phase PVDF crystalline structure to crystal planes (002) (Mohammadpourfazeli et al., 2023). It can be analysed that this peak for NC/GR/TiO_2 decreased in intensity which means that the crystallinity of PVDF is reduced. The reduction in crystallinity can be explained by several synergistic effects. NC with its high surface area and hydrogen bonding capacity, acts as a nucleating agent at low concentrations, but at higher loadings it can impede crystallinity (Janićijević et al., 2024; Xu et al., 2022). Other than that, the rigidity and planar conformation of GR might constrain PVDF chain mobility, thus preventing polymer segments from forming organized crystalline structures (J. hui Yang et al., 2021). In addition, TiO_2 is known to either promote or suppress crystallinity depending on its dispersion as well as interaction with the polymer (Almeida et al., 2024). In this study, the results indicate that the three fillers combinations inevitably conspired to disrupt the crystallization of PVDF, thus yielding lower peak intensities. Out of the sharp peaks, absence of TiO_2 or graphene indicates that these fillers have good dispersion and compatibility with the PVDF matrix without agglomeration which aligns with the SEM findings.

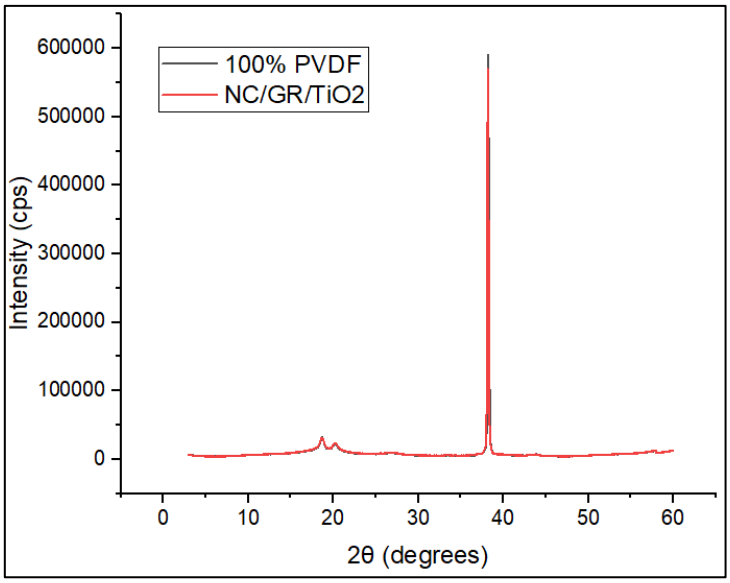

Figure 4.30: XRD analysis of NC/GR/TiO_2 and pure PVDF membranes.

4.4.3.4 Measurement of Membrane Porosity and Mean Pore Size for Nanocomposite Membrane

The porosity and mean pore size of the NC/GR/ TiO_2 as well as the pure PVDF membranes are tabulated in Table 4.6. The results show that NC/GR/ TiO_2 membrane has a greater porosity of 91.37% in comparison to 87.73% for the pure PVDF membrane. This porosity increase aligns with SEM morphological analysis which reveals more profound pore features in the nanocomposite membrane as seen at ×5,000 magnification. The increase in porosity associated with NC/GR/TiO_2 membrane is primarily caused by the synergistic effects of NC combined with TiO_2. The presence of hydroxyl groups in NC facilitates greater water uptake during phase inversion therefore allowing the formation of a porous matrix (Geleta et al., 2023). On top of that, TiO_2 makes porous material because of its active surface, which promotes pore creation by solvent-non-solvent exchange and accelerates phase separation (Geleta et al., 2023). Moreover, the usage of NMP solvent also enhances the porosity of both membranes as NMP is very well known in increasing porosity due to its miscibility with water and its ability to form a thin external skin layer which leads to less

macrovoids and higher overall porosity (Sueraya et al., 2024). In addition, the average pore size of both membranes is between 2-100 nm which is within an ultrafiltration (UF) range, verifying their classification as UF membranes (Qin et al., 2023). Organic dyes and macromolecules are best separated with UF membranes because of their high selectivity and moderate flux, which is beneficial for wastewater treatment (Feng et al., 2022; Siagian et al., 2021). Increasing porosity enhances permeability, but selectivity, antifouling behaviour, and the size of the pores influence the overall behaviour which will be explained in the next section.

Table 4.6: The porosity of GR/NC/TiO_2 nanocomposite membrane.

Sample	Porosity (%)	Pore size (nm)
NC/GR/TiO_2	91.37 ± 0.40	20.82
Pristine	87.73 ± 2.00	4.87

4.4.3.5 Membrane Permeation Test for Nanocomposite Membrane

Figure 4.31 shows the water flux and MB dye rejection performance of the pristine PVDF membrane in comparison to the NC/GR/TiO_2 nanocomposite membrane. According to Figure 4.31 (a), it is clear that the NC/GR/TiO_2 membrane has a water flux greatly surpassing that of the PVDF membrane, with values at 512.76 L/m².h.bar and 109.48 L/m².h.bar, respectively. The drastic enhancement in water permeability is explained by the synergistic effects caused by the nanocomposite fillers. As discussed earlier, the presence of nanocellulosic compounds significantly improves the membrane's hydrophilicity because these structures contain numerous hydroxyl functionalities (Mbakop et al., 2021). GR also plays a role in enhancing porosity and increased permeable resistance because of its 2D geometry and its good compatibility with PVDF at lower concentration (Pusty & Shirage,

2022). The nanoparticles of TiO_2 also enhance the water flux by improving membrane surface roughness and creating more hydrophilic surfaces for easier passage of water (Shawky et al., 2024).

Based on Figure 4.31 (b), NC/GR/ TiO_2 membrane has a greater MB dye removal which is 92.13% compared to PVDF membrane which is only 54.28%. The increase in MB dye removal is significantly better because of the more proficient hydrophilicity, enhanced surface charge interactions and pore structure of the nanocomposite membrane. Both NC and TiO_2 have functional groups that can form hydrogen bonds and electrostatically interact with the dye molecules which allows more effective adsorption and separation of MB dye (Mohammed et al., 2021; Oyarce et al., 2022). In addition, the incorporation of GR improves the MB dye removal as the aromatic structure of the dye is rejected by GR due to its large surface area and π bonds (Ederer et al., 2022). Therefore, the combination of these nanomaterials provides several rejection mechanisms such as size exclusion, surface adsorption, and electrostatic repulsion.

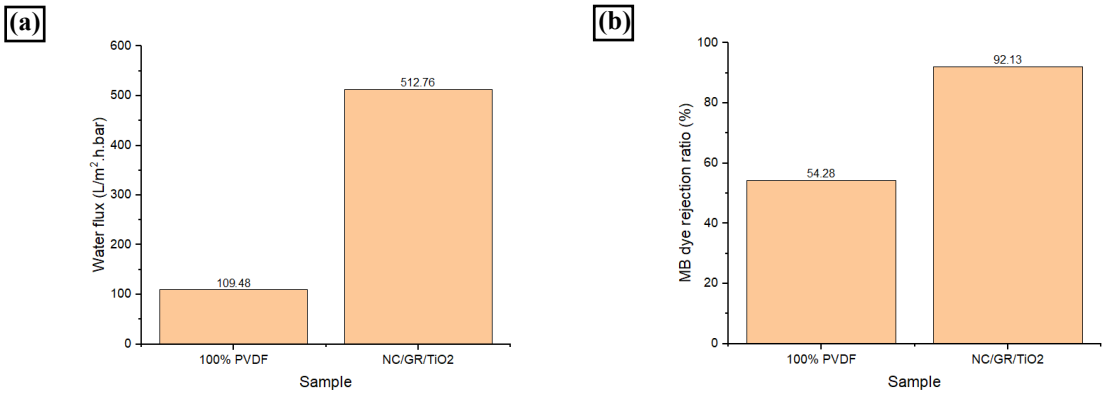

Figure 4.31: The trendline for water flux and MB dye rejection for GR/NC nanocomposite membrane, (a) Water flux, (b) MB dye rejection.

4.4.3.6 Membrane Antifouling and Reusability Test for Nanocomposite Membrane

FRR is an essential indicator of a membrane's antifouling capability and its potential for reuse in long-term applications. Figure 4.32 presents the FRR values of the pristine PVDF membrane and the NC/GR/TiO_2 nanocomposite membrane. The pristine membrane exhibits a relatively low FRR of 35.44%, indicating severe membrane fouling and poor recovery after cleaning. In contrast, the NC/GR/TiO_2 membrane shows a significantly higher FRR of 95.95%, suggesting excellent antifouling performance and effective flux recovery. This significant enhancement in FRR for the nanocomposite membrane can be attributed to its improved surface properties and hydrophilicity. The nanocomposite membrane with the incorporation of NC, GR and TiO_2 is expected to enhance hydrophilic nature of the surface, hence decreasing the surface adhesion of foulants and contaminants making it easier to remove them during the washing phase (Khurram et al., 2021; Steffi et al., 2022). Surfaces with hydrophilic characteristics are known to form a hydration layer that acts as a physical barrier to prevent organic fouling (Xiong et al., 2022). Apart from that, TiO_2 is widely known for its antifouling and self-cleaning properties along with its photocatalytic and hydrophilic characteristics (X. Wang, Li, et al., 2022).

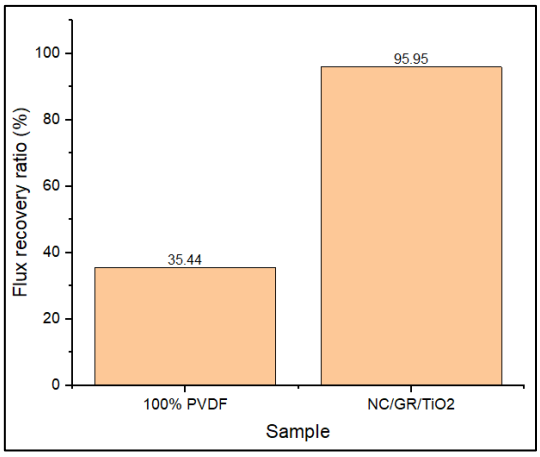

Figure 4.32: Flux recovery ratio of pristine and nanocomposite membrane.

Next, the antifouling performance of both pristine PVDF membrane and NC/GR/TiO_2 nanocomposite membrane was evaluated by analysing the total fouling, reversible fouling, and irreversible fouling ratios as shown in Figure 4.33. Based on the results, it is evident that the NC/GR/TiO_2 membrane exhibits remarkably improved antifouling performance compared to the pristine membrane. The total fouling ratio of the nanocomposite membrane was only 9.05%, whereas the pristine membrane showed a much higher total fouling of 70.89%. This significant reduction indicates that the incorporation of NC, GR, and TiO_2 into the PVDF matrix is able to effectively minimize the membrane fouling.

Furthermore, NC/GR/TiO_2 membrane also displayed a lower irreversible fouling ratio of 4.05% and reversible fouling of 5%, compared to the pristine membrane which exhibited 64.56% irreversible fouling and 6.33% reversible fouling. This shows that most of the fouling on the NC/GR/TiO_2 membrane was weakly adhered and could be easily removed by physical cleaning, such as backwashing with water (S. Park et al., 2022). On the other hand, the high irreversible fouling of the pristine membrane indicates that the dye molecules are strongly adhered into the membrane pores or surfaces, which makes it more difficult to

remove and requires chemical cleaning (Gul et al., 2021). Hence, the results shows that NC/GR/TiO_2 membrane has superior antifouling properties as it is more hydrophilic, has smoother surface morphology, and therefore the membrane material interacts less strongly with dye molecules.

On the other hand, the reusability of the membranes was also tested by subjecting the membranes to one cleaning cycle followed by reuse in MB dye removal. The MB dye rejection ratios are depicted in Figure 4.34 where it demonstrates that the NC/GR/TiO_2 membrane retained a high performance of 86.18% even after reuse, compared to its initial dye rejection of 92.13%, indicating only a slight decrease in performance. In comparison, the pristine membrane showed a major drop in dye rejection ratio from 54.28% to 36.39% even after one cycle. This significant drop in dye removal efficiency is due to the high degree of irreversible fouling observed in the pristine membrane, which leads to severe pore blockage and reduced selectivity (Kallem et al., 2022). Thus, the result in this study shows that incorporation of NC, GR, and TiO_2 into the PVDF membrane improves its antifouling properties and reusability, indicating its potential in practical water treatment applications.

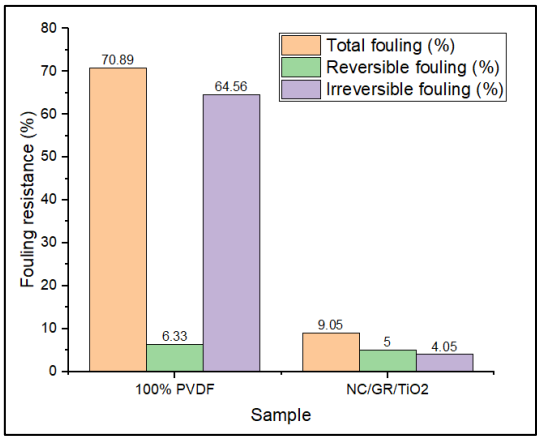

Figure 4.33: Results of total fouling, reversible fouling, and irreversible fouling for pristine and nanocomposite membrane.

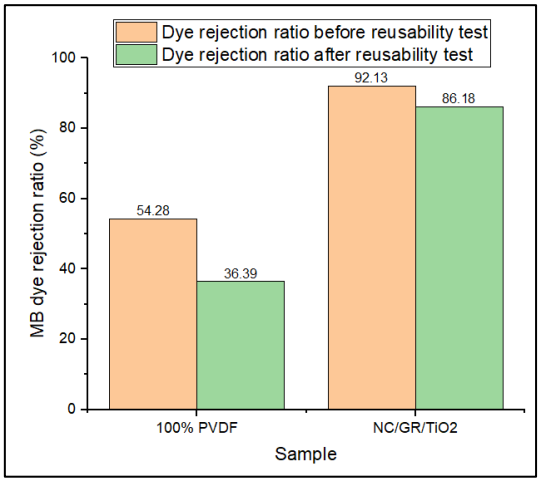

Figure 4.34: Results for membrane reusability test.

CHAPTER 5

CONCLUSION AND RECOMMENDATIONS

5.1 General Summary

This chapter presents all the conclusions made for each experiment including the findings of the study by summarizing all the analysis made based on the three nanocomposite membranes which are GR/NC, GR/TiO_2 and NC/GR/TiO_2. Each study is concluded individually in the following sections based on its contribution in improving the membrane performance such as water permeability, dye rejection, antifouling performance and reusability. The first section highlights GR/NC dye removal capability which emphasises the role of nanocellulose in enhancing porosity and hydrophilicity. Next, the second section concludes the improvement in permeability and antifouling performance by GR/TiO_2 nanocomposite membrane due to GR and TiO_2. Last but not least, the GR/NC/TiO_2 membrane focuses on the synergistic effects of combining all three nanomaterials which offer the most balanced performance across all metrics. Hence, these conclusions will support the objectives of the study in developing PVDF nanocomposite membranes incorporated with NC, GR, and TiO_2 for enhanced methylene blue dye removal along with recommendations for future studies in this field.

5.2 Conclusion

5.2.1 EXPERIMENT 1: Graphene/Nanocellulose Polyvinylidene Fluoride (PVDF) Nanocomposite Membrane to Intensify Methylene Blue Dye Removal and Antifouling Performance

As a conclusion, graphene/nanocellulose PVDF nanocomposite membranes with varying ratios were successfully fabricated, demonstrating high dye removal efficiency and

excellent antifouling performance. Extensive characterization methods were applied to evaluate the membrane performance. The FESEM-EDX analysis shows that 20% GR and 30% GR have no agglomeration in the membrane pores and the nanocomposites are dispersed evenly through the membrane matrix, allowing efficient dye removal. The TEM analysis indicated that the nanocellulose used in the nanocomposite membrane has a rod-like structure with a spherical morphology and this morphology enables the nanocomposite membrane to have better permeation and dye rejection. The XRD analysis revealed that all of the nanocomposite membranes are able to retain the crystallinity of PVDF except for 20% GR and 30% GR. The absence of characteristic PVDF peaks in the 20% GR and 40% GR membranes may indicate changes in PVDF crystallinity, which could contribute to the enhanced separation efficiency of MB dye molecules. Next, the membrane porosity and pore size measurements classified the nanocomposite membranes as UF membranes due to the pore size range, with all ratios displaying high porosities. The membrane permeation test shows that 20% GR exhibited the highest water flux results with the value of is 435.15 ± 1.73 L/m2.h.bar and highest dye removal efficiency which is 94.47% (± 0.16). This indicates that 20% GR has an excellent membrane permeation and selectivity. In addition, the antifouling and reusability test shows that 20% GR has the best antifouling performance as it has a high flux recovery ratio and low total fouling. Based on the total fouling results, all of the nanocomposite membranes have higher reversible fouling than irreversible fouling, enabling the membranes to be reused effectively compared to pristine membrane. Therefore, based on the characterization methods that have been conducted, it can be deduced that 20% GR is the optimum ratio for efficient dye removal and excellent antifouling properties in GR/NC PVDF nanocomposite membrane. There are several limitations that need to be considered for future improvements such as long-term stability of the membrane in industrial

wastewater treatment which contains various types of contaminants as this study only focuses on MB dye removal. Despite these limitations, the excellent dye removal and antifouling properties exhibited by the GR/NC PVDF nanocomposite membrane in this study is a promising approach in improving the membrane technologies for water purification. Hence, future studies should address the limitations mentioned and explore new techniques in the synergistic effects of GR and NC in PVDF membranes in wastewater treatment technologies.

5.2.2 EXPERIMENT 2: Impact of Titanium Dioxide/Graphene in Polyvinylidene Fluoride (PVDF) Nanocomposite Membrane to Intensify Methylene Blue Dye Removal, Antifouling Performance, and Reusability

In conclusion, a novel GR/TiO_2 nanocomposite membrane was produced with excellent dye removal efficiency and antifouling performance. Extensive characterization techniques were conducted to assess the fabricated GR/TiO_2 nanocomposite membranes. Field-emission scanning electron microscopy (FESEM) revealed that membranes containing 80% and 70% GR exhibited increased sponge-like structures compared to other ratios. This, along with energy-dispersive X-ray spectroscopy (EDX) analysis, indicates that reducing TiO_2 content minimizes particle agglomeration, promoting even distribution on the membrane surface. Fourier-transform infrared spectroscopy (FTIR) confirmed the presence of similar functional groups across all membranes despite varying GR/TiO_2 ratios. X-ray diffraction (XRD) analysis, however, highlighted differences in crystallinity. Especially, at 80% GR, the anatase phase of TiO_2 was largely absent, while other membranes retained the characteristic crystallinity of PVDF. For the membrane permeation analysis, graphene incorporation increased membrane porosity, thereby enhancing permeation. Consequently, both membrane flux and methylene blue (MB) dye rejection improved with increasing graphene content. Comprehensive analysis reveals that 80% GR represents the optimal ratio

for GR/TiO_2 composite membranes, maximizing MB dye rejection in PVDF membranes despite varied MB dye concentrations. 80% GR also has the best antifouling properties with flux recovery ratio (FRR) of 88.13%, and total fouling of 33.49%, along with excellent reusability up to 3 cycles. Hence, incorporating graphene and titanium dioxide has demonstrably enhanced the performance of pristine PVDF membranes in terms of porosity, water flux, MB dye rejection, and antifouling performance.

5.2.3 EXPERIMENT 3: Graphene/Nanocellulose/Titanium Dioxide Polyvinylidene Fluoride (PVDF) Nanocomposite Membrane to Improve Methylene Blue Dye Removal and Antifouling Performance

As a conclusion, the performance of the NC/GR/TiO_2 nanocomposite membrane in dye removal alongside its permeability, antifouling properties, and reusability were fabricated and evaluated with success. The developed membrane's characterization confirmed that incorporating NC, GR, and TiO_2 into a PVDF matrix outperformed the pristine PVDF membrane. The SEM-EDX analysis demonstrated the absence of agglomeration and enabled uniform dispersion of the nanoparticles within the membrane structure. This results in improved porosity along with membrane permeability. XRD analysis showed a slight reduction in the intensity of characteristic PVDF peaks in the nanocomposite membrane, possibly indicating reduced crystallinity or structural modification due to the introduction of nanomaterials, which in turn improved membrane hydrophilicity and separation efficiency. Additionally, the water flux of the nanocomposite membrane increased substantially to 512.76 L/m².h.bar, compared to 109.48 L/m².h.bar for the pristine membrane, demonstrating a significant enhancement in permeability. Similarly, the methylene blue (MB) dye rejection efficiency was significantly improved, with the nanocomposite membrane achieving a removal rate of 92.13%, compared to 54.28% for the pristine PVDF. Antifouling performance also improved drastically, with total fouling

reduced from 70.89% in the pristine membrane to only 9.05% in the nanocomposite membrane. The nanocomposite membrane also exhibited a flux recovery ratio (FRR) of 95.95%, far outperforming the pristine membrane with an FRR of 35.44%, indicating excellent antifouling resistance. Reusability tests further confirmed the robustness of the nanocomposite membrane, where it retained 86.18% of its dye rejection capacity after a single cleaning cycle, while the pristine membrane only retained 36.39%. These advancements are mainly due to the synergistic effects of NC, GR, and TiO_2, as the ternary membrane outperformed both binary nanocomposite membranes and the pristine PVDF membrane in permeance, antifouling resistance, and reusability.

5.2.4 Summary

This study successfully fabricated and characterized three PVDF-based nanocomposite membranes with different nanomaterial combinations which are GR/NC, GR/TiO_2, and NC/GR/TiO_2 using the phase inversion method, focusing on improving the conventional PVDF membranes used for water treatment processes. Each combination of nanomaterials was utilised based on their functional properties to enhance membrane performance with regards to permeability, dye rejection, antifouling capability, and reusability.

The first experiment with GR and NC showed the highest efficiency for dye removal at 94.47% percent along with four times increase in water flux compared to the pristine membrane. The uniform dispersion of nanomaterials along with the rod-like morphology of NC contributed to improved antifouling membrane performance and reusability. The membrane containing 20% GR displayed the best antifouling performance identifying it as the optimal loading ratio.

In the second experiment, enhanced antifouling performance and increased water flux were observed with the GR/TiO_2 membranes. The formulation containing 80% GR exhibited the best performance with a sponge-like morphology, low TiO_2 agglomeration, and higher dye rejection compared to other GR/TiO_2 ratios. Furthermore, this membrane showed high flux recovery ratio and maintained reusability over several cycles indicating practical applicability.

The water permeance and dye removal capabilities were highest for the nanocomposite membrane made using all three nanomaterials, NC, GR, and TiO_2 as water flux reached 512.76 L/m²·h·bar with 92.13% dye removal. In industrial filtration systems, the membrane typically operates around 200 until 450 L/m²·h·bar under standard operating pressure with dye removal over 90% as a standard (Patiu et al., 2025; Pundir et al., 2024; Rendón-Castrillón et al., 2023; Shahzad et al., 2021). Moreover, the membrane displayed remarkable antifouling properties with a FRR of 95.95%, retaining structural stability after being reused. Based on high-performance filtration membranes, the FRR typically range from 80% to 95% after cleaning cycles in testing on industrial scale (Awad et al., 2021; Darwish et al., 2023; Z. Li et al., 2025; Osman et al., 2024). The enhancement in hydrophilicity, porosity, and durability was due to the synergistic effects of the three nanomaterials, which performed better than the conventional PVDF membrane.

Flux recovery ratios (FRR) in high-performance ultrafiltration membranes typically range from 92–97% after cleaning cycles in industrial-style testing (Y. C. Lin et al., 2021). My nanocomposite NC/GR/TiO_2/PVDF membrane achieved an FRR of 95.95%, indicating excellent antifouling performance and robust structural stability. These results suggest competitive usability in large-scale applications with reduced cleaning frequency and associated operational costs.

Hence, the incorporation of functional nanomaterials has significantly enhanced the performance of PVDF membranes. In this study, optimal membrane performance was considered based on the high water permeance while maintaining methylene blue rejection above 90% and a flux recovery ratio exceeding 85%. Although the GR/NC membrane yielded the highest dye rejection, the NC/GR/TiO_2 membrane had the best balance and performed excellently in all parameters. These results provide crucial information for designing versatile and high-performance membranes for wastewater treatment and highlight an important starting point towards the future optimization of these membranes for practical use.

5.3 Recommendations

The overall findings of this study showed that the incorporation of NC, GR and TiO_2 into PVDF membranes significantly improves the water flux, dye rejection rate, and antifouling performance of the nanocomposite membranes. Among each of the tested formulations, every nanocomposite membrane demonstrated significant improvements which confirms the potential of the nanomaterials in water purification technologies. Based on these promising results, a few recommendations are proposed to improve the study in this area of research.

i. Future studies should explore other nanomaterial combinations or varying loading ratios of NC, GR, and TiO_2. This can further improve the analysis in efficient synergistic effects of nanomaterial combinations in improving membrane performance especially in water purification systems.
ii. As this study focused on MB dye as a model dye, future studies should include various dye types to analyse the versatility and selectivity of the fabricated membranes in a wide range of industrial wastewater.

iii. Future research should also apply advanced characterization techniques such as contact angle measurements, atomic force microscope (AFM), and mechanical testing. These characterization methods are able to provide a deeper understanding on the surface properties, hydrophilicity, and mechanical strength of the nanocomposite membranes.

REFERENCES

Abdi-Soojeede, M. I., & Nour, D. H. (2022). Assessments of Physical Analysis on Water Quality in Benadir Region, Somalia. *Integrated Journal for Research in Arts and Humanities*, *2*(4), 60–70. https://doi.org/10.55544/ijrah.2.4.48

Abouzeid, R. E., Khiari, R., El-Wakil, N., & Dufresne, A. (2019). Current State and New Trends in the Use of Cellulose Nanomaterials for Wastewater Treatment. In *Biomacromolecules* (Vol. 20, Issue 2, pp. 573–597). American Chemical Society. https://doi.org/10.1021/acs.biomac.8b00839

Agale, P., Salve, V., Arade, S., Balgude, S., & More, P. (2025). Tailoring structural and chemical properties of ZnO@ g-C3N4 nanocomposites through Sr doping: Insights from multi technique characterization. *Solid State Sciences*, *166*(April), 107960. https://doi.org/10.1016/j.solidstatesciences.2025.107960

Ahmed, B., Ashraf Hossain, M., Shamsuddin Ahmed, M., Thakare, J., Kausar, A., Ahmad, I., Zhao, T., Aldaghri, O., & Eisa, M. H. (2023). Graphene in Polymeric Nanocomposite Membranes—Current State and Progress. *Processes 2023, Vol. 11, Page 927*, *11*(3), 927. https://doi.org/10.3390/PR11030927

Al Harby, N. F., El-Batouti, M., & Elewa, M. M. (2022). Prospects of Polymeric Nanocomposite Membranes for Water Purification and Scalability and their Health and Environmental Impacts: A Review. *Nanomaterials 2022, Vol. 12, Page 3637*, *12*(20), 3637. https://doi.org/10.3390/NANO12203637

Alarif, W. M., Shaban, Y. A., Orif, M. I., Ghandourah, M. A., Turki, A. J., Alorfi, H. S., & Tadros, H. R. Z. (2023). Green Synthesis of TiO2 Nanoparticles Using Natural Marine

Extracts for Antifouling Activity. *Marine Drugs*, *21*(2), 62. https://doi.org/10.3390/MD21020062/S1

Ali, G. K., & Omer, K. M. (2022). Molecular imprinted polymer combined with aptamer (MIP-aptamer) as a hybrid dual recognition element for bio(chemical) sensing applications. Review. *Talanta*, *236*, 122878. https://doi.org/10.1016/J.TALANTA.2021.122878

Ali, M. E. A., Wang, L., Wang, X., & Feng, X. (2016). Thin film composite membranes embedded with graphene oxide for water desalination. *Desalination*, *386*, 67–76. https://doi.org/10.1016/j.desal.2016.02.034

Alkhouzaam, A., Qiblawey, H., & Khraisheh, M. (2021). Polydopamine Functionalized Graphene Oxide as Membrane Nanofiller: Spectral and Structural Studies. *Membranes 2021, Vol. 11, Page 86*, *11*(2), 86. https://doi.org/10.3390/MEMBRANES11020086

Almeida, M. L. A., Fernandes, M. A., Palhares, H. G., Silva, L. M. C., Xavier, L. G. O., Matencio, T., Silva, L. A., Faria, L. O., de Castro, V. G., de Souza, T. C., Houmard, M., & Nunes, E. H. M. (2024). Structural, electrical, and wettability properties of self-supporting PVDF/TiO2/GO composite films obtained by a solvent evaporation route. *REM - International Engineering Journal*, *77*(2), e230014. https://doi.org/10.1590/0370-44672023770014

AlShammari, A. S., Halim, M. M., Yam, F. K., & Kaus, N. H. M. (2020). Effect of precursor concentration on the performance of UV photodetector using TiO2/reduced graphene oxide (rGO) nanocomposite. *Results in Physics*, *19*, 103630. https://doi.org/10.1016/J.RINP.2020.103630

Alyarnezhad, S., Marino, T., Parsa, J. B., Galiano, F., Ursino, C., Garcìa, H., Puche, M., & Figoli, A. (2020). Polyvinylidene Fluoride-Graphene Oxide Membranes for Dye Removal under Visible Light Irradiation. *Polymers 2020, Vol. 12, Page 1509*, *12*(7), 1509. https://doi.org/10.3390/POLYM12071509

Anand, A., Meena, D., Dey, K. K., & Bhatnagar, M. C. (2020). Enhanced piezoelectricity properties of reduced graphene oxide (RGO) loaded polyvinylidene fluoride (PVDF) nanocomposite films for nanogenerator application. *Journal of Polymer Research*, *27*(12), 1–11. https://doi.org/10.1007/S10965-020-02323-X/METRICS

Anis, S. F., Hashaikeh, R., & Hilal, N. (2019). Microfiltration membrane processes: A review of research trends over the past decade. *Journal of Water Process Engineering*, *32*. https://doi.org/10.1016/J.JWPE.2019.100941

Armano, A., & Agnello, S. (2019). Two-Dimensional Carbon: A Review of Synthesis Methods, and Electronic, Optical, and Vibrational Properties of Single-Layer Graphene. *C 2019, Vol. 5, Page 67*, *5*(4), 67. https://doi.org/10.3390/C5040067

Ashfaq, J., Channa, I. A., Memon, A. G., Chandio, I. A., Chandio, A. D., Shar, M. A., Alsalhi, M. S., & Devanesan, S. (2023). Enhancement of Thermal and Gas Barrier Properties of Graphene-Based Nanocomposite Films. *ACS Omega*, *8*(44), 41054–41063. https://doi.org/10.1021/ACSOMEGA.3C02885

Ashok Kumar, S. S., Bashir, S., Ramesh, K., & Ramesh, S. (2022). A comprehensive review: Super hydrophobic graphene nanocomposite coatings for underwater and wet applications to enhance corrosion resistance. *FlatChem*, *31*, 100326. https://doi.org/10.1016/J.FLATC.2021.100326

Asif, K., Lock, S. S. M., Taqvi, S. A. A., Jusoh, N., Yiin, C. L., & Chin, B. L. F. (2023). A molecular simulation study on amine-functionalized silica/polysulfone mixed matrix membrane for mixed gas separation. *Chemosphere*, *311*, 136936. https://doi.org/10.1016/J.CHEMOSPHERE.2022.136936

Asif Khan, R. M., Ahmad, N. M., Nasir, H., Mahmood, A., Iqbal, M., & Janjua, H. A. (2023). Antifouling and Water Flux Enhancement in Polyethersulfone Ultrafiltration Membranes by Incorporating Water-Soluble Cationic Polymer of Poly [2-(Dimethyl amino) ethyl Methacrylate]. *Polymers*, *15*(13). https://doi.org/10.3390/POLYM15132868

Awad, E. S., Sabirova, T. M., Tretyakova, N. A., Alsalhy, Q. F., Figoli, A., & Salih, I. K. (2021). A Mini-Review of Enhancing Ultrafiltration Membranes (UF) for Wastewater Treatment: Performance and Stability. *ChemEngineering 2021, Vol. 5, Page 34*, *5*(3), 34. https://doi.org/10.3390/CHEMENGINEERING5030034

Aziz, S., & Abdel-Karim, A. (2023). Dual-functional ultrafiltration biocatalytic membrane containing laccase/ nanoparticle for removal of pollutants: A review. *Environmental Nanotechnology, Monitoring and Management*, *20*(March), 100852. https://doi.org/10.1016/j.enmm.2023.100852

Baghel, S. S., & Baranwal, E. (2022). Analyzing the Degradation of Rivers Using GI Science. *GIScience for the Sustainable Management of Water Resources*, 267–290. https://doi.org/10.1201/9781003284512-17

Basko, A., Lebedeva, T., Yurov, M., Ilyasova, A., Elyashevich, G., Lavrentyev, V., Kalmykov, D., Volkov, A., & Pochivalov, K. (2023). Mechanism of PVDF Membrane

Formation by NIPS Revisited: Effect of Precipitation Bath Nature and Polymer–Solvent Affinity. *Polymers*, *15*(21). https://doi.org/10.3390/polym15214307

Ben Dassi, R., & Chamam, B. (2025). Nanomaterial-enhanced membranes for advanced water and wastewater treatment: a comprehensive review. *Reviews in Environmental Science and Bio/Technology 2025*, 1–35. https://doi.org/10.1007/S11157-025-09723-9

Berg, T. van den, & Ulbricht, M. (2020). Polymer Nanocomposite Ultrafiltration Membranes: The Influence of Polymeric Additive, Dispersion Quality and Particle Modification on the Integration of Zinc Oxide Nanoparticles into Polyvinylidene Difluoride Membranes. *Membranes*, *10*(9), 1–19. https://doi.org/10.3390/MEMBRANES10090197

Bilal, A., Yasin, M., Akhtar, F. H., Gilani, M. A., Alhmohamadi, H., Younas, M., Mushtaq, A., Aslam, M., Hassan, M., Nawaz, R., Aqsha, A., Sunarso, J., Bilad, M. R., & Khan, A. L. (2024). Enhancing Water Purification by Integrating Titanium Dioxide Nanotubes into Polyethersulfone Membranes for Improved Hydrophilicity and Anti-Fouling Performance. *Membranes 2024, Vol. 14, Page 116*, *14*(5), 116. https://doi.org/10.3390/MEMBRANES14050116

Bohr, S. J., Wang, F., Metze, M., Vukušić, J. L., Sapalidis, A., Ulbricht, M., Nestler, B., & Barbe, S. (2023). State-of-the-art review of porous polymer membrane formation characterization—How numerical and experimental approaches dovetail to drive innovation. *Frontiers in Sustainability*, *4*, 1093911. https://doi.org/10.3389/FRSUS.2023.1093911/BIBTEX

Bortot Coelho, F. E., Deemter, D., Candelario, V. M., Boffa, V., Malato, S., & Magnacca, G. (2021). Development of a photocatalytic zirconia-titania ultrafiltration membrane with

anti-fouling and self-cleaning properties. *Journal of Environmental Chemical Engineering*, *9*(6), 106671. https://doi.org/10.1016/J.JECE.2021.106671

Boruah, P., Gupta, R., & Katiyar, V. (2023). Fabrication of cellulose nanocrystal (CNC) from waste paper for developing antifouling and high-performance polyvinylidene fluoride (PVDF) membrane for water purification. *Carbohydrate Polymer Technologies and Applications*, *5*, 100309. https://doi.org/10.1016/J.CARPTA.2023.100309

Brinkmann, T., & Filiz, V. (2021). Organic Solvent Nanofiltration. *Nanofiltration: Principles, Applications, and New Materials: Volume 1 and 2*, *1–2*, 889–932. https://doi.org/10.1002/9783527824984.CH20;JOURNAL:JOURNAL:BOOKS;WGROUP:STRING:PUBLICATION

Cevallos-Mendoza, J., Amorim, C. G., Rodríguez-Díaz, J. M., & Montenegro, M. da C. B. S. M. (2022). Removal of Contaminants from Water by Membrane Filtration: A Review. *Membranes 2022, Vol. 12, Page 570*, *12*(6), 570. https://doi.org/10.3390/MEMBRANES12060570

Chakrabarty, T., Giri, A. K., & Sarkar, S. (2022). Mixed-matrix gas separation membranes for sustainable future: A mini review. *Polymers for Advanced Technologies*, *33*(6), 1747–1761. https://doi.org/10.1002/PAT.5645

Chakraborty, M., & Hashmi, M. S. J. (2018). Graphene as a Material – An Overview of Its Properties and Characteristics and Development Potential for Practical Applications. *Reference Module in Materials Science and Materials Engineering*. https://doi.org/10.1016/B978-0-12-803581-8.10319-4

Chandio, T. A., Khan, M. N., Muhammad, M. T., Yalcinkaya, O., Wasim, A. A., & Kayis, A. F. (2020). Fluoride and arsenic contamination in drinking water due to mining activities

and its impact on local area population. *Environmental Science and Pollution Research 2020 28:2*, *28*(2), 2355–2368. https://doi.org/10.1007/S11356-020-10575-9

Cheng, L., Li, L., Pei, X., Ma, Y., Liu, F., & Li, J. (2022). PVDF/MOFs mixed matrix ultrafiltration membrane for efficient water treatment. *Frontiers in Chemistry*, *10*, 985750. https://doi.org/10.3389/FCHEM.2022.985750/BIBTEX

Concha, V. O. C., Timóteo, L., Duarte, L. A. N., Bahú, J. O., Munoz, F. L., Silva, A. P., Lodi, L., Severino, P., León-Pulido, J., & Souto, E. B. (2024). Properties, characterization and biomedical applications of polyvinylidene fluoride (PVDF): a review. *Journal of Materials Science 2024 59:31*, *59*(31), 14185–14204. https://doi.org/10.1007/S10853-024-10046-3

Cosquer, R., Pruvost, S., & Gouanvé, F. (2021). Improvement of Barrier Properties of Biodegradable Polybutylene Succinate/Graphene Nanoplatelets Nanocomposites Prepared by Melt Process. *Membranes 2021, Vol. 11, Page 151*, *11*(2), 151. https://doi.org/10.3390/MEMBRANES11020151

Crini, G., & Lichtfouse, E. (2018). Advantages and disadvantages of techniques used for wastewater treatment. *Environmental Chemistry Letters 2018 17:1*, *17*(1), 145–155. https://doi.org/10.1007/S10311-018-0785-9

Cui, J., Xie, A., Yan, Z., & Yan, Y. (2021). Fabrication of crosslinking modified PVDF/GO membrane with acid, alkali and salt resistance for efficient oil-water emulsion separation. *Separation and Purification Technology*, *265*(February), 118528. https://doi.org/10.1016/j.seppur.2021.118528

Dai, F., Zhang, S., Wang, Q., Chen, H., Chen, C., Qian, G., & Yu, Y. (2021). Preparation and Characterization of Reduced Graphene Oxide /TiO2 Blended Polyphenylene sulfone

Antifouling Composite Membrane With Improved Photocatalytic Degradation Performance. *Frontiers in Chemistry*, *9*, 753741. https://doi.org/10.3389/FCHEM.2021.753741/BIBTEX

Dai, Z., Ottesen, V., Deng, J., Helberg, R. M. L., & Deng, L. (2019). A brief review of nanocellulose based hybrid membranes for CO2 separation. In *Fibers* (Vol. 7, Issue 5). MDPI Multidisciplinary Digital Publishing Institute. https://doi.org/10.3390/FIB7050040

Darwish, N. Bin, Alalawi, A., Alromaih, H., Alotaibi, N., & Aleid, M. (2023). Synthesis and performance of ultrafiltration membranes incorporated with different oxide nanomaterials: experiments and modeling. *Water Reuse*, *13*(3), 492–505. https://doi.org/10.2166/WRD.2023.092/1287024/JWRD2023092.PDF

Davari, S., Omidkhah, M., & Salari, S. (2021). Role of polydopamine in the enhancement of binding stability of TiO2 nanoparticles on polyethersulfone ultrafiltration membrane. *Colloids and Surfaces A: Physicochemical and Engineering Aspects*, *622*, 126694. https://doi.org/10.1016/J.COLSURFA.2021.126694

Devrim, Y., & Bulanık Durmuş, G. N. (2022). Composite membrane by incorporating sulfonated graphene oxide in polybenzimidazole for high temperature proton exchange membrane fuel cells. *International Journal of Hydrogen Energy*, *47*(14), 9004–9017. https://doi.org/10.1016/J.IJHYDENE.2021.12.257

Dharma, H. N. C., Jaafar, J., Widiastuti, N., Matsuyama, H., Rajabsadeh, S., Othman, M. H. D., Rahman, M. A., Jafri, N. N. M., Suhaimin, N. S., Nasir, A. M., & Alias, N. H. (2022). A Review of Titanium Dioxide (TiO2)-Based Photocatalyst for Oilfield-

Produced Water Treatment. *Membranes 2022, Vol. 12, Page 345*, *12*(3), 345. https://doi.org/10.3390/MEMBRANES12030345

Dias, I. K. R., Lacerda, B. K., & Arantes, V. (2023). High-yield production of rod-like and spherical nanocellulose by controlled enzymatic hydrolysis of mechanically pretreated cellulose. *International Journal of Biological Macromolecules*, *242*, 125053. https://doi.org/10.1016/J.IJBIOMAC.2023.125053

Dong, Q., Zhang, X., Qian, J., He, S., Mao, Y., Brozena, A. H., Zhang, Y., Pollard, T. P., Borodin, O. A., Wang, Y., Chava, B. S., Das, S., Zavalij, P., Segre, C. U., Zhu, D., Xu, L., Liang, Y., Yao, Y., Briber, R. M., … Hu, L. (2022). A cellulose-derived supramolecule for fast ion transport. *Science Advances*, *8*(49). https://doi.org/10.1126/SCIADV.ADD2031;ISSUE:ISSUE:DOI

Dzinun, H., Ichikawa, Y., Honda, M., & Zhang, Q. (2020). Efficient Immobilised TiO2 in Polyvinylidene fluoride (PVDF) Membrane for Photocatalytic Degradation of Methylene Blue. *Journal of Membrane Science and Research*, *6*(2), 188–195. https://doi.org/10.22079/JMSR.2019.106656.1263

Eddy, D. R., Permana, M. D., Sakti, L. K., Sheha, G. A. N., Solihudin, G. A. N., Hidayat, S., Takei, T., Kumada, N., & Rahayu, I. (2023). Heterophase Polymorph of TiO2 (Anatase, Rutile, Brookite, TiO2 (B)) for Efficient Photocatalyst: Fabrication and Activity. *Nanomaterials 2023, Vol. 13, Page 704*, *13*(4), 704. https://doi.org/10.3390/NANO13040704

Ederer, J., Ecorchard, P., Slušná, M. Š., Tolasz, J., Smržová, D., Lupínková, S., & Janoš, P. (2022). A Study of Methylene Blue Dye Interaction and Adsorption by Monolayer

Graphene Oxide. *Adsorption Science & Technology*, *2022*. https://doi.org/10.1155/2022/7385541

Egan, J., & Salmon, S. (2021). Strategies and progress in synthetic textile fiber biodegradability. *SN Applied Sciences 2021 4:1*, *4*(1), 1–36. https://doi.org/10.1007/S42452-021-04851-7

El-Gendi, H., Taha, T. H., Ray, J. B., & Saleh, A. K. (2022). Recent advances in bacterial cellulose: a low-cost effective production media, optimization strategies and applications. *Cellulose 2022 29:14*, *29*(14), 7495–7533. https://doi.org/10.1007/S10570-022-04697-1

El-hadi, A. M. (2017). Increase the elongation at break of poly (lactic acid) composites for use in food packaging films. *Scientific Reports*, *7*(1), 46767. https://doi.org/10.1038/srep46767

Ezugbe, E. O., & Rathilal, S. (2020). Membrane Technologies in Wastewater Treatment: A Review. *Membranes*, *10*(5). https://doi.org/10.3390/MEMBRANES10050089

Faiz Norrrahim, M. N., Mohd Kasim, N. A., Knight, V. F., Mohamad Misenan, M. S., Janudin, N., Ahmad Shah, N. A., Kasim, N., Wan Yusoff, W. Y., Mohd Noor, S. A., Jamal, S. H., Ong, K. K., & Zin Wan Yunus, W. M. (2021). Nanocellulose: a bioadsorbent for chemical contaminant remediation. *RSC Advances*, *11*(13), 7347. https://doi.org/10.1039/D0RA08005E

Farooq, N., Kallem, P., ur Rehman, Z., Imran Khan, M., Kumar Gupta, R., Tahseen, T., Mushtaq, Z., Ejaz, N., & Shanableh, A. (2024). Recent trends of titania (TiO2) based materials: A review on synthetic approaches and potential applications. *Journal of King*

Saud University - Science, *36*(6), 103210. https://doi.org/10.1016/J.JKSUS.2024.103210

Feng, X., Peng, D., Zhu, J., Wang, Y., & Zhang, Y. (2022). Recent advances of loose nanofiltration membranes for dye/salt separation. *Separation and Purification Technology*, *285*, 120228. https://doi.org/10.1016/J.SEPPUR.2021.120228

FitzPatrick, J., Bera, S., Inman, A., Cabrera, A., Zhang, T., Parker, T., Mohammadlou, B. S., Roslyk, I., Ippolito, S., Shevchuk, K., Kadam, S. A., Pradhan, N. R., & Gogotsi, Y. (2025). Record Efficiency of β-Phase PVDF-MXene Composites in Thin-Film Dielectric Capacitors. *Advanced Materials*, *37*(12), 2419088. https://doi.org/10.1002/ADMA.202419088

Flamm, D. (2019, February 5). Meeting new challenges in pharmaceutical freeze-drying. *Processing*. https://www.processingmagazine.com/home/article/15587676/meeting-new-challenges-in-pharmaceutical-freezedrying

Fortunato, M., Bellagamba, I., Tamburrano, A., & Sarto, M. S. (2020). Flexible Ecoflex®/Graphene Nanoplatelet Foams for Highly Sensitive Low-Pressure Sensors. *Sensors 2020, Vol. 20, Page 4406*, *20*(16), 4406. https://doi.org/10.3390/S20164406

Frallicciardi, J., Melcr, J., Siginou, P., Marrink, S. J., & Poolman, B. (2022). Membrane thickness, lipid phase and sterol type are determining factors in the permeability of membranes to small solutes. *Nature Communications 2022 13:1*, *13*(1), 1–12. https://doi.org/10.1038/s41467-022-29272-x

Gan, P. G., Sam, S. T., Abdullah, M. F. bin, & Omar, M. F. (2020). Thermal properties of nanocellulose-reinforced composites: A review. *Journal of Applied Polymer Science*, *137*(11), 48544. https://doi.org/10.1002/APP.48544

Garg, M. C., Kumari, S., & Malik, N. (2024). Role of nanomaterials in advanced membrane technologies for groundwater purification. *Environmental Science: Water Research & Technology*, *10*(11), 2628–2645. https://doi.org/10.1039/D4EW00353E

Gayatri, R., Fizal, A. N. S., Yuliwati, E., Hossain, M. S., Jaafar, J., Zulkifli, M., Taweepreda, W., & Ahmad Yahaya, A. N. (2023). Preparation and Characterization of PVDF–TiO2 Mixed-Matrix Membrane with PVP and PEG as Pore-Forming Agents for BSA Rejection. *Nanomaterials 2023, Vol. 13, Page 1023*, *13*(6), 1023. https://doi.org/10.3390/NANO13061023

Ge, J., Zhang, Y., Heo, Y. J., & Park, S. J. (2019). Advanced design and synthesis of composite photocatalysts for the remediation of wastewater: A review. In *Catalysts* (Vol. 9, Issue 2). MDPI. https://doi.org/10.3390/catal9020122

Geleta, T. A., Maggay, I. V., Chang, Y., & Venault, A. (2023). Recent Advances on the Fabrication of Antifouling Phase-Inversion Membranes by Physical Blending Modification Method. *Membranes 2023, Vol. 13, Page 58*, *13*(1), 58. https://doi.org/10.3390/MEMBRANES13010058

Geng, H., Zhang, W., Zhao, X., Shao, W., & Wang, H. (2024). Research on Reverse Osmosis (RO)/Nanofiltration (NF) Membranes Based on Thin Film Composite (TFC) Structures: Mechanism, Recent Progress and Application. *Membranes 2024, Vol. 14, Page 190*, *14*(9), 190. https://doi.org/10.3390/MEMBRANES14090190

Giakoumis, T., Vaghela, C., & Voulvoulis, N. (2020). The role of water reuse in the circular economy. *Advances in Chemical Pollution, Environmental Management and Protection*, *5*, 227–252. https://doi.org/10.1016/BS.APMP.2020.07.013

Gohil, J. M., & Choudhury, R. R. (2019). Introduction to Nanostructured and Nano-enhanced Polymeric Membranes: Preparation, Function, and Application for Water Purification. *Nanoscale Materials in Water Purification*, 25–57. https://doi.org/10.1016/B978-0-12-813926-4.00038-0

Gontarek-castro, E., Di Luca, G., Lieder, M., & Gugliuzza, A. (2022). Graphene-Coated PVDF Membranes: Effects of Multi-Scale Rough Structure on Membrane Distillation Performance. *Membranes 2022, Vol. 12, Page 511*, *12*(5), 511. https://doi.org/10.3390/MEMBRANES12050511

Gontarek-Castro, E., Rybarczyk, M. K., Castro-Muñoz, R., Morales-Jiménez, M., Barragán-Huerta, B., & Lieder, M. (2021). Characterization of PVDF/Graphene Nanocomposite Membranes for Water Desalination with Enhanced Antifungal Activity. *Water 2021, Vol. 13, Page 1279*, *13*(9), 1279. https://doi.org/10.3390/W13091279

Gopakumar, D. A., Arumughan, V., Pasquini, D., Leu, S. Y., Abdul Khalil, H. P. S., & Thomas, S. (2019). Nanocellulose-Based Membranes for Water Purification. In *Nanoscale Materials in Water Purification* (pp. 59–85). Elsevier. https://doi.org/10.1016/B978-0-12-813926-4.00004-5

Goyat, R., Singh, J., Umar, A., Saharan, Y., Ibrahim, A. A., Akbar, S., & Baskoutas, S. (2024). Synthesis and characterization of nanocomposite based polymeric membrane (PES/PVP/GO-TiO2) and performance evaluation for the removal of various antibiotics (amoxicillin, azithromycin & ciprofloxacin) from aqueous solution. *Chemosphere*, *353*, 141542. https://doi.org/10.1016/J.CHEMOSPHERE.2024.141542

Gul, A., Hruza, J., & Yalcinkaya, F. (2021). Fouling and Chemical Cleaning of Microfiltration Membranes: A Mini-Review. *Polymers 2021, Vol. 13, Page 846*, *13*(6), 846. https://doi.org/10.3390/POLYM13060846

Haghighat, N., Vatanpour, V., Sheydaei, M., & Nikjavan, Z. (2020). Preparation of a novel polyvinyl chloride (PVC) ultrafiltration membrane modified with Ag/TiO2 nanoparticle with enhanced hydrophilicity and antibacterial activities. *Separation and Purification Technology*, *237*, 116374. https://doi.org/10.1016/J.SEPPUR.2019.116374

Han, J., Wang, S., Zhu, S., Huang, C., Yue, Y., Mei, C., Xu, X., & Xia, C. (2019). Electrospun Core-Shell Nanofibrous Membranes with Nanocellulose-Stabilized Carbon Nanotubes for Use as High-Performance Flexible Supercapacitor Electrodes with Enhanced Water Resistance, Thermal Stability, and Mechanical Toughness. *ACS Applied Materials and Interfaces*, *11*(47), 44624–44635. https://doi.org/10.1021/ACSAMI.9B16458/SUPPL_FILE/AM9B16458_SI_001.PDF

He, G., Li, H., Zhao, Z., Liu, Q., Yu, J., Ji, Z., Ning, X., & Ning, F. (2024). Antifouling coatings based on the synergistic action of biogenic antimicrobial agents and low surface energy silicone resins and their application to marine aquaculture nets. *Progress in Organic Coatings*, *195*, 108656. https://doi.org/10.1016/J.PORGCOAT.2024.108656

Holilah, H., Bahruji, H., Ediati, R., Asranudin, A., Jalil, A. A., Piluharto, B., Nugraha, R. E., & Prasetyoko, D. (2022). Uniform rod and spherical nanocrystalline celluloses from hydrolysis of industrial pepper waste (Piper nigrum L.) using organic acid and inorganic acid. *International Journal of Biological Macromolecules*, *204*, 593–605. https://doi.org/10.1016/j.ijbiomac.2022.02.045

Hou, J., Chen, Y., Shi, W., Bao, C., & Hu, X. (2020). Graphene oxide/methylene blue composite membrane for dyes separation: Formation mechanism and separation performance. *Applied Surface Science*, *505*, 144145. https://doi.org/10.1016/J.APSUSC.2019.144145

Hu, Y., Yue, M., Yuan, F., Yang, L., Chen, C., & Sun, D. (2021). Bio-inspired fabrication of highly permeable and anti-fouling ultrafiltration membranes based on bacterial cellulose for efficient removal of soluble dyes and insoluble oils. *Journal of Membrane Science*, *621*, 118982. https://doi.org/10.1016/J.MEMSCI.2020.118982

Huang, H., Xu, Y., Lu, Z., Zhang, A., Zhang, D., Xue, H., Dong, P., Zhang, J., & Goto, T. (2022). Highly permeable and dye-rejective nanofiltration membranes of TiO2and Bi2S3double-embedded Ti3C2Txwith a visible-light-induced self-cleaning ability. *Journal of Materials Research and Technology*, *18*, 4156–4168. https://doi.org/10.1016/j.jmrt.2022.04.104

Huang, Y., Yang, P., Yang, F., & Chang, C. (2021). Self-supported nanoporous lysozyme/nanocellulose membranes for multifunctional wastewater purification. *Journal of Membrane Science*, *635*, 119537. https://doi.org/10.1016/J.MEMSCI.2021.119537

Hube, S., Wang, J., Sim, L. N., Chong, T. H., & Wu, B. (2021). Direct membrane filtration of municipal wastewater: Linking periodical physical cleaning with fouling mechanisms. *Separation and Purification Technology*, *259*, 118125. https://doi.org/10.1016/J.SEPPUR.2020.118125

Huo, K., Wang, J., Zhang, J., Zhao, Y., Liu, S., Dou, M., Wang, X., Zhang, Q., Han, C., Wang, W., Zhou, C., & Xu, Y. (2023). Fabrication of a novel composite nanofiltration

membrane with effective treating dye wastewater via integration of phase inversion and interfacial polymerization. *Journal of Environmental Chemical Engineering*, *11*(5), 111013. https://doi.org/10.1016/J.JECE.2023.111013

Hussain, C. M., Paulraj, M. S., & Nuzhat, S. (2022). Source reduction, waste minimization, and cleaner technologies. *Source Reduction and Waste Minimization*, 23–59. https://doi.org/10.1016/B978-0-12-824320-6.00002-2

Hussain, S., Khan, N., Gul, S., Khan, S., Khan, H., Hussain, S., Khan, N., Gul, S., Khan, S., & Khan, H. (2019). Contamination of Water Resources by Food Dyes and Its Removal Technologies. *Water Chemistry*. https://doi.org/10.5772/INTECHOPEN.90331

Ibrahim, M., Statnik, E. S., Sadykova, I. A., Kovaleva, P., Korol, A., Olifirov, L., Zhevnenko, S., Golubnichiy, A. A., Khodan, A. N., Stafeev, I. A., Salimon, A. I., & Korsunsky, A. M. (2025). Preparation, optimization, and characterization of electrospun PVA/Alumina nanocomposite fibers using response surface methodology. *Emergent Materials*, 1–15. https://doi.org/10.1007/S42247-025-01099-4/METRICS

Ibrahim, Y., & Hilal, N. (2023). Enhancing ultrafiltration membrane permeability and antifouling performance through surface patterning with features resembling feed spacers. *Npj Clean Water 2023 6:1*, *6*(1), 1–15. https://doi.org/10.1038/s41545-023-00277-3

Im, D., Nakada, N., Fukuma, Y., & Tanaka, H. (2019). Effects of the inclusion of biological activated carbon on membrane fouling in combined process of ozonation, coagulation and ceramic membrane filtration for water reclamation. *Chemosphere*, *220*, 20–27. https://doi.org/10.1016/J.CHEMOSPHERE.2018.12.071

Ismail, A. F., Khulbe, K. C., & Matsuura, T. (2019). RO Membrane Preparation. *Reverse Osmosis*, 25–56. https://doi.org/10.1016/B978-0-12-811468-1.00002-5

Ismail, A. F., & Matsuura, T. (2022). Pervaporation. *Membrane Separation Processes*, 113–132. https://doi.org/10.1016/B978-0-12-819626-7.00014-4

Jafari, S., & Sillanpää, M. (2020). Adsorption of dyes onto modified titanium dioxide. *Advanced Water Treatment: Adsorption*, 85–160. https://doi.org/10.1016/B978-0-12-819216-0.00002-3

Jaffar, S. S., Saallah, S., Misson, M., Siddiquee, S., Roslan, J., Saalah, S., & Lenggoro, W. (2022). Recent Development and Environmental Applications of Nanocellulose-Based Membranes. *Membranes 2022, Vol. 12, Page 287*, *12*(3), 287. https://doi.org/10.3390/MEMBRANES12030287

James, A., Rahman, M. R., Mohamad Said, K. A., Kanakaraju, D., Sueraya, A. Z., Kuok, K. K., Bin Bakri, M. K., & Rahman, M. M. (2024). A review of nanocellulose modification and compatibility barrier for various applications. *Journal of Thermoplastic Composite Materials*, *37*(6), 2149–2199. https://doi.org/10.1177/08927057231205451;PAGE:STRING:ARTICLE/CHAPTER

James, A., Rezaur Rahman, M., Anwar Mohamed Said, K., Namakka, M., Kuok Kuok, K., Uddin Khandaker, M., Al-Humaidi, J. Y., Althomali, R. H., & Rahman, M. M. (2024). Lithium Chloride-Mediated enhancement of dye removal capacity in Borneo bamboo derived nanocellulose-based nanocomposite membranes (NCMs). *Journal of Molecular Liquids*, *413*(September), 125973. https://doi.org/10.1016/j.molliq.2024.125973

Janaswamy, S., Yadav, M. P., Hoque, M., Bhattarai, S., & Ahmed, S. (2022). Cellulosic fraction from agricultural biomass as a viable alternative for plastics and plastic products. *Industrial Crops and Products*, *179*, 114692. https://doi.org/10.1016/J.INDCROP.2022.114692

Jang, H., Kang, S., & Kim, J. (2024). Identification of Membrane Fouling with Greywater Filtration by Porous Membranes: Combined Effect of Membrane Pore Size and Applied Pressure. *Membranes 2024, Vol. 14, Page 46*, *14*(2), 46. https://doi.org/10.3390/MEMBRANES14020046

Jang, K., Nguyen, T. T., Yi, E., Kim, C. S., Kim, S. W., & Kim, I. S. (2022). Open Pore Ultrafiltration Hollow Fiber Membrane Fabrication Method via Dual Pore Former with Dual Dope Solution Phase. *Membranes*, *12*(11). https://doi.org/10.3390/membranes12111140

Jangam, K., Balgude, S., Pawar, H., Patange, S., & More, P. (2022). Effect of cobalt substitution in Zn1-xCoxFeCrO4 ferri-chromate: emerging light absorber for degradation of model textile dye. *Surfaces and Interfaces*, *33*(June), 102189. https://doi.org/10.1016/j.surfin.2022.102189

Janićijević, A., Pavlović, V. P., Kovačević, D., Đorđević, N., Marinković, A., Vlahović, B., Karoui, A., Pavlović, V. B., & Filipović, S. (2024). Impact of Nanocellulose Loading on the Crystal Structure, Morphology and Properties of PVDF/Magnetite@NC/BaTiO3 Multi-component Hybrid Ceramic/Polymer Composite Material. *Journal of Inorganic and Organometallic Polymers and Materials*, *34*(5), 2129–2139. https://doi.org/10.1007/S10904-023-02953-W/METRICS

Jankowska, A., Ejsmont, A., Galarda, A., & Goscianska, J. (2022). The outcome of human exposure to environmental contaminants. Importance of water and air purification processes. *Sustainable Materials for Sensing and Remediation of Noxious Pollutants*, 15–37. https://doi.org/10.1016/B978-0-323-99425-5.00003-7

Jeong, K. M., Li, Y., Yoo, D. G., Lee, N. K., Lee, H. G., Ando, S., & Ha, C. S. (2018). Effects of crosslinking agents on the physical properties of polyimide/amino-functionalized graphene oxide hybrid films. *Polymer International*, *67*(5), 588–597. https://doi.org/10.1002/pi.5555

Jiang, J., Ma, B., Yang, C., Duan, X., & Tang, Q. (2022). Fabrication of anti-fouling and photocleaning PVDF microfiltration membranes embedded with N-TiO2 photocatalysts. *Separation and Purification Technology*, *298*, 121673. https://doi.org/10.1016/J.SEPPUR.2022.121673

Jiang, L., Wen, Y., Zhu, Z., Liu, X., & Shao, W. (2021). A Double cross-linked strategy to construct graphene aerogels with highly efficient methylene blue adsorption performance. *Chemosphere*, *265*, 129169. https://doi.org/10.1016/J.CHEMOSPHERE.2020.129169

Jiang, Y. S., Zhang, S. B., Zhang, S. Y., & Peng, Y. X. (2021). Comparative study of high-intensity ultrasound and high-pressure homogenization on physicochemical properties of peanut protein-stabilized emulsions and emulsion gels. *Journal of Food Process Engineering*, *44*(6). https://doi.org/10.1111/jfpe.13710

Jin, J., Du, X., Yang, J., Li, K., Li, J., Qin, S., Yu, J., & He, M. (2022). Designed loose nanofiltration membrane for efficient separation of low molecular dye/salt. *Journal of Applied Polymer Science*, *139*(31), e52715. https://doi.org/10.1002/APP.52715

Joseph, B., Sagarika, V. K., Sabu, C., Kalarikkal, N., & Thomas, S. (2020). Cellulose nanocomposites: Fabrication and biomedical applications. *Journal of Bioresources and Bioproducts*, *5*(4), 223–237. https://doi.org/10.1016/J.JOBAB.2020.10.001

Junaidi, N. F. D., Othman, N. H., Fuzil, N. S., Mat Shayuti, M. S., Alias, N. H., Shahruddin, M. Z., Marpani, F., Lau, W. J., Ismail, A. F., & Aba, N. F. D. (2021). Recent development of graphene oxide-based membranes for oil–water separation: A review. *Separation and Purification Technology*, *258*, 118000. https://doi.org/10.1016/J.SEPPUR.2020.118000

Kadhim, R. J., Al-Ani, F. H., Al-Shaeli, M., Alsalhy, Q. F., & Figoli, A. (2020). Removal of Dyes Using Graphene Oxide (GO) Mixed Matrix Membranes. *Membranes 2020, Vol. 10, Page 366*, *10*(12), 366. https://doi.org/10.3390/MEMBRANES10120366

Kalla, S. (2021). Use of membrane distillation for oily wastewater treatment – A review. *Journal of Environmental Chemical Engineering*, *9*(1), 104641. https://doi.org/10.1016/J.JECE.2020.104641

Kallem, P., Ouda, M., Bharath, G., Hasan, S. W., & Banat, F. (2022). Enhanced water permeability and fouling resistance properties of ultrafiltration membranes incorporated with hydroxyapatite decorated orange-peel-derived activated carbon nanocomposites. *Chemosphere*, *286*, 131799. https://doi.org/10.1016/J.CHEMOSPHERE.2021.131799

Kammakakam, I., & Lai, Z. (2023). Next-generation ultrafiltration membranes: A review of material design, properties, recent progress, and challenges. *Chemosphere*, *316*, 137669. https://doi.org/10.1016/J.CHEMOSPHERE.2022.137669

Kamran, U., Rhee, K. Y., Lee, S.-Y., & Park, S.-J. (2022). Innovative progress in graphene derivative-based composite hybrid membranes for the removal of contaminants in wastewater: A review. *Chemosphere*, 135590.

Kang, G. dong, & Cao, Y. ming. (2021). Hydrophilic Modification of PVDF Membrane: a Review. *Journal of Membranes and Materials*, *1*(1), 1–9. https://doi.org/10.1016/J.MEMSCI.2014.03.055

Kannathasan, K., Jaafar, J., Ahmad, S. N. A., Samitsu, S., Ismail, A. F., Matsuura, T., Othman, M. H. D., Rahman, M. A., Rasool Qtaishat, M., Saidina Amin, N. A., Ersoz, M., & Mohamed Nasir, M. F. (2025). A scalable and chemical-free strategy for antifouling ultrafiltration PVDF membranes via hydrophilic macromolecular surface modification. *Journal of Materials Science 2025 60:44*, *60*(44), 21900–21924. https://doi.org/10.1007/S10853-025-11677-W

Karimi, A., Rajabi, M., & Zahedi, P. (2020). Effect of graphene oxide content on morphology and topography of polysulfone-based mixed matrix membrane for permeability and selectivity of carbon dioxide and methaneEinfluss von Graphenoxidgehalten von polysulfonbasierter Mischmatrixmembran auf Morphologie und Topographie für die Permeabilität und Selektivität von Kohlenstoffdioxid und Methan. *Materialwissenschaft Und Werkstofftechnik*, *51*(8), 1137–1147. https://doi.org/10.1002/MAWE.201900263

Khan, A. U., Hazaraimi, M. H., Othman, M. H. D., Younas, M., Karim, Z. A., Tai, Z. S., Samuel, O., Puteh, M. H., Kurniawan, T. A., Wong, K. Y., & Yoshida, N. (2024). A comprehensive review on dual-layer organic hollow fiber membranes fabrication via co-extrusion: Mechanistic insights, water treatment and gas separation applications.

Journal of Environmental Chemical Engineering, *12*(2), 112434. https://doi.org/10.1016/J.JECE.2024.112434

Khan, B., Haider, S., Khurram, R., Wang, Z., & Wang, X. (2020). Preparation of an Ultrafiltration (UF) Membrane with Narrow and Uniform Pore Size Distribution via Etching of SiO2 Nano-Particles in a Membrane Matrix. *Membranes 2020, Vol. 10, Page 150*, *10*(7), 150. https://doi.org/10.3390/MEMBRANES10070150

Khassi, K., Youssefi, M., & Semnani, D. (2020). PVDF/TiO2/graphene oxide composite nanofiber membranes serving as separators in lithium-ion batteries. *Journal of Applied Polymer Science*, *137*(23), 48775. https://doi.org/10.1002/APP.48775

Khorsandi, D., Jenson, S., Zarepour, A., Khosravi, A., Rabiee, N., Iravani, S., & Zarrabi, A. (2024). Catalytic and biomedical applications of nanocelluloses: A review of recent developments. *International Journal of Biological Macromolecules*, *268*, 131829. https://doi.org/10.1016/J.IJBIOMAC.2024.131829

Khurram, R., Javed, A., Ke, R., Lena, C., & Wang, Z. (2021). Visible Light-Driven GO/TiO2-CA Nano-Photocatalytic Membranes: Assessment of Photocatalytic Response, Antifouling Character and Self-Cleaning Ability. *Nanomaterials 2021, Vol. 11, Page 2021*, *11*(8), 2021. https://doi.org/10.3390/NANO11082021

Kolya, H., & Kang, C. W. (2023). Next-Generation Water Treatment: Exploring the Potential of Biopolymer-Based Nanocomposites in Adsorption and Membrane Filtration. *Polymers 2023, Vol. 15, Page 3421*, *15*(16), 3421. https://doi.org/10.3390/POLYM15163421

Kouzi, Y., Chafiq Elidrissi, Z., Essate, A., Beqqour, D., Achiou, B., Alami Younssi, S., Rabiller-Baudry, M., Bouhria, M., & Ouammou, M. (2025). Tailored rGO-TiO2-pPD

low-cost ceramic membrane for dye wastewater filtration: A synergistic strategy of GO reduction, intercalation and crosslinking. *Separation and Purification Technology*, *378*, 134643. https://doi.org/10.1016/J.SEPPUR.2025.134643

Kumar Purkait, M., Singh, R., Mondal, P., & Haldar, D. (2020). Pervaporation. *Thermal Induced Membrane Separation Processes*, 99–120. https://doi.org/10.1016/B978-0-12-818801-9.00006-2

Kumar, T. S. M., Kumar, K. S., Rajini, N., Siengchin, S., Ayrilmis, N., & Rajulu, A. V. (2019). A comprehensive review of electrospun nanofibers: Food and packaging perspective. *Composites Part B: Engineering*, *175*, 107074. https://doi.org/10.1016/J.COMPOSITESB.2019.107074

Kumari, P., Bahadur, N., & Dumée, L. F. (2020). Photo-catalytic membrane reactors for the remediation of persistent organic pollutants – A review. *Separation and Purification Technology*, *230*, 115878. https://doi.org/10.1016/J.SEPPUR.2019.115878

Kumari, P., Tripathi, K. M., Jangir, L. K., Gupta, R., & Awasthi, K. (2021). Recent advances in application of the graphene-based membrane for water purification. *Materials Today Chemistry*, *22*, 100597. https://doi.org/10.1016/J.MTCHEM.2021.100597

Kuok, K. K., Khusairy, M., Bakri, B., Chan, P., Namakka, M., Mohamad, A., Yun, M., Kuok, K. K., Khusairy, M., Bakri, B., & Chan, P. (2024). *Merits of Bamboo Utilization in Earth Preservation , Water , and Wastewater Treatment : A Mini Review Merits of Bamboo Utilization in Earth Preservation , Water and Wastewater Treatment : A Mini Review*. *19*(2), 3921–3944. https://doi.org/10.15376/biores.19.2.Kuok

Kusworo, T. D., Kumoro, A. C., Aryanti, N., Lingga, F. F., Widiastuti, A., Vetcher, A. A., & Dalanta, F. (2023). Development of anti-foulant ultraviolet-assisted polyvinyl alcohol

layer on the polysulfone-based nanohybrid membrane for industrial rubber wastewater decontamination. *Frontiers in Environmental Science*, *11*, 1175957. https://doi.org/10.3389/FENVS.2023.1175957/BIBTEX

Kusworo, T. D., Yulfarida, M., Kumoro, A. C., & Utomo, D. P. (2023). Purification of bioethanol fermentation broth using hydrophilic PVA crosslinked PVDF-GO/TiO2 membrane. *Chinese Journal of Chemical Engineering*, *55*, 123–136. https://doi.org/10.1016/J.CJCHE.2022.04.028

Lasrado, D., Ahankari, S., & Kar, K. (2020). Nanocellulose-based polymer composites for energy applications—A review. In *Journal of Applied Polymer Science* (Vol. 137, Issue 27). John Wiley and Sons Inc. https://doi.org/10.1002/app.48959

Leam, J. J., Bilad, M. R., Wibisono, Y., Wirzal, M. D. H., & Ahmed, I. (2020). Membrane Technology for Microalgae Harvesting. *Microalgae Cultivation for Biofuels Production*, 97–110. https://doi.org/10.1016/B978-0-12-817536-1.00007-2

Lee, C., Lee, S., & Kang, S. W. (2024). Enhanced porous membrane fabrication using cellulose acetate and citric acid: Improved structural integrity, thermal stability, and gas permeability. *Carbohydrate Polymers*, *324*, 121571. https://doi.org/10.1016/J.CARBPOL.2023.121571

Li, J., Hu, M., Pei, H., Ma, X., Yan, F., Dlamini, D. S., Cui, Z., He, B., Li, J., & Matsuyama, H. (2020). Improved water permeability and structural stability in a polysulfone-grafted graphene oxide composite membrane used for dye separation. *Journal of Membrane Science*, *595*, 117547. https://doi.org/10.1016/J.MEMSCI.2019.117547

Li, W., Shen, Y., Liu, H., Huang, X., Xu, B., Zhong, C., & Jia, S. (2022). Bioconversion of lignocellulosic biomass into bacterial nanocellulose: challenges and perspectives. *Green Chemical Engineering*. https://doi.org/10.1016/J.GCE.2022.04.007

Li, Y., Wang, M., Meng, Y., Wang, Q., Fu, Q., Yu, C., Zhu, L., Cai, L., Chen, C., Xia, C., & Wang, S. (2025). Nanocellulose Hybrid Membranes for Green Flexible Electronics: Interface Design and Functional Assemblies. *ACS Applied Materials and Interfaces*. https://doi.org/10.1021/ACSAMI.5C04027/ASSET/IMAGES/MEDIUM/AM5C04027_0016.GIF

Li, Y., Wang, S., Li, H., Kang, G., Sun, Y., Yu, H., Jin, Y., & Cao, Y. (2022). Preparation of highly selective nanofiltration membranes by moderately increasing pore size and optimizing microstructure of polyamide layer. *Journal of Membrane Science*, *643*, 120056. https://doi.org/10.1016/J.MEMSCI.2021.120056

Li, Z., Jin, R., Gong, J., Liu, W., & Li, J. (2025). Recent advances in anti-fouling oil–water separation membranes: a review focusing on active and passive anti-fouling strategies. *Journal of Materials Chemistry A*, *13*(29), 23418–23438. https://doi.org/10.1039/D5TA03722K

Liangdy, A. (2024). *Fabrication of catalytic ceramic membrane in hybrid catalytic oxidation filtration process for water treatment*. https://doi.org/10.32657/10356/182061

Lim, Y. J., Goh, K., Nadzri, N., & Wang, R. (2025). Thin-film composite (TFC) membranes for sustainable desalination and water reuse: A perspective. *Desalination*, *599*, 118451. https://doi.org/10.1016/J.DESAL.2024.118451

Lin, L., Shi, L., Liu, S., & He, J. (2023). Preparation of TiO2Grafted on Graphene and Study on their Photocatalytic Properties. *International Journal of Photoenergy*, *2023*. https://doi.org/10.1155/2023/8676430

Lin, Y. C., Tseng, H. H., & Wang, D. K. (2021). Uncovering the effects of PEG porogen molecular weight and concentration on ultrafiltration membrane properties and protein purification performance. *Journal of Membrane Science*, *618*, 118729. https://doi.org/10.1016/J.MEMSCI.2020.118729

Liu, J., & Lv, C. (2021). Research Progress on Durability of Cellulose Fiber-Reinforced Cement-Based Composites. *International Journal of Polymer Science*, *2021*. https://doi.org/10.1155/2021/1014531

Liu, L., Luo, X. B., Ding, L., & Luo, S. L. (2019). Application of Nanotechnology in the Removal of Heavy Metal From Water. *Nanomaterials for the Removal of Pollutants and Resource Reutilization*, 83–147. https://doi.org/10.1016/B978-0-12-814837-2.00004-4

Liu, Y., Ahmed, S., Sameen, D. E., Wang, Y., Lu, R., Dai, J., Li, S., & Qin, W. (2021). A review of cellulose and its derivatives in biopolymer-based for food packaging application. *Trends in Food Science & Technology*, *112*, 532–546. https://doi.org/10.1016/J.TIFS.2021.04.016

Liu, Y., Liu, H., & Shen, Z. (2021). Nanocellulose based filtration membrane in industrial waste water treatment: A review. *Materials*, *14*(18). https://doi.org/10.3390/ma14185398

Lizundia, E., Reizabal, A., Costa, C. M., Maceiras, A., & Lanceros-Méndez, S. (2020). Electroactive γ-Phase, Enhanced Thermal and Mechanical Properties and High Ionic

Conductivity Response of Poly (Vinylidene Fluoride)/Cellulose Nanocrystal Hybrid Nanocomposites. *Materials 2020, Vol. 13, Page 743*, *13*(3), 743. https://doi.org/10.3390/MA13030743

Lü, X., Yu, T., Meng, F., & Bao, W. (2021). Wide-Range and High-Stability Flexible Conductive Graphene/Thermoplastic Polyurethane Foam for Piezoresistive Sensor Applications. *Advanced Materials Technologies*, *6*(10), 2100248. https://doi.org/10.1002/ADMT.202100248;WGROUP:STRING:PUBLICATION

Luo, X., Zhong, J., Zhou, Q., Du, S., Yuan, S., & Liu, Y. (2018). Cationic Reduced Graphene Oxide as Self-Aligned Nanofiller in the Epoxy Nanocomposite Coating with Excellent Anticorrosive Performance and Its High Antibacterial Activity. *ACS Applied Materials and Interfaces*, *10*(21), 18400–18415. https://doi.org/10.1021/ACSAMI.8B01982/SUPPL_FILE/AM8B01982_SI_001.PDF

Ma, J., Tang, X., He, Y., Fan, Y., Chen, J., & HaoYu. (2020). Robust stable MoS2/GO filtration membrane for effective removal of dyes and salts from water with enhanced permeability. *Desalination*, *480*, 114328. https://doi.org/10.1016/J.DESAL.2020.114328

Maiti, S., Islam, S. S., & Bose, S. (2025). Nano-Engineering for Purity: Advances in PVDF Membrane Water Purification. *Chemistry - An Asian Journal*, *20*(24), e00788. https://doi.org/10.1002/ASIA.202500788;REQUESTEDJOURNAL:JOURNAL:1861471X;WGROUP:STRING:PUBLICATION

Manfo, A. T., Singh, P. K., Mehra, R. M., Singh, R. C., & Gupta, M. (2020). Structural, Vibrational, Electrical, Electrochemical and Capacitive Investigations on Ionic Liquid Doped P (VDF-HFP) + NaSCN Based Polymer Electrolytes. *Recent Innovations in*

Chemical Engineering (Formerly Recent Patents on Chemical Engineering), *14*(1), 21–34. https://doi.org/10.2174/2405520413999200719141337

Mansoori, S., Davarnejad, R., Matsuura, T., & Ismail, A. F. (2020). Membranes based on non-synthetic (natural) polymers for wastewater treatment. In *Polymer Testing* (Vol. 84). Elsevier Ltd. https://doi.org/10.1016/j.polymertesting.2020.106381

Marshall, J. E., Zhenova, A., Roberts, S., Petchey, T., Zhu, P., Dancer, C. E. J., McElroy, C. R., Kendrick, E., & Goodship, V. (2021). On the Solubility and Stability of Polyvinylidene Fluoride. *Polymers 2021, Vol. 13, Page 1354*, *13*(9), 1354. https://doi.org/10.3390/POLYM13091354

Matindi, C. N., Kadanyo, S., Liu, G., Hu, M., Hu, Y., Cui, Z., Ma, X., Yan, F., He, B., & Li, J. (2022). Hydrophilic polyethyleneimine-TiO2 hybrid layer on polyethersulfone/sulfonated polysulfone blend membrane with antifouling characteristics for the effective separation of oil-in-water emulsions. *Journal of Water Process Engineering*, *49*, 102982. https://doi.org/10.1016/J.JWPE.2022.102982

Mbakop, S., Nthunya, L. N., & Onyango, M. S. (2021). Recent Advances in the Synthesis of Nanocellulose Functionalized–Hybrid Membranes and Application in Water Quality Improvement. *Processes 2021, Vol. 9, Page 611*, *9*(4), 611. https://doi.org/10.3390/PR9040611

Memisoglu, G., Murugesan, R. C., Zubia, J., & Rozhin, A. G. (2023). Graphene Nanocomposite Membranes: Fabrication and Water Treatment Applications. *Membranes 2023, Vol. 13, Page 145*, *13*(2), 145. https://doi.org/10.3390/MEMBRANES13020145

M.Hamad, E., Al-Gharabli, S., & Kujawa, J. (2022). Tunable hydrophobicity and roughness on PVDF surface by grafting to mode – Approach to enhance membrane performance in membrane distillation process. *Separation and Purification Technology*, *291*, 120935. https://doi.org/10.1016/J.SEPPUR.2022.120935

Mishra, J. R., Samal, S. K., Mohanty, S., & Nayak, S. K. (2021). Polyvinylidene fluoride (PVDF)/Ag@TiO2 nanocomposite membrane with enhanced fouling resistance and antibacterial performance. *Materials Chemistry and Physics*, *268*, 124723. https://doi.org/10.1016/J.MATCHEMPHYS.2021.124723

Mohamat, R., Bakar, S. A., Mohamed, A., Muqoyyanah, M., Othman, M. H. D., Mamat, M. H., Malek, M. F., Ahmad, M. K., Yulkifli, Y., & Ramakrishna, S. (2023). Incorporation of graphene oxide/titanium dioxide with different polymer materials and its effects on methylene blue dye rejection and antifouling ability. *Environmental Science and Pollution Research*, *30*(28), 72446–72462. https://doi.org/10.1007/S11356-023-27207-7/METRICS

Mohammadpourfazeli, S., Arash, S., Ansari, A., Yang, S., Mallick, K., & Bagherzadeh, R. (2023). Future prospects and recent developments of polyvinylidene fluoride (PVDF) piezoelectric polymer; fabrication methods, structure, and electro-mechanical properties. *RSC Advances*, *13*(1), 370–387. https://doi.org/10.1039/D2RA06774A

Mohammed, N., Lian, H., Islam, M. S., Strong, M., Shi, Z., Berry, R. M., Yu, H. Y., & Tam, K. C. (2021). Selective adsorption and separation of organic dyes using functionalized cellulose nanocrystals. *Chemical Engineering Journal*, *417*, 129237. https://doi.org/10.1016/J.CEJ.2021.129237

Mohsenpour, S., Leaper, S., Shokri, J., Alberto, M., & Gorgojo, P. (2022). Effect of graphene oxide in the formation of polymeric asymmetric membranes via phase inversion. *Journal of Membrane Science*, *641*, 119924. https://doi.org/10.1016/J.MEMSCI.2021.119924

Moradi, G., & Zinadini, S. (2020). A high flux graphene oxide nanoparticles embedded in PAN nanofiber microfiltration membrane for water treatment applications with improved anti-fouling performance. *Iranian Polymer Journal (English Edition)*, *29*(9), 827–840. https://doi.org/10.1007/S13726-020-00842-4/METRICS

Mubarak, M. F., Selim, H., Hawash, H. B., & Hemdan, M. (2023). Flexible, durable, and anti-fouling maghemite copper oxide nanocomposite-based membrane with ultra-high flux and efficiency for oil-in-water emulsions separation. *Environmental Science and Pollution Research 2023 31:2*, *31*(2), 2297–2313. https://doi.org/10.1007/S11356-023-31240-X

Muhammad, S., & Usman, Q. A. (2022). Heavy metal contamination in water of Indus River and its tributaries, Northern Pakistan: evaluation for potential risk and source apportionment. *Toxin Reviews*, *41*(2), 380–388. https://doi.org/10.1080/15569543.2021.1882499

Nagaraj, K., Radha, S., Deepa, C. G., Raja, K., Umapathy, V., Badgujar, N. P., Parekh, N. M., Manimegalai, T., Archana Devi, L., & Uthra, C. (2025). Photocatalytic advancements and applications of titanium dioxide (TiO_2): Progress in biomedical, environmental, and energy sustainability. *Next Research*, *2*(1), 100180. https://doi.org/10.1016/J.NEXRES.2025.100180

Nair, R., Tripathi, B., Jain, A., & Shehata, N. (2024). Vibrational energy harvesting and tactile sensing applications based on PVDF-TPU piezoelectric nanofibers. *Journal of Materials Science: Materials in Electronics*, *35*(12), 1–21. https://doi.org/10.1007/S10854-024-12635-Z/METRICS

Namakka, M., Rahman, M. R., Mohamad Bin Said, K. A., Kuok, K. K., Md Yusof, F. A., Al-Saleem, M. S. M., Al-Humaidi, J. Y., & Rahman, M. M. (2024). Unveiling the synergistic effect of an nZVI–SiO 2 –TiO 2 nanocomposite for the remediation of dye contaminated wastewater. *Materials Advances*, 9292–9313. https://doi.org/10.1039/D4MA00853G

Namakka, M., Rahman, Md. R., Said, K. A. M. Bin, Abdul Mannan, M., & Patwary, A. M. (2023). A review of nanoparticle synthesis methods, classifications, applications, and characterization. *Environmental Nanotechnology, Monitoring & Management*, *20*(November), 100900. https://doi.org/10.1016/j.enmm.2023.100900

Nannan, N., Neethling, I., Cois, A., Laubscher, R., Turawa, E. B., Pacella, R., Bradshaw, D., & Pillay-van Wyk, V. (2022). Estimating the changing burden of disease attributable to unsafe water and lack of sanitation and hygiene in South Africa for 2000, 2006 and 2012. *South African Medical Journal*, 729–736. https://doi.org/10.7196/SAMJ.2022.v112i8b.16498

Narayanam, P. K., Vishwakarma, R. K., & Polaki, S. R. (2022). Fabrication of free standing graphene oxide membranes for efficient adsorptive removal of cationic dyes. *Journal of Molecular Liquids*, *368*, 120787. https://doi.org/10.1016/j.molliq.2022.120787

Nawaz, H., Umar, M., Ullah, A., Razzaq, H., Zia, K. M., & Liu, X. (2021). Polyvinylidene fluoride nanocomposite super hydrophilic membrane integrated with Polyaniline-

Graphene oxide nano fillers for treatment of textile effluents. *Journal of Hazardous Materials*, *403*, 123587. https://doi.org/10.1016/J.JHAZMAT.2020.123587

Ndeh, N. T., Sairiam, S., & Nuisin, R. (2024). Graphene oxide-chitosan coated PVDF adsorptive microfiltration membrane: Enhancing dye removal and antifouling properties. *International Journal of Biological Macromolecules*, *282*(Pt 3). https://doi.org/10.1016/j.ijbiomac.2024.137005

Nie, L., Fu, P., Cai, K., Deng, P., Bai, Y., Chaochao, C., He, X., Song, H., & Guo, D. (2024). *Tailoring the Pvdf Phase Structure in High Permittivity Mxene/Pvdf Composite Films Via Super-Cooling of the Polymer Melt*. https://doi.org/10.2139/SSRN.4871063

Nissilä, T., Wei, J., Geng, S., Teleman, A., & Oksman, K. (2021). Ice-Templated Cellulose Nanofiber Filaments as a Reinforcement Material in Epoxy Composites. *Nanomaterials 2021, Vol. 11, Page 490*, *11*(2), 490. https://doi.org/10.3390/NANO11020490

Noguchi, H., Oo, M. H., Niwa, T., Fong, E., Yin, R., & Supaat, N. (2019). Applications of flat sheet ceramic membrane for surface water and seawater treatments – introduction of performance in large-scale drinking water plant and seawater pretreatment pilot system in Singapore. *Water Practice and Technology*, *14*(2), 289–296. https://doi.org/10.2166/WPT.2019.013

Noor Azammi, A. M., Ilyas, R. A., Sapuan, S. M., Ibrahim, R., Atikah, M. S. N., Asrofi, M., & Atiqah, A. (2020). Characterization studies of biopolymeric matrix and cellulose fibres based composites related to functionalized fibre-matrix interface. *Interfaces in Particle and Fibre Reinforced Composites: Current Perspectives on Polymer, Ceramic, Metal and Extracellular Matrices*, 29–93. https://doi.org/10.1016/B978-0-08-102665-6.00003-0

Norfarhana, A. S., Ilyas, R. A., & Ngadi, N. (2022). A review of nanocellulose adsorptive membrane as multifunctional wastewater treatment. *Carbohydrate Polymers*, *291*, 119563. https://doi.org/10.1016/J.CARBPOL.2022.119563

Norizan, M. N., Shazleen, S. S., Alias, A. H., Sabaruddin, F. A., Asyraf, M. R. M., Zainudin, E. S., Abdullah, N., Samsudin, M. S., Kamarudin, S. H., & Norrrahim, M. N. F. (2022). Nanocellulose-Based Nanocomposites for Sustainable Applications: A Review. *Nanomaterials*, *12*(19), 3483. https://doi.org/10.3390/NANO12193483

Norrrahim, M. N. F., Kasim, N. A. M., Knight, V. F., Ong, K. K., Noor, S. A. M., Halim, N. A., Shah, N. A. A., Jamal, S. H., Janudin, N., Misenan, M. S. M., Ahmad, M. Z., Yaacob, M. H., & Yunus, W. M. Z. W. (2021). Emerging Developments Regarding Nanocellulose-Based Membrane Filtration Material against Microbes. *Polymers*, *13*(19). https://doi.org/10.3390/POLYM13193249

Nowak, D., & Jakubczyk, E. (2020). The freeze-drying of foods—The characteristic of the process course and the effect of its parameters on the physical properties of food materials. In *Foods* (Vol. 9, Issue 10). MDPI AG. https://doi.org/10.3390/foods9101488

Nursiah, K., Musteata, V.-E., Cerneaux, S., & Barboiu, M. (2023). Artificial water channels-embedded PVDF membranes for direct contact membrane distillation and ultrafiltration. *Frontiers in Membrane Science and Technology*, *2*, 1241526. https://doi.org/10.3389/FRMST.2023.1241526

Obaideen, K., Shehata, N., Sayed, E. T., Abdelkareem, M. A., Mahmoud, M. S., & Olabi, A. G. (2022). The role of wastewater treatment in achieving sustainable development goals (SDGs) and sustainability guideline. *Energy Nexus*, *7*, 100112. https://doi.org/10.1016/J.NEXUS.2022.100112

Odabaşi, Ç., Döhğlu, P., Gülmez, F., Kuşoğlu, G., & Çağlar, Ö. (2021). Machine Learning Analysis of the Feed Water Parameters Affecting Reverse Osmosis Membrane Operation. *Computer Aided Chemical Engineering*, *50*, 235–240. https://doi.org/10.1016/B978-0-323-88506-5.50038-3

Oladoyinbo, F. O., Elebiju, D., Akinwunmi, F., Ejeromedoghene, O., Alli, Y. A., Alayande, S. O., Amolegbe, S. A., Olayide, A. R., Diaz, D. D., & Dare, E. O. (2024). Ceramic Bowl-Supported Nanofibrous Membrane with Fluorinated Silsesquioxane-inspired Switchable Surfaces for Successive Crude Oil/Water Separation and Secondary Water Treatment. *Colloids and Surfaces A: Physicochemical and Engineering Aspects*, *686*(November 2023), 133224. https://doi.org/10.1016/j.colsurfa.2024.133224

Oliveira, C. P. M. de, Moreira, V. R., Lebron, Y. A. R., Vasconcelos, C. K. B. de, Koch, K., Viana, M. M., Drewes, J. E., & Amaral, M. C. S. (2022). Converting recycled membranes into photocatalytic membranes using greener TiO2-GRAPHENE oxide nanomaterials. *Chemosphere*, *306*, 135591. https://doi.org/10.1016/J.CHEMOSPHERE.2022.135591

Omar, A., Gomaa, I., Mohamed, O. A., Magdy, H., Kalloub, H. S., Hamza, M. H., Mohamed, T. M., Rabee, M. M., Tareq, N., Hesham, H., Abdallah, T., Elhaes, H., & Ibrahim, M. A. (2023). Investigation of morphological, structural and electronic transformation of PVDF and ZnO/rGO/PVDF hybrid membranes. *Optical and Quantum Electronics*, *55*(4), 1–21. https://doi.org/10.1007/S11082-023-04663-6/FIGURES/9

Omar, N. M. A., Othman, M. H. D., Tai, Z. S., Kurniawan, T. A., Puteh, M. H., Jaafar, J., Rahman, M. A., Ismail, A. F., Rajamohan, N., Abdullah, H., & Wong, K. Y. (2024). Recent strategies for enhancing the performance and lifespan of low-cost ceramic

membranes in water filtration and treatment processes: A review. *Journal of Water Process Engineering*, *62*, 105399. https://doi.org/10.1016/J.JWPE.2024.105399

Osman, A. I., Chen, Z., Elgarahy, A. M., Farghali, M., Mohamed, I. M. A., Priya, A. K., Hawash, H. B., & Yap, P. S. (2024). Membrane Technology for Energy Saving: Principles, Techniques, Applications, Challenges, and Prospects. *Advanced Energy and Sustainability Research*, *5*(5), 2400011. https://doi.org/10.1002/AESR.202400011;PAGEGROUP:STRING:PUBLICATION

Oyarce, E., Cantero-López, P., Yañez, O., Roa, K., Boulett, A., Pizarro, G. D. C., Zhang, Y., Xu, C., Willför, S., & Sánchez, J. (2022). Nanocellulose bio-based composites for the removal of methylene blue from water: An experimental and theoretical exploration. *Journal of Molecular Liquids*, *357*, 119089. https://doi.org/10.1016/J.MOLLIQ.2022.119089

Pachaiappan, R., Cornejo-Ponce, L., Rajendran, R., Manavalan, K., Femilaa Rajan, V., & Awad, F. (2022). A review on biofiltration techniques: recent advancements in the removal of volatile organic compounds and heavy metals in the treatment of polluted water. *Bioengineered*, *13*(4), 8432–8477. https://doi.org/10.1080/21655979.2022.2050538

Padmanabhan, N. T., Jayaraj, M. K., & John, H. (2020). Graphene hybridized high energy faceted titanium dioxide for transparent self-cleaning coatings. *Catalysis Today*, *348*, 63–71. https://doi.org/10.1016/J.CATTOD.2019.09.029

Pal, N., & Agarwal, M. (2021). Advances in materials process and separation mechanism of the membrane towards hydrogen separation. *International Journal of Hydrogen Energy*, *46*(53), 27062–27087. https://doi.org/10.1016/J.IJHYDENE.2021.05.175

Pal, P., Chaurasia, S. P., Upadhyaya, S., Kumar, R., & Sridhar, S. (2020). Development of hydrogen selective microporous PVDF membrane. *International Journal of Hydrogen Energy*, *45*(34), 16965–16975. https://doi.org/10.1016/J.IJHYDENE.2019.08.112

Park, M., Ko, Y. T., Ji, M., Cho, J. S., Wang, D. H., & Lee, Y. I. (2022). Facile self-assembly-based fabrication of a polyvinylidene fluoride nanofiber membrane with immobilized titanium dioxide nanoparticles for dye wastewater treatment. *Journal of Cleaner Production*, *378*, 134506. https://doi.org/10.1016/J.JCLEPRO.2022.134506

Park, S., Son, M., Shim, J., Jeong, K., & Cho, K. H. (2022). Physically-assisted removal of organic fouling by osmotic backwashing coupled with chemical cleaning. *Journal of Cleaner Production*, *378*, 134490. https://doi.org/10.1016/J.JCLEPRO.2022.134490

Parvin, F., Islam, S., Urmy, Z., Ahmed, S., & Islam, A. S. (2020). A Study on the Solutions of Environment Pollutions and Worker's Health Problems Caused by Textile Manufacturing Operations. *Biomedical Journal of Scientific & Technical Research*, *28*(4), 21831–21844. https://doi.org/10.13140/RG.2.2.13842.79048

Patil, K., Jangam, K., Patange, S., Balgude, S., Al-Sehemi, A. G., Pawar, H., & More, P. (2022). Influence of Cu–Mg substituted ZnFe2O4 ferrite as a highly efficient nanocatalyst for dye degradation and 4-nitrophenol reduction. *Journal of Physics and Chemistry of Solids*, *167*(August 2021), 110783. https://doi.org/10.1016/j.jpcs.2022.110783

Patiu, N. A. M. B., Austria, H. F. M., Carballo, G. V., Li, R., Leron, R. B., Hung, W. S., De Vera, F. C., Tsai, M. L., Cheng, C. H., & Don, T. M. (2025). Novel membrane-integrated ultrasonic atomization system for energy-efficient treatment of dye-polluted

wastewater. *Separation and Purification Technology*, *374*, 133732. https://doi.org/10.1016/J.SEPPUR.2025.133732

Peng, J., Deka, B. J., Wu, S., Luo, Z., Kharraz, J. A., & Jia, W. (2023). Rational Design of PDA/P-PVDF@PP Janus Membrane with Asymmetric Wettability for Switchable Emulsion Separation. *Membranes*, *13*(1), 14. https://doi.org/10.3390/MEMBRANES13010014/S1

Pervez, M. N., Talukder, M. E., Mishu, M. R., Buonerba, A., del Gaudio, P., Stylios, G. K., Hasan, S. W., Zhao, Y., Cai, Y., Figoli, A., Zarra, T., Belgiorno, V., Song, H., & Naddeo, V. (2022). One-Step Fabrication of Novel Polyethersulfone-Based Composite Electrospun Nanofiber Membranes for Food Industry Wastewater Treatment. *Membranes*, *12*(4). https://doi.org/10.3390/membranes12040413

Prabhakar, N., Isloor, A. M., Padaki, M., & Fauzi Ismail, A. (2024). Fabrication of TiO2@ZIF-67 metal organic framework composite incorporated PVDF membranes for the removal of hazardous reactive black 5 and Congo red dyes from contaminated water. *Chemical Engineering Journal*, *498*(July), 155270. https://doi.org/10.1016/j.cej.2024.155270

Pramono, E., Simamora, A. L., Radiman, C. L., & Wahyuningrum, D. (2017). Effects of PVDF concentration on the properties of PVDF membranes. *IOP Conference Series: Earth and Environmental Science*, *75*(1). https://doi.org/10.1088/1755-1315/75/1/012027

Prihatiningtyas, I., Hartanto, Y., & Van der Bruggen, B. (2021). Ultra-high flux alkali-treated cellulose triacetate/cellulose nanocrystal nanocomposite membrane for pervaporation

desalination. *Chemical Engineering Science*, *231*, 116276. https://doi.org/10.1016/J.CES.2020.116276

Pundir, A., Thakur, M. S., Radha, Goel, B., Prakash, S., Kumari, N., Sharma, N., Parameswari, E., Senapathy, M., Kumar, S., Dhumal, S., Deshmukh, S. V., Lorenzo, J. M., & Kumar, M. (2024). Innovations in textile wastewater management: a review of zero liquid discharge technology. *Environmental Science and Pollution Research*, *31*(9), 12597–12616. https://doi.org/10.1007/S11356-024-31827-Y/METRICS

Pusty, M., & Shirage, P. M. (2022). Insights and perspectives on graphene-PVDF based nanocomposite materials for harvesting mechanical energy. *Journal of Alloys and Compounds*, *904*, 164060. https://doi.org/10.1016/J.JALLCOM.2022.164060

Qamar, M. A., Javed, M., Shahid, S., & Sher, M. (2022). Fabrication of g-C3N4/transition metal (Fe, Co, Ni, Mn and Cr)-doped ZnO ternary composites: Excellent visible light active photocatalysts for the degradation of organic pollutants from wastewater. *Materials Research Bulletin*, *147*, 111630. https://doi.org/10.1016/J.MATERRESBULL.2021.111630

Qasem, N. A. A., Mohammed, R. H., & Lawal, D. U. (2021). Removal of heavy metal ions from wastewater: a comprehensive and critical review. *Npj Clean Water*, *4*(1), 1–15. https://doi.org/10.1038/s41545-021-00127-0

Qiao, A., Cui, M., Huang, R., Ding, G., Qi, W., He, Z., Klemeš, J. J., & Su, R. (2021). Advances in nanocellulose-based materials as adsorbents of heavy metals and dyes. In *Carbohydrate Polymers* (Vol. 272). Elsevier Ltd. https://doi.org/10.1016/j.carbpol.2021.118471

Qiao, Z., Wang, Z., Zhang, C., Yuan, S., Zhu, Y., & Wang, J. (2012). PVAm–PIP/PS composite membrane with high performance for CO2/N2 separation. *AIChE Journal*, *59*(4), 215–228. https://doi.org/10.1002/aic

Qin, J., Ziemann, E., Bar-Zeev, E., Bone, S. E., Liang, Y., Mauter, M. S., Herzberg, M., & Bernstein, R. (2023). Microporous Polyethersulfone Membranes Grafted with Zwitterionic Polymer Brushes Showing Microfiltration Permeance and Ultrafiltration Bacteriophage Removal. *ACS Applied Materials and Interfaces*, *15*(14), 18343–18353. https://doi.org/10.1021/ACSAMI.3C01495/SUPPL_FILE/AM3C01495_SI_001.PDF

Rahman, M. R., James, A., Mohamed Said, K. A., Namakka, M., Khandaker, M. U., Jiunn, W. H., Al-Humaidi, J. Y., Althomali, R. H., & Rahman, M. M. (2024). A TiO 2 grafted bamboo derivative nanocellulose polyvinylidene fluoride (PVDF) nanocomposite membrane for wastewater treatment by a photocatalytic process . *Materials Advances*, 7617–7636. https://doi.org/10.1039/d4ma00716f

Rahman, M. R., Rashid, Md. M., Islam, Md. M., & Akanda, Md. M. (2019). Electrical and Chemical Properties of Graphene over Composite Materials: A Technical Review. *Material Science Research India*, *16*(2), 142–163. https://doi.org/10.13005/MSRI/160208

Ramutshatsha-Makhwedzha, D., & Nomngongo, P. N. (2022). *Application of Ultrafiltration Membrane Technology for Removal of Dyes from Wastewater*. 37–47. https://doi.org/10.1007/978-981-16-4823-6_3

Ranjit, P., Jhansi, V., & Reddy, K. V. (2021). *Conventional Wastewater Treatment Processes*. 455–479. https://doi.org/10.1007/978-981-15-8999-7_17

Rath, R., Kumar, P., Rana, D., Mishra, V., Kumar, A., Mohanty, S., & Nayak, S. K. (2022). Sulfonated PVDF nanocomposite membranes tailored with graphene oxide nanoparticles: Improved proton conductivity and membrane selectivity thereof. *Journal of Materials Science*, *57*(5), 3565–3585. https://doi.org/10.1007/s10853-021-06803-3

Ravi, J., Othman, M. H. D., Tai, Z. S., El-badawy, T., Matsuura, T., & Kurniawan, T. A. (2021). Comparative DCMD performance of hydrophobic-hydrophilic dual-layer hollow fibre PVDF membranes incorporated with different concentrations of carbon-based nanoparticles. *Separation and Purification Technology*, *274*, 118948. https://doi.org/10.1016/J.SEPPUR.2021.118948

Ray, P., Singh, P. S., & Polisetti, V. (2020). Synthetic polymeric membranes for the removal of toxic pollutants and other harmful contaminants from water. *Removal of Toxic Pollutants through Microbiological and Tertiary Treatment: New Perspectives*, 43–99. https://doi.org/10.1016/B978-0-12-821014-7.00002-2

Ren, L., Deng, R., Yang, J., Li, J., Jin, J., & Lei, T. (2023). Improved hydrophilicity and antifouling performances of PVDF ultrafiltration membrane via in situ cross-linking. *Journal of Materials Science 2023 58:34*, *58*(34), 13854–13864. https://doi.org/10.1007/S10853-023-08879-5

Rendón-Castrillón, L., Ramírez-Carmona, M., Ocampo-López, C., González-López, F., Cuartas-Uribe, B., & Mendoza-Roca, J. A. (2023). Treatment of water from the textile industry contaminated with indigo dye: A hybrid approach combining bioremediation and nanofiltration for sustainable reuse. *Case Studies in Chemical and Environmental Engineering*, *8*, 100498. https://doi.org/10.1016/J.CSCEE.2023.100498

Reshmy, R., Philip, E., Madhavan, A., Pugazhendhi, A., Sindhu, R., Sirohi, R., Awasthi, M. K., Pandey, A., & Binod, P. (2022). Nanocellulose as green material for remediation of hazardous heavy metal contaminants. *Journal of Hazardous Materials*, *424*, 127516. https://doi.org/10.1016/J.JHAZMAT.2021.127516

Reshmy, R., Thomas, D., Philip, E., Paul, S. A., Madhavan, A., Sindhu, R., Binod, P., Pugazhendhi, A., Sirohi, R., Tarafdar, A., & Pandey, A. (2021). Potential of nanocellulose for wastewater treatment. *Chemosphere*, *281*, 130738. https://doi.org/10.1016/J.CHEMOSPHERE.2021.130738

Rihayat, T., Mawardi, I., Munadi, R., Tadjuddin, M., Moentamaria, D., Suharti, P., Lianda, J., Custer, J., Siregar, J. P., Safitri, A., Ilmi, A., & Aida, A. (2025). POLYOLEFIN LITHIUM ION BATTERY (LIB) SEPARATOR TECHNOLOGY WITH ADDITION OF PVDF/NANO CHITOSAN COMPOSITE BLENDING MEMBRANE METHOD. *Rasayan J. Chem*, *18*(1), 624 – +31. https://doi.org/10.31788/RJC.2025.1819079

Robert, M., El Kaddouri, A., Perrin, J. C., Mozet, K., Daoudi, M., Dillet, J., Morel, J. Y., André, S., & Lottin, O. (2020). Effects of conjoint mechanical and chemical stress on perfluorosulfonic-acid membranes for fuel cells. *Journal of Power Sources*, *476*, 228662. https://doi.org/10.1016/J.JPOWSOUR.2020.228662

Rudolph, G., Al-Rudainy, B., Thuvander, J., & Jönsson, A. S. (2021). Comprehensive Analysis of Foulants in an Ultrafiltration Membrane Used for the Treatment of Bleach Plant Effluent in a Sulfite Pulp Mill. *Membranes*, *11*(3), 201. https://doi.org/10.3390/MEMBRANES11030201

Sadare, O. O., Yoro, K. O., Moothi, K., & Daramola, M. O. (2022). Lignocellulosic Biomass-Derived Nanocellulose Crystals as Fillers in Membranes for Water and Wastewater

Treatment: A Review. *Membranes 2022, Vol. 12, Page 320*, *12*(3), 320. https://doi.org/10.3390/MEMBRANES12030320

Safarpour, M., Najjarizad-Peyvasti, S., Khataee, A., & Karimi, A. (2022). Polyethersulfone ultrafiltration membranes incorporated with CeO2/GO nanocomposite for enhanced fouling resistance and dye separation. *Journal of Environmental Chemical Engineering*, *10*(3), 107533. https://doi.org/10.1016/J.JECE.2022.107533

Sakarkar, S., Muthukumaran, S., & Jegatheesan, V. (2020). Evaluation of polyvinyl alcohol (PVA) loading in the PVA/titanium dioxide (TiO2) thin film coating on polyvinylidene fluoride (PVDF) membrane for the removal of textile dyes. *Chemosphere*, *257*, 127144. https://doi.org/10.1016/J.CHEMOSPHERE.2020.127144

Sakarkar, S., Muthukumaran, S., & Jegatheesan, V. (2021). Tailoring the Effects of Titanium Dioxide (TiO2) and Polyvinyl Alcohol (PVA) in the Separation and Antifouling Performance of Thin-Film Composite Polyvinylidene Fluoride (PVDF) Membrane. *Membranes 2021, Vol. 11, Page 241*, *11*(4), 241. https://doi.org/10.3390/MEMBRANES11040241

Salama, A., Abouzeid, R., Leong, W. S., Jeevanandam, J., Samyn, P., Dufresne, A., Bechelany, M., & Barhoum, A. (2021). Nanocellulose-based materials for water treatment: Adsorption, photocatalytic degradation, disinfection, antifouling, and nanofiltration. In *Nanomaterials* (Vol. 11, Issue 11). MDPI. https://doi.org/10.3390/nano11113008

Saleem, H., & Zaidi, S. J. (2020). Nanoparticles in reverse osmosis membranes for desalination: A state of the art review. *Desalination*, *475*, 114171. https://doi.org/10.1016/J.DESAL.2019.114171

Saleh, T. A., Mustaqeem, M., & Khaled, M. (2022). Water treatment technologies in removing heavy metal ions from wastewater: A review. *Environmental Nanotechnology, Monitoring & Management*, *17*, 100617. https://doi.org/10.1016/J.ENMM.2021.100617

Saud, A., Saleem, H., & Zaidi, S. J. (2022). Progress and Prospects of Nanocellulose-Based Membranes for Desalination and Water Treatment. In *Membranes* (Vol. 12, Issue 5). MDPI. https://doi.org/10.3390/membranes12050462

Saxena, P., & Shukla, P. (2021). A comprehensive review on fundamental properties and applications of poly(vinylidene fluoride) (PVDF). *Advanced Composites and Hybrid Materials 2021 4:1*, *4*(1), 8–26. https://doi.org/10.1007/S42114-021-00217-0

Schweizer, P., Dolle, C., Dasler, D., Abellán, G., Hauke, F., Hirsch, A., & Spiecker, E. (2020). Mechanical cleaning of graphene using in situ electron microscopy. *Nature Communications 2020 11:1*, *11*(1), 1–9. https://doi.org/10.1038/s41467-020-15255-3

Seraj, S., Mohammadi, T., & Tofighy, M. A. (2022). Graphene-based membranes for membrane distillation applications: A review. *Journal of Environmental Chemical Engineering*, *10*(3), 107974. https://doi.org/10.1016/J.JECE.2022.107974

Shahzad, A., Oh, J. M., Azam, M., Iqbal, J., Hussain, S., Miran, W., & Rasool, K. (2021). Advances in the Synthesis and Application of Anti-Fouling Membranes Using Two-Dimensional Nanomaterials. *Membranes 2021, Vol. 11, Page 605*, *11*(8), 605. https://doi.org/10.3390/MEMBRANES11080605

Sharifalhoseini, Z., Entezari, M. H., & Shahidi, M. (2018). Sonication affects the quantity and the morphology of ZnO nanostructures synthesized on the mild steel and changes

the corrosion protection of the surface. *Ultrasonics Sonochemistry*, *41*(October 2017), 492–502. https://doi.org/10.1016/j.ultsonch.2017.10.012

Sharma, P. R., Sharma, S. K., Lindström, T., & Hsiao, B. S. (2020). Nanocellulose-Enabled Membranes for Water Purification: Perspectives. *Advanced Sustainable Systems*, *4*(5), 1900114. https://doi.org/10.1002/ADSU.201900114

Shawky, A. M., Kotp, Y. H., Mousa, M. A., Aboelfadl, M. M. S., Hekal, E. E., & Zakaria, K. (2024). Effect of titanium oxide/reduced graphene (TiO2/rGO) addition onto water flux and reverse salt diffusion thin-film nanocomposite forward osmosis membranes. *Environmental Science and Pollution Research*, *31*(16), 24584–24598. https://doi.org/10.1007/S11356-024-32500-0/FIGURES/8

Shi, S., Jia, M., Li, M., Zhou, S., Zhao, Y., Zhong, J., Dai, D., & Qiu, J. (2023). ZnO@g-C3N4 S-scheme photocatalytic membrane with visible-light response and enhanced water treatment performance. *Colloids and Surfaces A: Physicochemical and Engineering Aspects*, *667*(March), 131259. https://doi.org/10.1016/j.colsurfa.2023.131259

Shin, Y., Hwang, T. M., Nam, S. H., Kim, E., Park, J. B., Choi, Y. J., Kye, H., & Koo, J. W. (2024). Evaluating Nanofiltration and Reverse Osmosis Membranes for Pharmaceutically Active Compounds Removal: A Solution Diffusion Model Approach. *Membranes*, *14*(12), 250. https://doi.org/10.3390/MEMBRANES14120250

Shirazi, M. M. A., Bazgir, S., & Meshkani, F. (2020). Electrospun Nanofibrous Membranes for Water Treatment. In A. Abdelrasoul (Ed.), *Advances in Membrane Technologies*. IntechOpen. https://doi.org/10.5772/intechopen.87948

Siagian, U. W. R., Khoiruddin, K., Wardani, A. K., Aryanti, P. T. P., Widiasa, I. N., Qiu, G., Ting, Y. P., & Wenten, I. G. (2021). High-Performance Ultrafiltration Membrane: Recent Progress and Its Application for Wastewater Treatment. *Current Pollution Reports*, *7*(4), 448–462. https://doi.org/10.1007/S40726-021-00204-5/METRICS

Siddique, I. (2022). Sustainable Water Management in Urban Environments. *SSRN Electronic Journal*. https://doi.org/10.2139/SSRN.4885908

Silva, J. A. (2023). Water Supply and Wastewater Treatment and Reuse in Future Cities: A Systematic Literature Review. *Water (Switzerland)*, *15*(17), 3064. https://doi.org/10.3390/W15173064/S1

Smith, A. T., LaChance, A. M., Zeng, S., Liu, B., & Sun, L. (2019). Synthesis, properties, and applications of graphene oxide/reduced graphene oxide and their nanocomposites. *Nano Materials Science*, *1*(1), 31–47. https://doi.org/10.1016/J.NANOMS.2019.02.004

Sreedharan, M., Vijayamma, R., Liyaskina, E., Revin, V. V., Ullah, M. W., Shi, Z., Yang, G., Grohens, Y., Kalarikkal, N., Ali Khan, K., & Thomas, S. (2024). Nanocellulose-Based Hybrid Scaffolds for Skin and Bone Tissue Engineering: A 10-Year Overview. *Biomacromolecules*, *25*(4), 2136–2155. https://doi.org/10.1021/ACS.BIOMAC.3C00975/ASSET/IMAGES/MEDIUM/BM3C00975_0008.GIF

Srivastava, A., & Adesina, N. O. (2022). Graphene—Technology and integration with semiconductor electronics. *Theoretical and Computational Chemistry*, *21*, 1–40. https://doi.org/10.1016/B978-0-12-819514-7.00006-3

Steffi, A. P., Balaji, R., Prakash, N., Rajesh, T. P., Ethiraj, S., Samuel, M. S., Nadda, A. K., & Chandrasekar, N. (2022). Incorporation of SiO2 functionalized gC3N4 sheets with

TiO2 nanoparticles to enhance the anticorrosion performance of metal specimens in aggressive Cl− environment. *Chemosphere*, *290*, 133332. https://doi.org/10.1016/J.CHEMOSPHERE.2021.133332

Su, C., Li, Z., Zhang, D., Wang, Z., Zhou, X., Liao, L., & Xiao, X. (2020). A highly sensitive sensor based on a computer-designed magnetic molecularly imprinted membrane for the determination of acetaminophen. *Biosensors and Bioelectronics*, *148*, 111819. https://doi.org/10.1016/J.BIOS.2019.111819

Subrahmanya, T. M., Arshad, A. bin, Lin, P. T., Widakdo, J., Makari, H. K., Austria, H. F. M., Hu, C. C., Lai, J. Y., & Hung, W. S. (2021). A review of recent progress in polymeric electrospun nanofiber membranes in addressing safe water global issues. *RSC Advances*, *11*(16), 9638–9663. https://doi.org/10.1039/D1RA00060H

Sueraya, A. Z., Rahman, M. R., Kanakaraju, D., Said, K. A. M., James, A., Othman, A. K. Bin, Bakri, M. K. Bin, & Uddin, J. (2023). A comprehensive review on nanocellulose-based membranes: methods, mechanism, and applications in wastewater treatment. *Polymer Bulletin 2023 81:9*, *81*(9), 7519–7549. https://doi.org/10.1007/S00289-023-05084-X

Sueraya, A. Z., Rahman, M. R., Said, K. A. B. M., Namakka, M., Kanakaraju, D., Al-Humaidi, J. Y., Al-Baqami, S. M., Rahman, M. M., & Khandaker, M. U. (2024). Impact of titanium dioxide/graphene in polyvinylidene fluoride nanocomposite membrane to intensify methylene blue dye removal, antifouling performance, and reusability. *Journal of Applied Polymer Science*, e56257. https://doi.org/10.1002/APP.56257

Sun, L., Zhang, X., Liu, H., Liu, K., Du, H., Kumar, A., Sharma, G., & Si, C. (2020). Recent Advances in Hydrophobic Modification of Nanocellulose. *Current Organic Chemistry*, *25*(3), 417–436. https://doi.org/10.2174/1385272824999201210191041

Sun, Y. (2025). PCERAMIC MEMBRANE CATALYTIC REACTORS FOR WASTEWATER PURIFICATION: RECENT ADVANCES, CURRENT CHALLENGES AND FUTURE PERSPECTIVES. *Ceramics-Silikáty*, *69*(2), 204–221. https://doi.org/10.13168/cs.2025.0006

Taghipour, A., Karami, P., Manikantan Sandhya, M., & Sadrzadeh, M. (2024). An Innovative Surface Modification Technique for Antifouling Polyamide Nanofiltration Membranes. *ACS Applied Materials and Interfaces* , *16*(28), 37197–37211. https://doi.org/10.1021/ACSAMI.4C06082/ASSET/IMAGES/MEDIUM/AM4C06082_0009.GIF

Tan, H. F., Ooi, B. S., & Leo, C. P. (2020). Future perspectives of nanocellulose-based membrane for water treatment. *Journal of Water Process Engineering*, *37*, 101502. https://doi.org/10.1016/J.JWPE.2020.101502

Tavakolmoghadam, M., Mokhtare, A., Rekabdar, F., Esmaeili, M., & Hossein Khanli Khaneghah, A. (2019). A predictive model for tuning additives for the fabrication of porous polymeric membranes. *Materials Research Express*, *7*(1). https://doi.org/10.1088/2053-1591/ab5f6c

Tetteh, E. K., Rathilal, S., Asante-Sackey, D., & Chollom, M. N. (2021). Prospects of Synthesized Magnetic TiO2-Based Membranes for Wastewater Treatment: A Review. *Materials 2021, Vol. 14, Page 3524*, *14*(13), 3524. https://doi.org/10.3390/MA14133524

Toriello, M., Afsari, M., Shon, H. K., & Tijing, L. D. (2020). Progress on the fabrication and application of electrospun nanofiber composites. In *Membranes* (Vol. 10, Issue 9, pp. 1–35). MDPI AG. https://doi.org/10.3390/membranes10090204

Ullah, A., Tanudjaja, H. J., Ouda, M., Hasan, S. W., & Chew, J. W. (2021). Membrane fouling mitigation techniques for oily wastewater: A short review. *Journal of Water Process Engineering*, *43*, 102293. https://doi.org/10.1016/J.JWPE.2021.102293

van den Berg, T., & Ulbricht, M. (2020). Polymer nanocomposite ultrafiltration membranes: The influence of polymeric additive, dispersion quality and particle modification on the integration of zinc oxide nanoparticles into polyvinylidene difluoride membranes. *Membranes*, *10*(9), 197. https://doi.org/10.3390/membranes10090197

Vatanpour, V., Mousavi Khadem, S. S., Dehqan, A., Al-Naqshabandi, M. A., Ganjali, M. R., Sadegh Hassani, S., Rashid, M. R., Saeb, M. R., & Dizge, N. (2021). Efficient removal of dyes and proteins by nitrogen-doped porous graphene blended polyethersulfone nanocomposite membranes. *Chemosphere*, *263*, 127892. https://doi.org/10.1016/J.CHEMOSPHERE.2020.127892

Verma, Y. K., Singh, A. K., Paswan, M. K., & Gurmaita, P. K. (2024). Preparation and characterization of bamboo based nanocellulose by ball milling and used as a filler for preparation of nanocomposite. *Polymer*, *308*(March), 127396. https://doi.org/10.1016/j.polymer.2024.127396

Vilela, C., Moreirinha, C., Almeida, A., Silvestre, A. J. D., & Freire, C. S. R. (2019). Zwitterionic nanocellulose-based membranes for organic dye removal. *Materials*, *12*(9). https://doi.org/10.3390/ma12091404

Vivod, V., Neral, B., Mihelič, A., & Kokol, V. (2018). Highly efficient film-like nanocellulose-based adsorbents for the removal of loose reactive dye during textile laundering. *Https://Doi.Org/10.1177/0040517518760752*, *89*(6), 975–988. https://doi.org/10.1177/0040517518760752

Wan, Z., & Jiang, Y. (2021). Synthesis-structure-performance relationships of nanocomposite polymeric ultrafiltration membranes: A comparative study of two carbon nanofillers. *Journal of Membrane Science*, *620*, 118847. https://doi.org/10.1016/J.MEMSCI.2020.118847

Wang, C., Chen, Y., Yang, K., Hu, X., & Zhang, Y. (2022). Fabrication of tight GO/PVDF hollow fiber membranes with improved permeability for efficient fractionation of dyes and salts in textile wastewater. *Polymer Bulletin*, *79*(1), 443–462. https://doi.org/10.1007/S00289-020-03513-9/METRICS

Wang, G., Shen, Y., Lu, W., Tian, B., Zhang, J., & Chu, J. (2024). *Electrical and Optical Dielectric Constants of B-Phase P(Vdf-Trfe) Ferroelectric Films*. https://doi.org/10.2139/SSRN.4801361

Wang, J., Chen, S., Zeng, Q., Jiang, H., Chang, H., Zhang, T. C., Tian, X., Li, Y., Liang, Y., & Wang, K. (2023). Polydopamine/UiO-66-NH2 induced photothermal antibacterial electrospun membrane for efficient point-of-use drinking water treatment. *Colloids and Surfaces A: Physicochemical and Engineering Aspects*, *658*(September 2022), 130640. https://doi.org/10.1016/j.colsurfa.2022.130640

Wang, J., Wang, Y., Zhu, J., Zhang, Y., Liu, J., & Van der Bruggen, B. (2017). Construction of TiO2@graphene oxide incorporated antifouling nanofiltration membrane with

elevated filtration performance. *Journal of Membrane Science*, *533*, 279–288. https://doi.org/10.1016/J.MEMSCI.2017.03.040

Wang, P., He, M., & Maeda, Y. (2025). Fouling of Reverse Osmosis (RO) and Nanofiltration (NF) Membranes by Low Molecular Weight Organic Compounds (LMWOCs), Part 2: Countermeasures and Applications. *Membranes 2025, Vol. 15, Page 94*, *15*(3), 94. https://doi.org/10.3390/MEMBRANES15030094

Wang, X., Ding, H., Lv, G., Zhou, R., Ma, R., Hou, X., Zhang, J., & Li, W. (2022). Fabrication of superhydrophilic self-cleaning SiO2–TiO2 coating and its photocatalytic performance. *Ceramics International*, *48*(14), 20033–20040. https://doi.org/10.1016/J.CERAMINT.2022.03.278

Wang, X., Feng, M., Liu, Y., Deng, H., & Lu, J. (2019). Fabrication of graphene oxide blended polyethersulfone membranes via phase inversion assisted by electric field for improved separation and antifouling performance. *Journal of Membrane Science*, *577*(September 2018), 41–50. https://doi.org/10.1016/j.memsci.2019.01.055

Wang, X., Li, S., Chen, P., Li, F., Hu, X., & Hua, T. (2022). Photocatalytic and antifouling properties of TiO2-based photocatalytic membranes. *Materials Today Chemistry*, *23*, 100650. https://doi.org/10.1016/J.MTCHEM.2021.100650

Wang, Y. (Alex), Smith, S. J. D., Liu, Y., Lu, P., Zhang, X., Ng, D., & Xie, Z. (2022). Surface hydrophilicity modification of thin-film composite membranes with metal−organic frameworks (MOFs) Ti-UiO-66 for simultaneous enhancement of anti-fouling property and desalination performance. *Separation and Purification Technology*, *302*, 122001. https://doi.org/10.1016/J.SEPPUR.2022.122001

Wang, Z., Chen, Z., Zheng, Z., Liu, H., Zhu, L., Yang, M., & Chen, Y. (2023). Nanocellulose-based membranes for highly efficient molecular separation. *Chemical Engineering Journal*, *451*, 138711. https://doi.org/10.1016/J.CEJ.2022.138711

Wang, Z., Feng, G., Yan, Z., Li, S., Xu, M., Wang, C., & Li, Y. (2023). Improving the hydrophilicity and antifouling performance of PVDF membranes via PEI amination and further poly (methyl vinyl ether-alt-maleic anhydride) modification. *Reactive and Functional Polymers*, *189*, 105610. https://doi.org/10.1016/J.REACTFUNCTPOLYM.2023.105610

Wei, D., Zhou, S., Li, M., Xue, A., Zhang, Y., Zhao, Y., Zhong, J., & Yang, D. (2019). PVDF/palygorskite composite ultrafiltration membranes: Effects of nano-clay particles on membrane structure and properties. *Applied Clay Science*, *181*, 105171. https://doi.org/10.1016/J.CLAY.2019.105171

Wu, Z., Huang, W., Shan, X., & Li, Z. (2020). Preparation of a porous graphene oxide/alkali lignin aerogel composite and its adsorption properties for methylene blue. *International Journal of Biological Macromolecules*, *143*, 325–333. https://doi.org/10.1016/J.IJBIOMAC.2019.12.017

Xia, L., Guan, K., He, S., Luo, P., Matsuyama, H., Zhong, Z., & Zou, D. (2024). Engineering high-flux poly (vinylidene fluoride) membranes with symmetric structure for membrane distillation via delayed phase inversion. *Separation and Purification Technology*, *338*, 126499. https://doi.org/10.1016/J.SEPPUR.2024.126499

Xiong, Z., Liu, J., Yang, Y., Lai, Q., Wu, X., Yang, J., Zeng, Q., Zhang, G., & Zhao, S. (2022). Reinforcing hydration layer on membrane surface via nano-capturing and hydrothermal

crosslinking for fouling reduction. *Journal of Membrane Science*, *644*, 120076. https://doi.org/10.1016/J.MEMSCI.2021.120076

Xu, Y., Chiam, S. L., Leo, C. P., & Hu, Z. (2025). Recent Advances in Photocatalytic TiO2-based Membranes for Eliminating Water Pollutants. *Separation and Purification Reviews*. https://doi.org/10.1080/15422119.2025.2487991;JOURNAL:JOURNAL:LSPR19;WGROUP:STRING:PUBLICATION

Xu, Y., Xu, Y., Chen, H., Gao, M., Yue, X., & Ni, Y. (2022). Redispersion of dried plant nanocellulose: A review. *Carbohydrate Polymers*, *294*, 119830. https://doi.org/10.1016/J.CARBPOL.2022.119830

Yang, C., Wang, P., Li, J., Wang, Q., Xu, P., You, S., Zheng, Q., & Zhang, G. (2021). Photocatalytic PVDF ultrafiltration membrane blended with visible-light responsive Fe(III)-TiO2 catalyst: Degradation kinetics, catalytic performance and reusability. *Chemical Engineering Journal*, *417*, 129340. https://doi.org/10.1016/J.CEJ.2021.129340

Yang, C., Xu, W., Nan, Y., Wang, Y., Hu, Y., Gao, C., & Chen, X. (2020). Fabrication and characterization of a high performance polyimide ultrafiltration membrane for dye removal. *Journal of Colloid and Interface Science*, *562*, 589–597. https://doi.org/10.1016/J.JCIS.2019.11.075

Yang, G., Xie, Z., Cran, M., Wu, C., & Gray, S. (2020). Dimensional Nanofillers in Mixed Matrix Membranes for Pervaporation Separations: A Review. *Membranes 2020, Vol. 10, Page 193*, *10*(9), 193. https://doi.org/10.3390/MEMBRANES10090193

Yang, J. hui, Zhang, Y. sheng, Xue, F., Liu, D. feng, Zhang, N., Huang, T., & Wang, Y. (2021). Structural relaxation and dielectric response of PVDF/PMMA blend in the presence of graphene oxide. *Polymer*, *229*, 123998. https://doi.org/10.1016/J.POLYMER.2021.123998

Yang, X., Sun, H., Li, G., An, T., & Choi, W. (2021). Fouling of TiO2 induced by natural organic matters during photocatalytic water treatment: Mechanisms and regeneration strategy. *Applied Catalysis B: Environmental*, *294*, 120252. https://doi.org/10.1016/J.APCATB.2021.120252

Yao, X., Raine, T. P., Liu, M., Zakaria, M., Kinloch, I. A., & Bissett, M. A. (2021). Effect of graphene nanoplatelets on the mechanical and gas barrier properties of woven carbon fibre/epoxy composites. *Journal of Materials Science*, *56*(35), 19538–19551. https://doi.org/10.1007/S10853-021-06467-Z/FIGURES/10

Yin, J., Roso, M., Boaretti, C., Lorenzetti, A., Martucci, A., & Modesti, M. (2021). PVDF-TiO2 core-shell fibrous membranes by microwave-hydrothermal method: Preparation, characterization, and photocatalytic activity. *Journal of Environmental Chemical Engineering*, *9*(5), 106250. https://doi.org/10.1016/J.JECE.2021.106250

Youcai, Z. (2018). Physical and Chemical Treatment Processes for Leachate. *Pollution Control Technology for Leachate from Municipal Solid Waste*, 31–183. https://doi.org/10.1016/B978-0-12-815813-5.00002-4

Yu, K., Spiesz, E. M., Balasubramanian, S., Schmieden, D. T., Meyer, A. S., & Aubin-Tam, M. E. (2021). Scalable bacterial production of moldable and recyclable biomineralized cellulose with tunable mechanical properties. *Cell Reports Physical Science*, *2*(6), 100464. https://doi.org/10.1016/J.XCRP.2021.100464

Yue, X., Li, W., Li, Z., Qiu, F., Pan, J., & Zhang, T. (2020). Laminated superwetting aerogel/membrane composite with large pore sizes for efficient separation of surfactant-stabilized water-in-oil emulsions. *Chemical Engineering Science*, *215*, 115450. https://doi.org/10.1016/J.CES.2019.115450

Zaki, M., Atiqah, M. S. N., Khalil, H. P. S. A., Ikram, H., Alfatah, T., Mistar, E. M., Adisalamun, A., & Yahya, E. B. (2022). Microbial enhancement of nanocellulose isolation from sawn timber industrial wastes and fabrication of biocomposite membranes. *Bioresource Technology Reports*, *20*, 101242. https://doi.org/10.1016/J.BITEB.2022.101242

Zakuwan, S. Z., & Ahmad, I. (2018). Synergistic Effect of Hybridized Cellulose Nanocrystals and Organically Modified Montmorillonite on κ-Carrageenan Bionanocomposites. *Nanomaterials 2018, Vol. 8, Page 874*, *8*(11), 874. https://doi.org/10.3390/NANO8110874

Zeng, X., Cai, W., Fu, S., Lin, X., Lu, Q., Liao, S., Hu, H., Zhang, M., Zhou, C., Wen, X., & Tan, S. (2022). A novel Janus sponge fabricated by a green strategy for simultaneous separation of oil/water emulsions and dye contaminants. *Journal of Hazardous Materials*, *424*, 127543. https://doi.org/10.1016/J.JHAZMAT.2021.127543

Zhang, B., Gao, H., Tong, X., Liu, S., Gan, L., & Chen, Y. (2019). Pressure retarded osmosis and reverse electrodialysis as power generation membrane systems. In *Current Trends and Future Developments on (Bio-) Membranes: Renewable Energy Integrated with Membrane Operations* (pp. 133–152). Elsevier. https://doi.org/10.1016/B978-0-12-813545-7.00006-4

Zhang, F., Yang, K., Liu, G., Chen, Y., Wang, M., Li, S., & Li, R. (2022). Recent advances on graphene: Synthesis, properties and applications. *Composites Part A: Applied Science and Manufacturing*, *160*, 107051. https://doi.org/10.1016/J.COMPOSITESA.2022.107051

Zhang, F., Zhang, Y., He, P., Chen, H., Gao, J., & Liang, J. (2023). Multifunctional granulated blast furnace slag-based inorganic membrane for highly efficient separation of oil and dye from wastewater. *Process Safety and Environmental Protection*, *170*(13), 380–391. https://doi.org/10.1016/j.psep.2022.12.015

Zhang, H. C., Yu, C. N., Li, X. Z., Wang, L. F., Huang, J., Tong, J., Lin, Y., Min, Y., & Liang, Y. (2022). Recent Developments of Nanocellulose and its Applications in Polymeric Composites. *ES Food and Agroforestry*, *9*, 1–14. https://doi.org/10.30919/ESFAF768

Zhang, H., Lin, S., Pan, Y., Wang, X., Zhang, H., Liu, S., Li, Z., & Wei, N. (2025). Nanocellulose–Graphene Derivative Composite Membranes: Recent Advances, Functional Mechanisms, and Water Purification Applications. *Membranes 2025, Vol. 15, Page 347*, *15*(12), 347. https://doi.org/10.3390/MEMBRANES15120347

Zhang, H., Zhu, Y., & Li, L. (2020). Fabrication of PVDF/graphene composites with enhanced β phase via conventional melt processing assisted by solid state shear milling technology. *RSC Advances*, *10*(6), 3391–3401. https://doi.org/10.1039/C9RA09459H

Zhang, J., Zheng, M., Zhou, Y., Yang, L., Zhang, Y., Wu, Z., Liu, G., & Zheng, J. (2022). Preparation of Nano-TiO2-Modified PVDF Membranes with Enhanced Antifouling Behaviors via Phase Inversion: Implications of Nanoparticle Dispersion Status in Casting Solutions. *Membranes 2022, Vol. 12, Page 386*, *12*(4), 386. https://doi.org/10.3390/MEMBRANES12040386

Zhang, S., Chen, Y., Zang, X., & Zhang, X. (2020). Harvesting of Microcystis aeruginosa using membrane filtration: Influence of pore structure on fouling kinetics, algogenic organic matter retention and cake formation. *Algal Research*, *52*, 102112. https://doi.org/10.1016/J.ALGAL.2020.102112

Zhang, W., Wang, X., Zhang, Y., van Bochove, B., Mäkilä, E., Seppälä, J., Xu, W., Willför, S., & Xu, C. (2020). Robust shape-retaining nanocellulose-based aerogels decorated with silver nanoparticles for fast continuous catalytic discoloration of organic dyes. *Separation and Purification Technology*, *242*. https://doi.org/10.1016/J.SEPPUR.2020.116523

Zhang, W., Zhang, Y., Wang, Y., Tian, S., Han, N., Li, W., Wang, W., Liu, H., Yan, X., & Zhang, X. (2022). Fluffy-like amphiphilic graphene oxide (f-GO) and its effects on improving the antifouling of PAN-based composite membranes. *Desalination*, *527*, 115575. https://doi.org/10.1016/J.DESAL.2022.115575

Zhang, Y., & Park, S. J. (2019). Facile construction of MoO3@ZIF-8 core-shell nanorods for efficient photoreduction of aqueous Cr (VI). *Applied Catalysis B: Environmental*, *240*, 92–101. https://doi.org/10.1016/J.APCATB.2018.08.077

Zhang, Y., Zhang, C., & Wang, Y. (2021). Recent progress in cellulose-based electrospun nanofibers as multifunctional materials. *Nanoscale Advances*, *3*(21), 6040–6047. https://doi.org/10.1039/D1NA00508A

Zhao, D. L., Feng, F., Shen, L., Huang, Z., Zhao, Q., Lin, H., & Chung, T. S. (2023). Engineering metal–organic frameworks (MOFs) based thin-film nanocomposite (TFN) membranes for molecular separation. *Chemical Engineering Journal*, *454*, 140447. https://doi.org/10.1016/J.CEJ.2022.140447

Zhou, W., Huang, H., Wang, Z., Sharshir, S. W., Wang, C., An, M., Wang, L., & Yuan, Z. (2024). Impact of functional groups on cellulose nanofibers on the state of water molecules, photocatalytic water splitting, and photothermal water evaporation. *Journal of Materials Chemistry A*, *12*(7), 4046–4056. https://doi.org/10.1039/D3TA06600B

Zhou, W., Lin, Y., Zou, K., Zhou, C., Gong, X., Cao, Y., & Jiang, S. (2021). Enhancement of piezoelectricity in polymer PVDF based on molecular chain structure. *Journal of Materials Science: Materials in Electronics*, *32*(24), 28708–28717. https://doi.org/10.1007/S10854-021-07250-1/METRICS

Zhou, Y., Song, P., Pan, M., Wang, H., Liu, Z., Di, J., Liu, D., Low, J., & Yang, R. (2023). Super hydrophilic-electrons acceptor regulated rutile TiO2 nanorods for promoting photocatalytic H2 evolution. *Applied Surface Science*, *623*, 157098. https://doi.org/10.1016/J.APSUSC.2023.157098

Zhu, C., Liu, G., Han, K., Ye, H., Wei, S., & Zhou, Y. (2017). One-step facile synthesis of graphene oxide/TiO2 composite as efficient photocatalytic membrane for water treatment: Crossflow filtration operation and membrane fouling analysis. *Chemical Engineering and Processing - Process Intensification*, *120*, 20–26. https://doi.org/10.1016/J.CEP.2017.06.012

Zhu, T., Zuo, X., Lin, X., Su, Z., Li, J., Zeng, R., & Nan, J. (2022). High-Wettability Composite Separator Embedded with in Situ Grown TiO2 Nanoparticles for Advanced Sodium-Ion Batteries. *Energy Technology*, *10*(10), 2200409. https://doi.org/10.1002/ENTE.202200409;PAGEGROUP:STRING:PUBLICATION

Zubair, M., Yasir, M., Ponnamma, D., Mazhar, H., Sedlarik, V., Hawari, A. H., Al-Harthi, M. A., & Al-Ejji, M. (2024). Recent advances in nanocellulose-based two-dimensional

nanostructured membranes for sustainable water purification: A review. *Carbohydrate Polymers*, *329*(September 2023), 121775. https://doi.org/10.1016/j.carbpol.2024.121775

Zulkefli, N. F., Alias, N. H., Jamaluddin, N. S., Abdullah, N., Manaf, S. F. A., Othman, N. H., Marpani, F., Mat-Shayuti, M. S., & Kusworo, T. D. (2021). Recent Mitigation Strategies on Membrane Fouling for Oily Wastewater Treatment. *Membranes 2022, Vol. 12, Page 26*, *12*(1), 26. https://doi.org/10.3390/MEMBRANES12010026

Сергієнко, А. О., Донцова, Т. А., Янушевська, О. І., Нагірняк, С. В., & Ahmad, H.-B. (2020). CERAMIC MEMBRANES: NEW TRENDS AND PROSPECTS (SHORT REVIEW). *WATER AND WATER PURIFICATION TECHNOLOGIES. SCIENTIFIC AND TECHNICAL NEWS*, *27*(2), 4–31. https://doi.org/10.20535/2218-93002722020208817

APPENDICES

Appendix A: Journal Publications

1. **Sueraya, A. Z.**, Rahman, M. R., Said, K. A. B. M., Namakka, M., Kanakaraju, D., Al-Humaidi, J. Y., ... & Khandaker, M. U. (2024). Impact of titanium dioxide/graphene in polyvinylidene fluoride nanocomposite membrane to intensify methylene blue dye removal, antifouling performance, and reusability. *Journal of Applied Polymer Science*, *141*(47), e56257.
2. **Sueraya, A. Z.**, Rahman, M. R., Kanakaraju, D., Said, K. A. M., James, A., Othman, A. K. B., ... & Uddin, J. (2024). A comprehensive review on nanocellulose-based membranes: methods, mechanism, and applications in wastewater treatment. *Polymer Bulletin*, *81*(9), 7519-7549.
3. Rahman, M. R., **Sueraya, A. Z.,** Said, K. A. B. M., Namakka, M., James, A., Rahman, I. M. M., ... & Rahman, M. M. (2025). Impact of graphene/nanocellulose on nanocomposite membrane for methylene blue dye removal and antifouling performance. *Journal of Applied Polymer Science*, *142*(43), e57648.
4. **Sueraya, A. Z.**, Rahman, M. R., James, A. A., Bakri, M. K. B., & Namakka, M. (2025). Polymer nanocomposite membranes for dye removal. *Polymer Nanocomposite Membranes in Water Treatment and Desalination*, 187-207.
5. **Sueraya, A. Z.**, Rahman, M. R., Said, K. A. B. M., Matin, M. M., & Rahman, M. M. (2024). Impact on biocomposites using various types of nanocarbon and polymer. In *Advanced Nanocarbon Polymer Biocomposites* (pp. 217-254). Woodhead Publishing.